

Non-linear density wave solutions for different models of galaxies

M. Vukcevic^{1,2★}

¹*Military Academy, University of Defence, Pavla Jurisica Sturma 33, 11000 Belgrade, Serbia*

²*Isaac Newton Institute of Chile, Yugoslavia Branch, 11000 Belgrade, Serbia*

Accepted 2014 March 24. Received 2014 March 6; in original form 2013 December 11

ABSTRACT

We have studied different geometry of the galaxy and the influence of certain geometry on the possible derivation of non-linear equation. We discussed soliton solutions of the derived non-linear equations and the properties of the morphologies resulting from these solutions. For thick disc, perturbations of the equilibrium state cause the non-linear Korteweg de Vries equation, and the stable solution of that equation results in the ring shape, while for the thin disc, for the similar type of perturbations, non-linear Schrodinger equation is derived with stable solution of the spiral shape.

Key words: waves – galaxies: general – galaxies: spiral – galaxies: structure.

1 INTRODUCTION

Spiral structure in galaxies has been studied in both observational and theoretical field, mainly during the 20th century. First, B. Lindblad formulated the hypothesis that the large-scale spiral structure in galaxies is quasi-stationary, in spite of the presence of differential rotation in the disc (Lindblad 1963). Due to observed differential rotation, any material structure could not persist for a long time, but would be stretched on a very short time-scale. This is known as the winding dilemma. In contrast, as the conclusion of the Lindblad work, the idea was introduced in the early 1960s that the spiral arms, if associated with a wave phenomenon, could survive differential rotation as a quasi-stationary pattern (Lin & Shu 1964). There are a few levels at which validity of the density wave theory has been questioned. The main discussions are posed on generation and maintenance of density waves (Lin & Bertin 1995).

There are, in general, three different theoretical models that can be used to investigate stellar component of galaxies, orbital, kinematic and dynamical one. Here, we recall just two of them to underline difference and difficulties. A kinematic model specifies the spatial density of stars and their kinematics at each point without questioning whether a gravitational potential exists in which the given density distribution and kinematics constitute a steady state. To treat galaxy dynamically is more complex and plausible, since it is necessary to relate the galactic gravitational potential, in which there is substantial contribution to the local acceleration from a disc, a bulge and a dark halo, to the mass density. Recently, more dynamical models of our Galaxy have been explored by Binney (2012), using complex gravitational potential that is generated by three discs (gas and both thin and thick stellar discs), a bulge and a dark halo. There are a number of papers studying the same prob-

lem from different points of research interests, such as (El-Zanta & Haßler 1998; Bratek, Jalocha & Kutschera 2008).

Apart from these studies, there is also number of non-linear approaches to density waves. In numerical studies, using simulations, complex system has been treated in non-linear regime (Sellwood 1985, 1986). Turbulent behaviour of the interstellar medium was studied by number of authors such as Wada, Meurer & Norman (2002), and this kind of research is very useful since the turbulence is transient phase that could lead, under certain conditions, to soliton formation. There is also non-linear study of the accretion disc (Heinemann & Papaloizou 2012), resulting in a non-linear Burgers' equation and sawtooth waves, that could be used to understand transient physical processes from linear waves to possible stable non-linear structure. Theoretical research concerning possible soliton solution was given by Norman (1978) for the first time.

In this paper, our aim is not to investigate complexity but rather to study theoretically, weakly non-linear dynamics of different simplified galaxy models, using reductive perturbation method (RPM), with the primary emphasis on possible soliton solutions. Solitons are able to overcome mentioned difficulties in density wave theory. In order to use proper coordinate transformation, it is necessary to analyse stability of the linearized system of equations, and to define proper parameter regime. Each model is useful in verifying the more complex models, especially in testing the simulations and numerics used to explain dynamics of galaxies.

2 GOVERNING EQUATIONS

The density wave model consists of transport equations for the mass density ρ and the momentum ρv , together with the Poisson's equation that relates the density to the gravitational potential ϕ . The equilibrium state of the system is described as a rotation with an angular velocity $\Omega(r)$ about z -axis under the balance of centrifugal and gravitational forces in a frame rotating with constant angular velocity Ω_0 . Then, the equilibrium velocity is $v_{0\phi} = (\Omega - \Omega_0)r$,

★E-mail: vuk.mira@gmail.com

where $\Omega^2 r = \partial\phi_0/\partial r$. The quantities ϕ_0 and ρ_0 are the equilibrium potential and the density, respectively.

The dispersive property originates from the coupled Poisson equation, which is a second-order elliptic partial differential equation.

Depending on the Poisson equation three different geometries could be considered.

Case (a): the infinitely long cylinder. The simplest solution of Poisson's equation is obtained concerning one-dimensional motion of the infinite fluid. The Poisson equation reads as

$$\frac{\partial^2 \phi}{\partial x^2} = \rho - v^2 \quad (1)$$

if rotation is present in the system, or

$$\frac{\partial^2 \phi}{\partial x^2} = \rho - 1 \quad (2)$$

if there is no rotation.

Hence, the geometry of the model is infinitely long cylinder, and the coordinate x corresponds to azimuthal one. In this model, the galaxy is considered as fluid with both rotation and pressure, assuming radial velocity component to be much less than azimuthal one, and $\Omega = \text{const}$.

We consider the density wave that propagates in the φ direction and approximate spatial derivative as

$$\frac{1}{r} \frac{\partial}{\partial \varphi} = \frac{\partial}{\partial x}. \quad (3)$$

Then, the set of equations that describes this model has the form

$$\frac{\partial \rho}{\partial t} + \frac{\partial}{\partial x}(\rho v) = 0 \quad (4)$$

$$\frac{\partial v}{\partial t} + v \frac{\partial v}{\partial x} = -K \gamma \rho^{\gamma-2} \frac{\partial \rho}{\partial x} - \frac{\partial \phi}{\partial x} \quad (5)$$

$$\frac{\partial^2 \phi}{\partial x^2} = \rho - v^2, \quad (6)$$

where v is the x component of the velocity and all variables are normalized as: $\rho = \rho_0 \bar{\rho}$, $p = 2\pi G \rho_0^2 R^2 \bar{p}$, $v = (2\pi G \rho_0^2)^{1/2} R \bar{v}$, $\phi = 2\pi G \rho_0^2 R^2 \bar{\phi}$, $x = R/\sqrt{2\bar{x}}$, $t = (2\pi G \rho_0^2)^{-1/2} \bar{t}$.

We have supposed polytropic fluid and that the variations of ρ and p take place adiabatically: $\frac{1}{\rho} \nabla p = \nabla(\frac{\gamma K}{\gamma-1} \rho^{\gamma-1})$ for $\gamma \neq 1$, or $\frac{1}{\rho} \nabla p = \nabla(K \log \rho)$ for $\gamma = 1$.

Case (b): infinitely thin disc. The model of Lin and Shu assumes delta function for the density in z -direction and approximates Poisson's equation by

$$\frac{\partial \phi(r, z=0)}{\partial r} = \pm 2\pi i G \sigma \quad (7)$$

in the vicinity of spiral arms, where σ represents surface mass density. Then, relation between surface density and two-dimensional potential is $\sigma = -\frac{k}{2\pi G} \phi(z=0)$, where $k = -\frac{i}{\phi} \frac{\partial \phi}{\partial r}$ (Lin & Shu 1964). Here, the geometry of the model is infinitely thin disc.

Within this approximation it is necessary to examine more complicated two-dimensional motion of the fluid model of the galaxy, but we simplified it neglecting the pressure. This simplification will have no influence on the possibility of deriving integrable non-linear equation.

In the cylindrical coordinates, the governing equations for two-dimensional fluid model describing the galaxy, are written as

$$\frac{\partial \rho}{\partial t} + \frac{1}{r} \frac{\partial}{\partial r}(r \rho v_r) + \frac{1}{r} \frac{\partial}{\partial \varphi}(\rho v_\varphi) = 0 \quad (8)$$

$$\frac{\partial v_r}{\partial t} + v_r \frac{\partial v_r}{\partial r} + \frac{v_r}{r} \frac{\partial v_\varphi}{\partial \varphi} - \frac{v_\varphi^2}{r} = -\frac{\partial \phi}{\partial r} \quad (9)$$

$$\frac{\partial v_\varphi}{\partial t} + v_r \frac{\partial v_r}{\partial r} + \frac{v_\varphi}{r} \frac{\partial v_\varphi}{\partial \varphi} + \frac{v_r v_\varphi}{r} = -\frac{1}{r} \frac{\partial \phi}{\partial \varphi} \quad (10)$$

$$\frac{1}{r} \frac{\partial}{\partial r} \left(r \frac{\partial \phi}{\partial r} \right) + \frac{1}{r^2} \frac{\partial^2 \phi}{\partial \varphi^2} + \frac{\partial^2 \phi}{\partial z^2} = 4\pi G \rho, \quad (11)$$

where v_r and v_φ are radial and azimuthal velocity components.

The last equation will be approximated using Lin and Shu asymptotic solution, and we use notation ρ for surface density. Coordinates r and φ are normalized by mean wavelength of the carrier wave in the radial direction $2\pi R/\lambda$, where R is the radial size of the galaxy and $\lambda \gg 1$ is a dimensionless constant from the Lin–Shu derivation, t by the period of the carrier wave $2\pi/\omega$, ρ by ρ_0 , both components of velocity by the phase velocity $\omega R/\lambda$, ϕ by $\omega^2 R^2/\lambda^2$ and G by $\omega^2 R/(2\rho_0 \lambda)$.

Case (c): thick disc. In this paper, we propose more realistic solution, introducing Gaussians in the z -direction instead of delta function, $f(z)$ for potential and $g(z)$ for density. Then, we can approximately express Poisson's equation in dimensionless form as follows:

$$A \nabla_\perp^2 \bar{\phi} + B \bar{\phi} = \bar{\rho}, \quad (12)$$

where $\bar{\phi}$, $\bar{\rho}$ are two-dimensional potential and density, respectively, normalized in the same way as in case (b), $A = a/(4Gc)$, $B = b/(4Gc)$ are constants dependent on the thickness of the disc L by way of a , b and c given by

$$a = \frac{1}{2L} \int_{-L}^L f(z) dz = f_1(L) \quad (13)$$

$$b = \frac{1}{2L} \int_{-L}^L f''(z) dz = f_2(L) \quad (14)$$

$$c = \frac{1}{2L} \int_{-L}^L g(z) dz = f_3(L) \quad (15)$$

and ∇_\perp^2 denotes two-dimensional Laplacian in the plane perpendicular to z . In order to find analytical solution, we assume $\nabla_\perp^2 \ll \frac{\partial^2}{\partial z^2}$, and $v_z \ll v_\perp$, which is correct as long as the disc is not too thick. Note that for $B = 0$ we can restore infinitesimally thin disc approximation, taking $g(z) = \delta(z)$. Governing equations in this case are the same as in case (b), only the Poisson equation (11) is replaced by equation (12).

3 LINEAR STABILITY ANALYSIS

Before making the choice of transformation of coordinates and expansion of variables in order to derive possible non-linear equation, it is necessary to discuss parameter regime. Linear dispersion relation is very useful since its form can suggest the type of the non-linear equation. We do it invoking linear stability analysis for each case. The wavenumber and density for each case is defined separately, although the same notation is used.

Case (a): concerning the gravitational force, there is known Jeans criterion for the stability of a finite spherical, non-rotating system with gravity and pressure (Jeans 1902) as

$$k^2 c^2 > 4\pi G \rho, \quad (16)$$

where k is the total wavenumber in radial direction, due to spherical symmetry, and c is the sound velocity. Jeans criterion is valid only locally, as long as the inhomogeneity of the system needs to be recognized. For a uniformly rotating infinite-length cylindrical column, Chandrasekhar proved that Jeans criterion is unaffected by rotation, except for modes with wave numbers perpendicular to the axis of rotation (Chandrasekhar 1981). In the previous section, perturbing and linearizing the system equations (4)–(6), assuming that all quantities are proportional to $e^{i(\omega t - kx)}$, we obtain the dispersion relation

$$(\omega - k)^2 k^2 + k^2 - \gamma k^4 - 2(\omega - k)k = 0. \quad (17)$$

Note that in this model gravitational instability is suppressed by the rotation, since we treat perturbations in azimuthal direction. Then, we consider only linearly stable waves in order to apply RPM (Jaffrey & Kawahara 1982) and to obtain the non-linear equation.

Case (b): For differentially rotating thin disc, linearizing equations (8)–(10), using equation (7) and assuming plane wave type variation as $f = f(r)e^{i(kr + m\varphi - \omega t)}$, we obtain the dispersion relation

$$(\omega - m\Omega)^2 = \kappa^2 - 2\pi G \rho_0 |k|, \quad (18)$$

where $\omega - m\Omega$ is Doppler-shifted frequency and κ is epicyclic frequency due to differential rotation

$$\kappa^2 = 2\Omega \left(2\Omega + r \left(\frac{d\Omega}{dr} \right) \right). \quad (19)$$

Equation (18) is the same as obtained by Lin & Shu (1964), but for pressureless medium. For a pressureless medium, $(\omega - m\Omega)$ becomes negative if

$$\kappa^2 < 0, \quad (20)$$

so the disc is unstable. This is the rotational instability due to exponentially growing departure of particles from circular orbits, and the growing rate is given by κ .

Stability parameter is defined by $k_2 = \frac{\kappa^2}{2\pi G \rho_0}$, so all waves with $k < k_2$ are purely stable. For this parameter regime, dark soliton solution was obtained (Kondoh, Teramoto & Yoshida 2000). The problem is that such consideration results in dark soliton solution with diminishing density, and has no spiral pattern. It is due to improper coordinate transformation used in reductive perturbation expansion.

Taking initial limitation on the wavenumber into account, namely $k > k_1$, where $k_1 = \max \left\{ \frac{1}{r}, \frac{\rho_0'(r)}{\rho_0(r)} \right\}$ (sign ' denotes derivative with respect to r), one finds that observational data suggests having $k_1 \approx k_2$ in real galaxy (Bertin 2000). Marginal stability, as introduced above in terms of local dispersion relation, identifies a very important condition for the basic state. In fact, if the system is far from it on the side of instability, then it is expected to be subject to rapidly growing perturbations, which are bound to change the properties of the basic state in a short dynamical time-scale. It is often said for this point of astrophysical applications, that violently unstable models are just the wrong choice of basic state (Bertin 2000), (Toomre 1964). Observed systems are generally well beyond such a transient dynamical state, or such a rapidly evolving dynamical state would be very hard to catch by the observer. On the other side of marginal

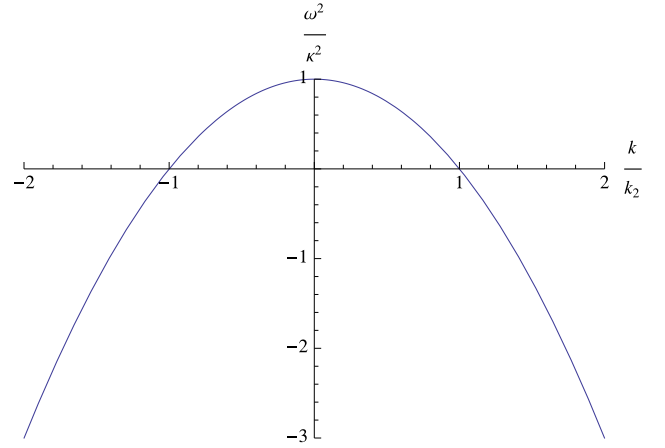


Figure 1. Marginal stability curve for the zero-thickness fluid model without pressure; ω^2 is Doppler-shifted frequency and is normalized by epicyclic frequency; wavenumber k is normalized by critical wavenumber k_2 ; part defined by $\frac{\omega^2}{\kappa^2} > 0$ is stable and for $\frac{\omega^2}{\kappa^2} < 0$ is unstable region.

stability, if the disc is well within a locally stable regime, not only would the local instabilities be absent, but wave propagation would also be inhibited altogether. Hence, the relevant regimes for the galaxy disc must be close to the threshold of instability (Fig. 1). In this case, new transformation of variables has to be introduced, different from the stable case (the reason is that in marginal stability frequency goes to zero, so group velocity becomes infinite).

Before taking thickness of the disc into account, it is necessary to underline two points. First, the sign of wavenumber can be positive or negative (equation 18) defining two possible branches of waves, leading and trailing. An important effect that might distinguish between these two branches is differential rotation. Density waves are propagated primarily by gravitational forces, but they would be modified by differential rotation, if the non-linear terms, omitted in linear description, were included. This effect is similar to that of fluid motion that leads to the distortion of acoustic waves. In that case, a density decrease in the direction of wave propagation tends to be accentuated into compression shock, while a density decrease would tend to be smoothed out by the motion of fluid. Thus, only the trailing waves are stable in the presence of non-linear effects. Next, inspecting the dispersion relation for gaseous disc when the pressure cannot be neglected, there is additional term $c^2 k^2$. However, pressure and differential rotation work in the same way, balancing the non-linearity. That means, omitting the pressure, the general conclusion on the non-linear effects is not reduced; it is just modified through the parameters related with dispersive and non-linear terms.

Case (c): finite thickness of the disc is responsible for the different value of critical wavenumber due to appearance of parameters A and B in Poisson's equation (12). It will result in the more complex dispersion relation, comparing to one obtained in Lin–Shu model, for the zero-thickness fluid model. Dispersion relation in this case has a form

$$(\omega - m\Omega)^2 = \kappa^2 - \frac{4\pi G \rho_0 m \hat{k}^2}{1 + \hat{k}^2}, \quad (21)$$

where $\hat{k}^2 = \frac{k^2}{n}$, and $m = 1/A$, $n = 1/B$.

Marginal stability criterion holds for this case as well, so the coordinate transformation can be used in the same way as for thin disc. Non-linear equation will be of the same type as for thin disc,

but with different coefficients of non-linear and dispersive terms. Using those coefficients, one can control the validity of applied finite thickness approximation, comparing with observed values for the galaxies.

4 NON-LINEAR EQUATIONS

In the previous section, we have summarized instabilities that are possible to occur in different galaxy models. Using WKJB analysis, Lin and Shu have proposed that gravitational instability is the basis for formation of the spiral pattern in the infinitesimally thin disc galaxies. Proposed theory resolved winding dilemma problem, assuming that the matter in the galaxy can maintain density waves through gravitational interaction in the presence of a differential rotation (even neglecting pressure). How density waves can persist quasi-stationary for a long time, remains unresolved. Several authors searched for different possible mechanisms that can replenish waves (Toomre 1969; Mark 1976; Bertin et al. 1989), but still there is no complete understanding. One possibility could be derivation of non-linear equation, that has stable soliton solution, mainly because that approach avoids involvement of some other objects which additionally complicate analysis.

We try to overcome that difficulty just keeping the higher order terms in perturbation expansions, which were omitted in linear approach, deriving the non-linear equation with localized solution. Such solutions exist whenever dispersive effects are counterbalanced by non-linear effects and coherent structure can be formed. The Korteweg de Vries (KdV) and the non-linear Schrodinger (NLS) equation are expressions of that balancing. Some of these coherent structures are stable and have been found experimentally (Mitchell & Driscoll 1996).

In order to obtain either of these two equations, we introduce asymptotic, RPM, which has been developed for non-linear dispersive wave problem (Jaffrey & Taniuti 1964). The scale transformation,

$$\xi = \epsilon^\alpha (x - \lambda t), \quad \tau = \epsilon^\beta t, \quad (22)$$

introduced by Gardner and Morikawa, may be derived from the linearized asymptotic behaviour of long waves (Jaffrey & Taniuti 1964). Using combination of this transformation of coordinates with a perturbation expansion of the dependent variables, one can obtain single non-linear equation (KdV or NLS). This type of perturbation has generally been developed and formulated by Taniuti and his collaborators (Jaffrey & Taniuti 1964).

Case (a): we transform coordinates and expand variables as

$$\xi = \epsilon^{1/2} (x - Vt), \quad \tau = \epsilon^{3/2} t \quad (23)$$

$$\rho = 1 + \sum_{n=1}^{\infty} \sum_{m=-\infty}^{\infty} \epsilon^n \rho^{(n,m)}(\xi, \tau) E, \quad (24)$$

$$v = 1 + \sum_{n=1}^{\infty} \sum_{m=-\infty}^{\infty} \epsilon^n v^{(n,m)}(\xi, \tau) E, \quad (25)$$

$$\phi = \sum_{n=1}^{\infty} \sum_{m=-\infty}^{\infty} \epsilon^n \phi^{(n,m)}(\xi, \tau) E, \quad (26)$$

where ϵ is a small parameter, $E = e^{i(\omega t - kx)}$ with k belonging to the linearly stable domain discussed in the previous section for this case

and V is group velocity. Set of equations is obtained from the lowest order of $\epsilon^{3/2}$:

$$v^{(1,0)} = \frac{1}{2} \rho^{(1,0)}, \quad \phi^{(1,0)} = \frac{1 - 4K\gamma}{4} \rho^{(1,0)}, \quad V = \frac{3}{2}. \quad (27)$$

KdV-type equation is obtained from the order of $\epsilon^{5/2}$, as following:

$$\frac{\partial}{\partial \tau} \phi^{(1,0)} + \frac{3}{1 - 4K\gamma} \phi^{(1,0)} - \frac{1 - 4K\gamma}{8} \frac{\partial^3}{\partial \xi^3} \phi^{(1,0)} = 0. \quad (28)$$

This type of non-linear equation has a solution in the form:

$$\phi(\xi, \tau) = \phi_\infty + a \operatorname{sech}^2 \left[(\xi - V\tau) \left(\frac{a}{12b} \right)^{1/2} \right], \quad (29)$$

where ϕ_∞ denotes the boundary value of $\phi^{(1,0)}$ at $(\xi - V\tau) \rightarrow \pm\infty$, a is amplitude of the wave relative to the constant solution ϕ_∞ at infinity, $b = \frac{27}{8(1-4K\gamma)^2}$ and V is the speed of the soliton. The solution of such non-linear equation represents the soliton, stable and localized solution, which, although derived under certain assumptions, can be used as a control parameter in numerical simulations. Also, it can be understood as a kind of equilibrium that could be perturbed and create some new structures. This soliton is travelling along azimuthal direction creating the ring structure. The width of the soliton b represents the width of the ring and could be used to compare properties of the obtained structure with the properties of observed rings.

Case (b): as we mentioned in the previous section, a new transformation of variables has to be introduced for this case, according to Watanabe (Watanabe 1969), contrary to the stable case (the reason is that frequency goes to zero in marginal stability, so group velocity becomes infinite). Stretched coordinates and expansion of variables in this case are given as

$$\xi = \epsilon(\tau - cr), \quad \eta = \epsilon^2 r, \quad (30)$$

where $\tau = t + \Omega\varphi$. Consequently, spatial and time derivatives will be

$$\frac{\partial}{\partial r} = -\epsilon c \frac{\partial}{\partial \xi} + \epsilon^2 \frac{\partial}{\partial \eta}, \quad \frac{\partial}{\partial \tau} = \epsilon \frac{\partial}{\partial \xi}, \quad (31)$$

together with $\frac{1}{r} = \epsilon^2 \frac{1}{\eta}$.

Variable expansions have the form

$$\rho = \rho_0 + \sum_{n=1}^{\infty} \sum_{m=-\infty}^{\infty} \epsilon^n \rho^{(n,m)}(\xi, \eta) E, \quad (32)$$

$$v_r = \sum_{n=1}^{\infty} \sum_{m=-\infty}^{\infty} \epsilon^n v^{(n,m)}_r(\xi, \eta) E, \quad (33)$$

$$v_\varphi = r\Omega + \sum_{n=1}^{\infty} \sum_{m=-\infty}^{\infty} \epsilon^n v^{(n,m)}_\varphi(\xi, \eta) E, \quad (34)$$

where $E = e^{i(kr - \omega\tau)}$.

Substituting equations (30) and (31) into equations (8)–(10) with respect to equation (7), we derive non-linear equation following procedure of RPM. We separate terms with respect to the order of small parameter ϵ as follows:

$$\epsilon^1 : m = 0, \quad v^{1,0}_\varphi = a_1 \rho^{1,0}, \quad a_1 = \frac{-i\pi G}{\Omega}, \quad v^{1,0}_r = 0; \quad (35)$$

$$m = 1, \quad \omega^2 = \kappa^2 - 2\pi G \rho_0 k, \quad v^{1,1}_r = a_2 \rho^{1,1}, \quad a_2 = \frac{-\omega}{k\rho_0}, \quad (36)$$

$$v_{\phi}^{1,1} = a_3 \rho^{1,1}, \quad a_3 = \frac{-i\kappa^2}{2\Omega k \rho_0}. \quad (37)$$

$$\epsilon^2 : m = 0, \quad \rho^{1,0} = 0, \quad v_{\phi}^{2,0} = a_4 \rho^{2,0}, \quad a_4 = \frac{-i\pi G}{\Omega}, \quad (38)$$

$$v_r^{2,0} = a_5 \rho^{1,1}, \quad a_5 = \frac{2\omega}{k \rho_0^2}; \quad (39)$$

$$m = 1, \quad \frac{\partial \omega}{\partial k} = \frac{\pi G \rho_0}{\omega} = c, \quad \rho^{2,1} = 0, \quad (40)$$

$$v_r^{2,1} = b_1 \frac{\partial}{\partial \xi} \rho^{1,1}, \quad b_1 = \frac{\rho_0 c a_2 - 1}{i \rho_0 k}, \quad (41)$$

$$v_{\phi}^{2,1} = b_2 \frac{\partial}{\partial \xi} \rho^{1,1}, \quad b_2 = \frac{a_3 - \frac{\kappa^2}{2\Omega} b_1}{i \omega}; \quad (42)$$

$$m = 2, \quad v_r^{2,2} = b_3 (\rho^{1,1})^2, \quad b_3 = \frac{\frac{1}{2} i k a_2^2 + \frac{1}{2} \frac{k \Omega}{\omega} a_2 a_3 + \frac{i \pi G k}{\omega} a_2}{i \omega + \frac{\kappa^2}{4 i \omega} - \frac{i \pi G k \rho_0}{\omega}}, \quad (43)$$

$$\rho^{2,2} = b_4 (\rho^{1,1})^2, \quad b_4 = \frac{k}{\omega} a_2 + \frac{\rho_0 k}{\omega}, \quad (44)$$

$$v_{\phi}^{2,2} = b_5 (\rho^{1,1})^2, \quad b_5 = \frac{1}{2} \frac{k}{\omega} a_2 a_3 - \frac{\kappa^2}{4 i \omega \Omega} b_3; \quad (45)$$

$$\epsilon^3 : m = 0, \rho^{2,0} = 0; \quad m = 1, \frac{\omega}{2\pi G} b_2 + \frac{2\Omega}{2i\pi G} b_3 = b_1; \quad (46)$$

From equation (46), after substituting all coefficients, we obtain the NLS equation:

$$i \frac{\partial}{\partial \eta} \rho^{1,1} + P \frac{\partial^2}{\partial \xi^2} \rho^{1,1} + Q |\rho^{1,1}|^2 \rho^{1,1} = 0, \quad (47)$$

where $P = -\frac{k_2}{\kappa^2} = \frac{1}{2} \frac{\partial^2 k}{\partial \omega^2} < 0$, and $Q = -\frac{3}{2} \frac{\kappa^2}{k_2 \rho_0^2} < 0$, which implies $PQ > 0$ and consequently bright soliton solution. The solution of equation (47) has the form:

$$\rho^{1,1}(\xi, \eta) = \rho_a \frac{e^{i\psi}}{ch \left(\sqrt{\frac{Q}{2P}} \rho_a (\xi - 2P\eta) \right)}, \quad (48)$$

$$\psi = P \left(\frac{Q}{2P} \rho_a^2 - 1 \right) \eta + \xi. \quad (49)$$

Here, ρ_a is relative amplitude of the soliton, its velocity of travel is the coefficient P , $\sqrt{Q/2P} \rho_a$ is the width of the soliton, all in dimensionless units, and ψ is the phase.

Going back to the original coordinates, we have obtained solitary structure with enhanced density along the spiral, which explains the observed pattern (Fig. 2). The solitary solution resolves the main difficulty from the linear theory is removed, e.g. the problem of searching for generators of spiral wave and mechanism that maintain waves for a long time-scale (quasi-stationarity assumption). Also, it is likely that the transport of the mass by solitons away from the considered region of the disc into outer regions will keep the disc in a state close to the threshold of stability for a long time. This fact might be responsible for the relative stability of the spiral structure as a whole. Finally, this solution provides a fine oscillatory structure inside the soliton, with a space period much smaller than the width

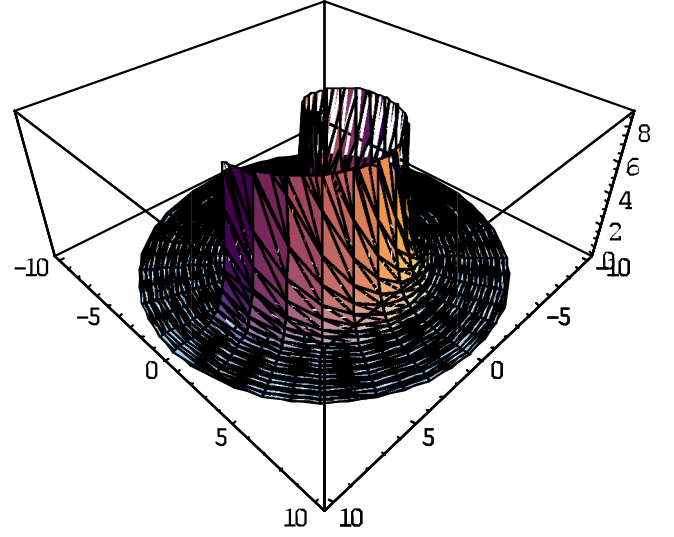


Figure 2. Bright soliton solution.

of the soliton. This property could explain the appearance of large density gradients within spiral arms, responsible for understanding the star formation process.

In order to make some rough estimates for the arms of the Galaxy in the neighbourhood of the Solar system, we take the following values from the observations: mass density in the disc $(1-3)10^{-24} \text{ g cm}^{-3}$, thickness of the flat system $(0.1-0.2) \text{ kpc}$, which implies surface density $(3-5)10^{-4} \text{ g cm}^{-2}$, half-width of the arm 0.5 kpc , enhancement of the mean density in the arm $\approx 5/100$, which implies $\rho_a \approx 0.3$, $\Omega \approx 10^{-15} \text{ 1/s}$, and $\kappa \approx \sqrt{2}\Omega$. Then, equation (48) indicates that group velocity of the soliton is $P = 3 \times 10^5 \text{ cm s}^{-1}$. A more detailed comparison of the observed structures with our proposed model would request solving the non-linear integro-differential equations involving the boundary conditions at the centre.

Case (c): we extend non-linear analysis in the more realistic case, taking finite thickness effect into account. It will result in the dispersion relation (21), in a contrast with the Lin-Shu model, where dispersion relation is linear with respect to k . Resulting non-linear equation will be of the same type as in case (b), but with different coefficients of non-linear and dispersive terms. Using those coefficients, one can control the validity of used finite thickness approximation, comparing it to the observed galactic parameters.

We transform coordinates as in case (b), invoking again physical restrictions for the galaxy (marginal stability case), and expanding variables in the same way, but we have approximated the potential using Poisson's equation given by equation (12), as follows:

$$\phi = -\frac{r^2 \Omega^2}{2} + \sum_{n=1}^{\infty} \sum_{m=-\infty}^{\infty} \epsilon^n \phi^{(n,m)}(\xi, \eta) e^{i(kr - \omega\tau)}. \quad (50)$$

Here, spatial and time derivatives are

$$\frac{\partial}{\partial r} = -\epsilon c \frac{\partial}{\partial \xi} + \epsilon^2 \frac{\partial}{\partial \eta}, \quad \frac{\partial}{\partial \tau} = \epsilon \frac{\partial}{\partial \xi}. \quad (51)$$

Following the same procedure as in case (b), one obtains the NLS equation

$$i \frac{\partial}{\partial \eta} \rho^{1,1} + W \frac{\partial^2}{\partial \xi^2} \rho^{1,1} + Z |\rho^{1,1}|^2 \rho^{1,1} = 0, \quad (52)$$

but in this case coefficients related to dispersive and non-linear terms, $W = -\frac{k_2}{n\kappa^2}$ and $Z = -\frac{3}{2}\frac{n\kappa^2}{k_2\rho_0}$ will be dependent on the thickness of the disc n . Since those coefficients give velocity and width of the soliton, respectively, comparing with observed structure, it is possible to evaluate when the finite thickness approximation is necessary to be involved for the given galaxy. Comparing these two soliton parameters for zero-thickness model and finite thickness model, one finds that spiral arm in the first case is wider than in the latter one. It is expectable because the same material amount would be redistributed taking vertical direction into account. Also, the fact that the same type of non-linear equation is obtained is in agreement with the linear stability analysis.

5 SUMMARY AND CONCLUSION

In this paper, we have studied weakly non-linear dynamics of different galaxy models, using RPM, with the primary emphasis on possible soliton solutions. Linear stability analysis of different galaxy models, which is necessary for defining parameter regime, has been conducted. We have studied the influence of finite-thickness of the galaxy disc on dispersive properties of the system. We underline that the purpose of this paper is not to describe full galactic dynamics but rather to derive possible non-linear equation which has stable localized solution for simplified models. The soliton existence gives physical answer for the permanent density wave phenomenon as a balance between the tendency of the dispersion to propagate the wave inwards, and non-linearity that tends to hold it up. This type of solution is useful for comparison with numerical simulations that treat more realistic models and with the observations, or for evaluation of dominance of each mechanism that occurs in real galaxy. We have not treated terms which we have already found that would not influence the type of the non-linear equation; for example, pressure, that undoubtedly exists in most galaxies, would not change the necessary and sufficient conditions for derivation of integrable non-linear equation. It will change only the parameters of non-linear and dispersive term, giving better agreement with observed patterns. In one-dimensional model, KdV type of non-linear equation has been derived. For a twodimensional model, using Lin–Shu approximation, the NLS equation has been derived. The solution is bright soliton propagating along the spiral. We have extended two-dimensional analysis for galaxies solving Poisson’s equation in a different manner and obtain NLS equation. The last one is with different coefficients for non-linear and dispersive terms, which means different properties of soliton. The first type of non-linear equation, namely KdV, is applicable as long as the azimuthal velocity is dominant, together with the assumption of relatively thick disc. In that case, the ring shape could be formed, with restriction that certain structure cannot be formed at any distance from the galactic centre, but the radial distance is defined by restriction $\ll \frac{1}{r} \frac{\partial}{\partial \varphi} = \frac{m}{r}$, where m is positive integer and could be understood as number of rings. The second type of non-linear equation, namely NLS, is applicable when radial and azimuthal components of motions are coupled, as long as $\frac{1}{kr} \ll 1$. The last restriction is related with the condition

of the finite amplitude perturbations. We have shown that derived velocity of the soliton is in good agreement with the observations. The advantage of the second type is fine structure inside the solitary envelope, that might be used to explain any process within spiral arms with scales shorter than the width of soliton. Comparing soliton properties with observational data, it is possible to control validity of the approximation that was made for each model. However, neither of these models is able to explain stretched structures, such as barred or elliptical galaxies. It would be very interesting to investigate the transient models, the dynamical scale on which the thickness of the galaxy changes and consequently, change the structure. If there is any correlation between the age of the galaxies and their thickness, how does it evolve? There is the remaining problem of the inner part of galaxy with the singularity in the centre, that would also be interesting to consider in non-linear regime. Both aspects will be treated in further research.

ACKNOWLEDGEMENTS

The author thanks Dr Vazha Bereziani for discussing the connection between the linear and non-linear regime, and Dr Vladimir Cadez for constructive questioning the linear stability and equilibrium states. Part of this work was supported by Monbukagakusho (Monbusho) Scholarship.

REFERENCES

- Bertin G., 2000, Dynamics of Galaxies. Cambridge Univ. Press, Cambridge
- Bertin G., Lin C. C., Lowe S. A., Thurstans R. P., 1989, ApJ, 338, 104
- Binney J., 2012, MNRAS, 426, 1328
- Bratek L., Jalocha J., Kutschera M., 2008, MNRAS, 391, 1373
- Chandrasekhar S., 1981, Hydrodynamic and Hydromagnetic Stability, Dover Press, New York
- El-Zanta A. A., Haß lera B., 1998, New Astron., 3, 493
- Heinemann T., Papaloizou J. C. B., 2012, MNRAS, 419, 1085
- Jaffrey A., Kawahara T., 1982, Asymptotic Methods in Nonlinear Wave Theory. Pitman, Boston, MA, p. 70
- Jaffrey A., Taniuti T., 1964, Non-linear Wave Propagation: with Applications to Physics and Magnetohydrodynamics. Academic Press, New York
- Jeans J. H., 1902, Phil. Trans. R. Soc., 199A, 49
- Kondoh S., Teramoto R., Yoshida Z., 2000, Phys. Rev. E, 61, 5710
- Lin C. C., Bertin G., 1995, Ann. New York Acad. Sci., 773, 125
- Lin C. C., Shu F. H., 1964, ApJ, 140, 646
- Lindblad B., 1963, Stockholm Obser. Ann., 22, 3
- Mark J. W. -K., 1976, ApJ, 205, 363
- Mitchell T. B., Driscoll C. F., 1996, Phys. Fluids, 8, 1828
- Norman C. A., 1978, MNRAS, 182, 457
- Sellwood J. A., 1985, MNRAS, 217, 127
- Sellwood J. A., 1986, MNRAS, 221, 213
- Toomre A., 1964, ApJ, 139, 1217
- Toomre A., 1969, ApJ, 158, 899
- Wada K., Meurer G., Norman C. A., 2002, ApJ, 577, 197
- Watanabe T., 1969, Phys. Soc. Japan, 27, 1341

This paper has been typeset from a \LaTeX file prepared by the author.

The scattering mean free path of cosmic ray particles in isotropic damped plasma wave turbulence

M. Vukcevic^{1,2}

¹ Institut für Theoretische Physik, Lehrstuhl IV: Weltraum- und Astrophysik, Ruhr-Universität Bochum, 44780 Bochum, Germany
 e-mail: vuk.mira@gmail.com

² University of Defence, Military Academy, Pavla Jurisica Sturma 33, 11000 Belgrade, Serbia

Received 30 January 2013 / Accepted 3 May 2013

ABSTRACT

An analytical expression for the mean free path of single-charged cosmic ray particles, especially for positrons, is derived in isotropic plasma wave turbulence, where the crucial scattering of cosmic ray particles with small pitch-angle cosines is caused by resonant cyclotron interactions with oblique magnetosonic waves. In this calculation, viscous damping effects are included, which results in broadening of the resonance function. It is demonstrated that including resonance function broadening ensures a finite mean free path for cosmic ray energies, for which previously reported types of turbulence predicted an infinitely large mean free path.

Key words. scattering

1. Introduction

A Galactic bulge-to-disk ratio of the luminosity of diffuse 511 keV positron annihilation radiation is, as measured by INTEGRAL, four times larger than a stellar bulge to disk ratio of the Galactic supernovae (SNe). SNe are thought to be the principal source of the annihilating positrons. This large discrepancy has started a search for new sources. It has been shown that the measured 511 keV luminosity ratio can be understood well in the context of a Galactic SN origin when the differential propagation of these MeV positrons in the various phases of the interstellar medium is taken into consideration (Higdon et al. 2009), since these relativistic positrons must first slow down to energies less than 10 eV before they can annihilate.

A large number of potential sources have been proposed over the years: cosmic ray interaction with the interstellar medium (Ramaty et al. 1970), pulsars (Sturrock 1971), radioactive nuclei produced in SN (Clayton 1973), compact objects (Ramaty & Lingelfelter 1979), dark matter (Boehm 2004), and microquasars (Guessoum et al. 2006). Some of these theories either are problematic or have a wide range of uncertainties. For example, the predicted distributions of positrons from radionuclei synthesized in SN are only marginally compatible with observations (Milne et al. 2002). However, the recent mapping of the Galaxy at 511 KeV (Knödlseider et al. 2005) has placed severe constraints on the possible positron sources.

On the other hand, the positron excess in Galactic cosmic ray positrons above 10 GeV has been confirmed by PAMELA (Adriani et al. 2009). The most recent confirmation of the PAMELA result on positrons in the Galaxy cosmic ray spectrum has just been published (Aguilar et al. 2013). There are several astrophysical explanations for possible sources of these positrons, such as dark matter annihilation (Hooper et al. 2009) or decay (Arvanitaki et al. 2009). According to a recent investigation (Pohl & Eichler 2009), Fermi measurements of the high-latitude γ -ray background (Abdo et al. 2009) constrain

a decaying-dark-matter origin for the GeV Galactic positron anomaly measured by PAMELA.

To quantify scattering mean free paths for MeV interstellar positrons, an analytic approximation has been used (Teufel & Schlickeiser 2002) for slab-like dynamical turbulence, which predict that is a mean free path in MeV energies proportional to $r^{1/3}$, where r is defined as particle rigidity. This model for GeV particles predicts an infinitely large mean free path. The other slab plasma-wave turbulence model (Schlickeiser et al. 2010), which is more plausible when compared to the dynamical one, predicts an infinite positron scattering mean free path at MeV energies, while it has finite values proportional to $r^{1/3}$ for GeV energies.

Here, we propose a damped plasma wave turbulence model, which can assure a finite mean free path for MeV and GeV positrons, and compare our result with results of previously mentioned models.

A key parameter for the cosmic ray transport is the parallel spatial diffusion coefficient $\kappa = v\lambda/3$, which is conventionally expressed in terms of the mean free path λ along the background magnetic field and the particle speed v . In many studies, the parallel mean free path also controls the perpendicular spatial diffusion coefficient $\kappa_{\perp} = \alpha\kappa_{\parallel}$, which is assumed to be proportional to κ_{\parallel} due to the lack of a rigorous theory of perpendicular diffusion. When discussing the ratio of perpendicular and parallel mean free path, it has been published from proton observations that $0.02 < \lambda_{\perp}/\lambda_{\parallel} < 0.083$ over the rigidity range of $0.5MV < R < 5GV$ (Palmer 1982), which assures parallel mean free path values to be high enough that we can neglect the perpendicular component. Hereafter, we only consider parallel mean free path.

The scattering mean free path is the result of resonant particle-wave interactions of cosmic ray particles with the turbulent component of cosmic magnetic fields, and thus depends on the nature and geometry of cosmic turbulent magnetic fields (Schlickeiser 2002). Many observations of plasma turbulence

in the solar wind indicate that the turbulent magnetic field is a mixture of slab (i.e., parallel to the ordered background magnetic field) waves, a dominating 2D component (Bieber et al. 1996) with a negligible contribution to particle scattering (Shalchi & Schlickeiser 2004), and obliquely propagating magnetosonic waves that reveal through electron density fluctuations because of their compressive nature. In the static magnetosonic limit, the scattering rate from the 2D component vanishes (Shalchi & Schlickeiser 2004).

For small amplitude waves, an appreciable interaction between a wave and a particle arises only when the particle is moving at nearly the parallel wave phase speed. The interaction is resonant and the subsequent physics is close to that of Fermi acceleration: particles with v_{\parallel} slightly greater than ω/k_{\parallel} suffer a trailing collision with a wave compression and slow down, while particles with v_{\parallel} slightly less than ω/k_{\parallel} are stuck by a compression and speed up. This process could be called resonant Fermi acceleration, but the usual term is transit-time acceleration or transit-time damping (TTD). The name is given because the resonance condition can be rewritten as $\lambda_{\parallel}/v_{\parallel} \approx t$, where t is the wave period and $\lambda_{\parallel} = 2\pi/k_{\parallel}$ is the parallel wavelength. That means a wave and a particle will interact strongly when the particle transit time across the wave compression is approximately equal to the period.

Schlickeiser & Miller (1998) and Schlickeiser & Vainio (1999) have investigated the quasilinear interactions of charged particles with Alfvén and magnetosonic plasma modes. A cosmic ray particle of given velocity v , Lorentz factor $\gamma = (1 - (v^2/c^2))^{-1/2}$, pitch angle cosine $\mu = v_{\parallel}/v$, mass m , the speed of light c , charge $q_i = e|Z_i|Q$ with $Q = \text{sgn}(Z_i)$, and gyrofrequency $\Omega_c = Q\Omega$ with $\Omega = q_i B_0/(mc\gamma)$ interacts with waves whose wavenumber k , cosine of propagation angle $\eta = k_{\parallel}/k$, and real frequency f obey the resonance condition $f(k) = v\mu k\eta + n\Omega_c$ for entire $n \in [-\infty, \infty]$. For slab ($\eta = 1$) Alfvén waves, only gyroresonant interactions with $n = 1$ are possible. In contrast, the $n = 0$ resonance for obliquely propagating fast magnetosonic waves, which do not include gyroresonance interactions ($n \neq 1$), is possible due to their compressive magnetic field component. The $n = 0$ interactions are referred to as transit-time damping (TTD). Using $n = 0$ the resonance condition requires the parallel cosmic ray velocity $v\mu = f/(k\eta)f/k \simeq V_A$ to be greater than the finite phase velocity of magnetosonic waves, which is given by the Alfvén speed. TTD interactions therefore only occur for cosmic ray particles with pitch-angle cosines $\mu > |V_A/v| = \epsilon$. At these pitch angle cosines, TTD interactions provide most of the particle scattering.

Thus, the crucial scattering in small μ is provided for energetic particles by only gyroresonances with slab plasma waves and oblique magnetosonic waves (Schlickeiser et al. 2010):

$$\lambda = \frac{3v}{8} \int_{-\epsilon}^{\epsilon} d\mu \frac{(1 - \mu^2)}{D_{\mu\mu}^{\text{slab}}(\mu) + D_{\mu\mu}^{\text{g-ms}}(\mu)} \simeq \frac{3V_A}{4[D_{\mu\mu}^{\text{slab}}(0) + D_{\mu\mu}^{\text{g-ms}}(0)]}. \quad (1)$$

According to Schlickeiser & Miller (1998), the magnetosonic contribution $D_{\mu\mu}^{\text{g-ms}}(0) \simeq \epsilon D_{\mu\mu}^{\text{slab}}(0)$ for energetic particles ($\epsilon \ll 1$) is much smaller than the slab contribution for similar turbulence power spectra of slab and magnetosonic waves. However, this latter reduction is not justified for cosmic ray positrons with Lorentz factors $\gamma < m_p/m_e = 1836$. These positrons no LH polarized slab waves to find resonantly interact with, so that $D_{\mu\mu}^{\text{slab}}(0) \rightarrow 0$. In this case, the contribution from gyroresonant interactions with magnetosonic waves provides small but finite scattering (Schlickeiser et al. 2010).

It is the purpose of this work to involve oblique magnetosonic waves and quantitatively investigate the influence of wave damping on the quasilinear scattering mean free paths of cosmic rays, especially for positrons with Lorentz factors $\gamma < m_p/m_e = 1836$. In a plasma in rough equipartition of kinetic and magnetic pressure, oblique magnetosonic waves are expected to be overdamped by Landau absorption (Fedorenko 1992). Thus, the second-order Fermi acceleration using oblique fast magnetosonic waves cannot work in a plasma in rough equipartition (Achterberg 1979). It is possible to overcome this difficulty either by considering that this mechanism works, in the interstellar medium with small β (relatively cold medium) or by including the finite wave cascading that exists in the interstellar medium. Due to the large amplitude of interstellar turbulence, there is no doubt that wave cascading exists and will then transfer this spectral energy to higher wavenumbers. One property of the diffusion equation for isotropic turbulence (Eq. (11.3.6), Schlickeiser 2002) is that it yields finite positive wave spectral energy densities at all wavenumbers k , even if the net damping rate is negative in some wavenumber intervals.

We show then that the inclusion of resonance broadening caused by wave damping in the resonance function guarantees that the transit-time damping contribution holds at small pitch angle cosines $\mu \leq |V_A/v|$, unlike the case of negligible wave damping (Vukcevic & Schlickeiser 2007). We expect that TTD makes an overwhelming contribution to particle scattering because the cosmic ray particle interacts with the whole wave spectrum in this interaction. This contrasts gyroresonances that single out individual resonant wave numbers (Schlickeiser 2003). However, quantitative analysis of gyroresonance contribution in damped plasma wave turbulence will be studied in a separate, forthcoming investigation. Therefore we only consider the TTD-contribution to particle scattering in the following and assume $n = 0$ both in the resonance function and in the calculation of the Fokker-Planck coefficients.

In Sect. 2, we present the general plasma wave turbulence and relevant magnetohydrodynamic plasma modes. In Sect. 3, we calculate the Fokker-Planck coefficient for fast mode waves and discuss relevant domains for application to cosmic ray positrons. In Sect. 4, we derived the Fokker-Planck coefficient for slow mode waves. The analytical expressions of a mean free path for fast and slow plasma waves and the comparison with different previously reported turbulence models are given in Sect. 5. The summary and conclusion are presented in the last section.

2. Plasma wave turbulence

According to our discussion in the paragraph above and in the two paragraphs after Eq. (1), the relevant mean free path for the positrons with Lorentz factor $\gamma < m_p/m_e = 1836$ in small pitch-angle cosine becomes

$$\lambda \simeq \frac{3V_A}{4D_{\mu\mu}^{\text{TTD}}(0)}. \quad (2)$$

Hereafter, we omit TTD notation and keep only notation for relevant magnetosonic waves. The Fokker-Planck coefficient $D_{\mu\mu}$ is computed by employing the Kubo formula (Kubo 1957),

$$D_{\mu\mu} = \int_0^{\infty} dt \langle \dot{\mu}(t) \dot{\mu}(0) \rangle. \quad (3)$$

The pitch-angle variation $\mu(t)$ is obtained from the Newton-Lorentz equation:

$$\dot{\mu} = \frac{\Omega \sqrt{1-\mu^2}}{B_0} \left[\frac{c}{v} \sqrt{1-\mu^2} \delta E_{\parallel} + \frac{i}{\sqrt{2}} \left[e^{i\phi} \left(\delta B_r + i\mu \frac{c}{v} \delta E_r \right) - e^{-i\phi} \left(\delta B_l - i\mu \frac{c}{v} \delta E_l \right) \right] \right]. \quad (4)$$

In these equations, we use pitch-angle cosine μ , the particle speed v , the gyrophase ϕ , the cosmic ray particle gyrofrequency in the background field B_0 and the turbulent fields $\delta B_{l,r}$ and $\delta E_{l,r}$, which are related to the left-handed and right-handed polarized field components. The term δE_{\parallel} is parallel component relative to the background magnetic field.

The simplest method to calculate $D_{\mu\mu}$ is the application of perturbation theory (Jokipii 1966). In this case, we have applied a quasilinear approximation for a fluctuating electric and magnetic field, a quasistationary turbulence condition, and the existence of a finite correlation time t_c . The last two assumptions guarantee a diffusive behavior of transport (Shalchi & Schlickeiser 2004). The assumption of homogeneous turbulence will imply that the turbulence fields at different wavevectors are uncorrelated.

Next, we define the properties of the plasma turbulence that will be considered. We follow the approach for the electromagnetic turbulence that represents the Fourier transforms of the magnetic and electric field fluctuations as a superposition of N individual weakly damped plasma modes of frequencies:

$$\omega = \omega_j(\mathbf{k}) = \omega_{R,j}(\mathbf{k}) - i\gamma_j(\mathbf{k}), \quad (5)$$

where $j = 1, \dots, N$, which can have both the real and imaginary parts with $|\gamma_j| \ll |\omega_{R,j}|$, so that

$$[\mathbf{B}(\mathbf{k}, t), \mathbf{E}(\mathbf{k}, t)] = \sum_{j=1}^N [\mathbf{B}^j(\mathbf{k}), \mathbf{E}^j(\mathbf{k})] e^{-i\omega_j t}. \quad (6)$$

Damping of the waves is counted with a positive $\gamma^j > 0$.

In the case we consider here, the time integration of the Fokker-Planck coefficient $D_{\mu\mu}$ yields the Lorentzian resonance function:

$$\mathcal{R}_j(\gamma_j) = \int_0^\infty du e^{-i(k_{\parallel}v_{\parallel} + \omega_{R,j} + n\Omega)u - \gamma_j u} = \frac{\gamma_j(\mathbf{k})}{\gamma_j^2(\mathbf{k}) + [k_{\parallel}v_{\parallel} + \omega_{R,j}(\mathbf{k}) + n\Omega]^2}. \quad (7)$$

The detailed derivation of the Fokker-Planck coefficient for this case (vanishing magnetic helicity and isotropic turbulence) is performed in the PhD Thesis of Vukcevic (2007), which contrasts the case of negligible damping $\gamma \rightarrow 0$ (Schlickeiser 2001) in which the use of the δ -function representation

$$\lim_{\gamma \rightarrow 0} \frac{\gamma}{\gamma^2 + \xi^2} = \pi \delta(\xi), \quad (8)$$

reduces the resonance function (7) to sharp δ -functions,

$$\mathbf{R}^j(\gamma = 0) = \pi \delta(k_{\parallel}v_{\parallel} + \omega_{R,j} + n\Omega). \quad (9)$$

Next, it is necessary to specify the geometry of the plasma wave turbulence itself through the correlation tensors, which will be adopted throughout this work in the form (Mattheus & Smith 1981) of

$$P_{\alpha\beta}^j(\mathbf{k}) = \frac{g_i^j(\mathbf{k})}{k^2} \left[\delta_{\alpha\beta} - \frac{\mathbf{k}_{\alpha} k_{\beta}}{k^2} + i\sigma(\mathbf{k}) \epsilon_{\alpha\beta\lambda} \frac{k_{\lambda}}{k} \right], \quad (10)$$

where $\sigma(\mathbf{k})$ is the magnetic helicity and the function $g(\mathbf{k})$ determines different turbulence geometries. This was to illustrate the result, although this model is not in accord with the known polarization properties of fast-mode waves at oblique angles.

2.1. Relevant magnetohydrodynamic plasma modes

It has been already emphasized that there is no TTD for shear Alfvén waves (Teufel et al. 2003) in the case of negligible damping, and the gyroresonant interactions provided by shear Alfvén waves is small compared to the same contribution provided by fast magnetosonic waves (Vukcevic & Schlickeiser 2007). As a consequence, we consider only fast and slow magnetosonic waves.

2.1.1. Fast magnetosonic plasma modes

For the fast plasma modes, we use a simplified dispersion relation,

$$\omega_R \simeq jkV_A, \quad (11)$$

which is relevant at wavenumbers $k_c \ll k \ll \xi k_c$, where $k_c = \omega_{p,i}/c$ is the inverse ion skin length, and $\xi = \sqrt{m_p/m_e} = 43$.

In the dispersion equation, forward ($j = 1$) and backward ($j = -1$) moving fast mode waves are described. The associated electric field and magnetic field polarizations are (Dogan et al. 2006)

$$\delta E_L = -\delta E_R, \quad \delta E_{\parallel} = 0, \quad \delta B_L = \delta B_R, \quad \delta B_{\parallel} \neq 0. \quad (12)$$

2.1.2. Slow magnetosonic plasma modes

The dispersion relation for slow magnetosonic waves in low- β plasma reads (Dogan et al. 2006)

$$\omega_R^2 \simeq k^2 V_A^2 \left(\frac{\eta^2 \beta}{1 + \beta} + \frac{\eta^4 \beta^2}{(1 + \beta)^3} \right) \quad (13)$$

with $\eta = \cos \theta$ and β as the ratio of thermal and magnetic pressure. In the last equation, we neglect the second term in brackets in the first approximation, since it is one order smaller than the first term. The associated electric field and magnetic field polarizations are

$$\delta E_L = -\delta E_R, \quad \delta E_{\parallel} = 0, \quad \delta B_L = \delta B_R, \quad \delta B_{\parallel} \neq 0. \quad (14)$$

Consideration of the dispersion relation in high frequencies could change the result, since we expect nondispersive effects in that range. The polarization of the waves in that domain could also affect the transport coefficients through the correlation tensors. However, a detailed inspection of the dispersion relation in the high-frequency domain is needed to draw a quantitative conclusion, and it will be discussed in a separate investigation.

2.2. Damping rate

The damping of magnetosonic waves is caused by both collisionless Landau damping and collisional viscous damping and by Joule damping and ion-neutral friction. The dominant contribution is provided by viscous damping with the rate calculated

for plasma parameters of the diffuse intercloud medium (Spanier & Schlickeiser 2005)

$$\gamma_F = \frac{1}{12} \beta V_A^2 \tau_i k^2 [\sin^2 \theta + 5 \times 10^{-9} \cos^2 \theta] \\ = 2.9 \times 10^5 \beta V_A^2 k^2 [\sin^2 \theta + 5 \times 10^{-9} \cos^2 \theta] \quad (15)$$

in terms of the ion-ion collisional time $\tau_i = 3.5 \times 10^6$ s. Except at very small propagation angles, the second term in Eq. (15) is negligible, and we infer

$$\gamma_F \simeq 2.9 \times 10^5 \beta V_A^2 k^2 \sin^2 \theta = \alpha_F k^2 \sin^2 \theta, \quad (16)$$

where $\alpha_F = \frac{1}{12} \beta V_A^2 \tau_i$.

3. Fast mode waves

With Eqs. (11) and (16), the resonance function (7) for forward and backward moving fast mode waves becomes

$$\mathcal{R}_F^j(n) = \frac{\alpha_F k^2 \sin^2 \theta}{(\alpha_F k^2 \sin^2 \theta)^2 + [kv\mu \cos \theta + jV_A k + n\Omega]^2}, \quad (17)$$

which describes both gyroresonant ($n \neq 0$) and transit-time damping ($n = 0$) wave-particle interactions.

The non-vanishing parallel magnetic field component $B_{\parallel} \neq 0$ (see Eq. (12)) of fast mode waves allows TTD interactions with $n = 0$, so that we proceed with $n = 0$. The resonance function (17) becomes

$$\mathcal{R}_F^j(0) = \frac{\alpha_F k^2 \sin^2 \theta}{(\alpha_F k^2 \sin^2 \theta)^2 + [kv\mu \cos \theta + jV_A k]^2} \\ = \frac{\alpha_F (1 - \eta^2)}{(\alpha_F k (1 - \eta^2))^2 + [v\mu\eta + jV_A]^2}. \quad (18)$$

Throughout this work, we consider isotropic turbulence $g^j(\mathbf{k}) = g^j(k)$. Modifications due to different turbulence geometries are possible and will be the subject of further analysis (in particular anisotropic turbulence).

For energetic cosmic ray particles with $v \gg V_A$, the pitch-angle Fokker-Planck coefficient then simplifies as

$$D_{\mu\mu}^F \simeq \frac{\Omega^2}{4B_0^2} (1 - \mu^2) \sum_{j=\pm 1} \int_{-\infty}^{\infty} dk \int_{-1}^1 d\eta \mathcal{R}_F^j(0) g^j(k) J_1^2(W) (1 + \eta^2), \quad (19)$$

where $J_1(W)$ is a Bessel function with the argument $W = \frac{v}{|\Omega|} \cdot k_{\perp} \sqrt{1 - \mu^2} = R_L \cdot k_{\perp} \sqrt{1 - \mu^2}$ that involves the ray Larmor radius $R_L = v/|\Omega|$.

We further simplify Eq. (19) by assuming equal intensity of forward and backward waves (a vanishing cross helicity of each plasma mode):

$$g^+(k) = g^-(k) = \frac{1}{2} g_{\text{tot}}(k), \quad (20)$$

which reads as

$$D_{\mu\mu}^F \simeq \frac{\Omega^2}{8B_0^2} (1 - \mu^2) \sum_{j=\pm 1} \int_{-\infty}^{\infty} dk \int_{-1}^1 d\eta \mathcal{R}_F^j(0) g_{\text{tot}}^j(k) J_1^2(W) (1 + \eta^2). \quad (21)$$

To illustrate our results, we adopt a Kolmogorov-type power law dependence on $g^j(k)$ above and below some minimum and maximum wavenumber k_{\min} and k_{\max} , respectively

$$g_{\text{tot}}(k) = g_{\text{tot}} k^{-q} \quad (22)$$

for $k_{\min} < k < k_{\max}$.

The magnetic energy density in wave component j is given by

$$(\delta B_j)^2 = \int_0^{\infty} dk g^j(k) \quad (23)$$

which implies

$$g_{\text{tot}} = (q - 1)(\delta B)^2 / (k_{\min}^{1-q} - k_{\max}^{1-q}) \simeq (q - 1)(\delta B)^2 k_{\min}^{q-1} \quad (24)$$

for $k_{\max} \gg k_{\min}$.

With Eqs. (22), (23), (24) the pitch-angle Fokker-Planck coefficient $D_{\mu\mu}^F$ reads as

$$D_{\mu\mu}^F \simeq \frac{\Omega^2}{4B_0^2} (q - 1)(\delta B)^2 k_{\min}^{q-1} (1 - \mu^2) \int_{k_{\min}}^{k_{\max}} dk k^{-q} \\ \int_{-1}^1 d\eta \mathcal{R}_F(0) J_1^2(W) (1 + \eta^2). \quad (25)$$

Now, we must approximate the resonance function (Eq. (18)). In doing this, we consider two cases:

- a) $\eta < \eta_c$;
- b) $\eta > \eta_c$,

where $\epsilon = V_A/v$ and $\eta_c = \epsilon/\mu$. The parameter η_c divides the integration domain with respect to η , in which either V_A , $v\mu\eta$ or both values are relevant. By using $D_{\mu\mu}^F(-\mu) = D_{\mu\mu}^F(\mu)$ and the substitution $s = R_L k \sqrt{1 - \mu^2}$ and $R_L = v/|\Omega|$, we derive

$$D_{\mu\mu}^F \simeq \alpha_F (q - 1) (k_{\min} R_L)^{q-1} \left(\frac{\delta B}{B_0} \right)^2 (1 - \mu^2)^{\frac{q+1}{2}} \int_{k_{\min} R_L \sqrt{1 - \mu^2}}^{\infty} ds s^{-q} \\ \times \left[\int_0^{\min(1, \epsilon/\mu)} d\eta (1 - \eta^4) J_1^2 \left(s \sqrt{1 - \eta^2} \right) \frac{1}{\frac{\alpha_F^2 (1 - \eta^2)^2 s^2}{R_L^2 (1 - \mu^2)} + V_A^2} \right. \\ \left. + \int_{\min(1, \epsilon/\mu)}^1 d\eta (1 - \eta^4) J_1^2 \left(s \sqrt{1 - \eta^2} \right) \frac{1}{\frac{\alpha_F^2 (1 - \eta^2)^2 s^2}{R_L^2 (1 - \mu^2)} + (v\mu\eta)^2} \right]. \quad (26)$$

3.1. High values of $\mu > \epsilon$

For large pitch-angles $\mu > \epsilon$ we obtain

$$D_{\mu\mu}^F(\mu > \epsilon) \simeq \frac{(q - 1)}{\alpha_F} (k_{\min} R_L)^{q-1} \left(\frac{\delta B}{B_0} \right)^2 (1 - \mu^2)^{\frac{q+3}{2}} \\ \times \int_{k_{\min} R_L \sqrt{1 - \mu^2}}^{\infty} ds s^{-q} \left[\int_0^{\epsilon/\mu} d\eta (1 - \eta^4) J_1^2 \left(s \sqrt{1 - \eta^2} \right) \right. \\ \left. + \frac{1}{(1 - \eta^2)^2 s^2 + \frac{R_L^2 (1 - \mu^2) V_A^2}{\alpha_F^2}} + \int_{\epsilon/\mu}^1 d\eta (1 - \eta^4) J_1^2 \left(s \sqrt{1 - \eta^2} \right) \right. \\ \left. \times \frac{1}{(1 - \eta^2)^2 s^2 + \frac{R_L^2 (1 - \mu^2) (v\mu\eta)^2}{\alpha_F^2}} \right]. \quad (27)$$

3.2. Small values $\mu < \epsilon$

This case is important when treating damped waves. For the small pitch-angles $\mu < \epsilon$, we obtain

$$D_{\mu\mu}^F(\mu < \epsilon) \simeq \alpha_F(q-1)(k_{\min}R_L)^{q-1} \left(\frac{\delta B}{B_0}\right)^2 (1-\mu^2)^{\frac{q+1}{2}} \times \int_{k_{\min}R_L}^{\infty} \frac{ds s^{-q}}{\sqrt{1-\mu^2}} \left[\int_0^1 d\eta (1-\eta^4) J_1^2\left(s\sqrt{1-\eta^2}\right) \times \frac{1}{\frac{\alpha_F^2(1-\eta^2)^2 s^2}{R_L^2(1-\mu^2)} + V_A^2} \right]. \quad (28)$$

We have already discussed that inclusion of resonance broadening due to wave damping in the resonance function guarantees dominance of transit-time damping. The main contribution of wave damping comes exactly in the region $|\mu| < \epsilon$ that is relevant for deriving the spatial diffusion coefficient and related mean free path, both of which are given by the average over μ of the inverse of $D_{\mu\mu}$. Therefore, we can further consider only the case $D_{\mu\mu}(\mu = 0)$, which simplifies the analysis enormously and reads as

$$D_{\mu\mu}^F(\mu = 0) \simeq \frac{\Omega^2(q-1)R_L^2}{4\alpha_F}(k_{\min}R_L)^{q-1} \left(\frac{\delta B}{B_0}\right)^2 \int_{k_{\min}R_L}^{\infty} ds s^{-q} \times \int_0^1 d\eta (1-\eta^4) J_1^2\left(s\sqrt{1-\eta^2}\right) \frac{1}{(1-\eta^2)^2 s^2 + \frac{V_A^2 R_L^2}{\alpha_F^2}}. \quad (29)$$

In the last equation, $s = kR_L$, and each term under integration is dimensionless.

4. Slow mode waves

With Eqs. (13) and (16), the resonance function (7) for slow mode waves becomes

$$\mathcal{R}_S^j(n) = \frac{2.9 \times 10^5 \beta V_A^2 k^2 \sin^2 \theta}{(2.9 \times 10^5 \beta V_A^2 k^2 \sin^2 \theta)^2 + \left[kv\mu \cos \theta + jV_A k\eta \sqrt{\frac{\beta}{1+\beta}} + n\Omega \right]^2}. \quad (30)$$

The non-vanishing parallel magnetic field component $B_{\parallel} \neq 0$ (see Eq. (14)) of slow mode waves allows TTD interactions with $n = 0$, so that we proceed with $n = 0$. The resonance function (30) becomes

$$\mathcal{R}_S^j(0) = \frac{2.9 \times 10^5 \beta V_A^2 k^2 \sin^2 \theta}{(2.9 \times 10^5 \beta V_A^2 k^2 \sin^2 \theta)^2 + \left[kv\mu \cos \theta + jV_A k\eta \sqrt{\frac{\beta}{1+\beta}} \right]^2} = \frac{\alpha_F \sin^2 \theta}{(\alpha_F k \sin^2 \theta)^2 + \left[v\mu \cos \theta + jV_A \eta \sqrt{\frac{\beta}{1+\beta}} \right]^2}, \quad (31)$$

where α_F is the same as in the fast mode case.

Following the same procedure for fast mode waves in Sect. 3, we assume (20), (22), (23), and imply (24). We derive

$$D_{\mu\mu}^S \simeq \frac{\Omega^2}{4B_0^2} (1-\mu^2) \sum_{j=\pm 1} \int_{-\infty}^{\infty} dk \int_{-1}^1 d\eta \mathcal{R}_S^j(0) g^j(k) J_1^2(W) \times \left[(1+\eta^2) \left(1 + \mu^2 \epsilon^2 \eta^2 \frac{\beta}{1+\beta} \right) - 4\mu j\epsilon \eta \sqrt{\frac{\beta}{1+\beta}} \right], \quad (32)$$

which can be simplified if we consider the energetic cosmic ray particles $v \gg V_A$, or namely, the last two terms, to be small (order of ϵ and ϵ^2) and neglected. Then, we obtain the same expression as in the case for fast mode waves:

$$D_{\mu\mu}^S \simeq \frac{\Omega^2}{4B_0^2} (q-1)(\delta B)^2 k_{\min}^{q-1} (1-\mu^2) \int_{k_{\min}}^{k_{\max}} dk k^{-q} \times \int_{-1}^1 d\eta \mathcal{R}_S(0) J_1^2(W) (1+\eta^2). \quad (33)$$

Next, we have to approximate the resonance function for slow mode waves. As in the fast mode case, there are two cases:

$$\text{a) } \eta < \eta_c^S;$$

$$\text{b) } \eta > \eta_c^S,$$

where

$$\eta_c^S = \frac{\epsilon}{\mu} \frac{\beta}{1+\beta}. \quad (34)$$

Note that $\eta_c^S < \eta_c^F$. Using $D_{\mu\mu}^S(-\mu) = D_{\mu\mu}^S(\mu)$ and the substitution $s = R_L k \sqrt{1-\mu^2}$, we derive

$$D_{\mu\mu}^S \simeq \alpha_F(q-1)(k_{\min}R_L)^{q-1} \left(\frac{\delta B}{B_0}\right)^2 (1-\mu^2)^{\frac{q+1}{2}} \times \int_{k_{\min}}^{\infty} R_L \frac{ds s^{-q}}{\sqrt{1-\mu^2}} \left[\int_0^{\min\left(1, \frac{\epsilon}{\mu} \frac{\beta}{1+\beta}\right)} d\eta (1-\eta^4) \times J_1^2\left(s\sqrt{1-\eta^2}\right) \frac{1}{\frac{\alpha_F^2(1-\eta^2)^2 s^2}{R_L^2(1-\mu^2)} + V_A^2 \eta^2 \frac{\beta}{1+\beta}} + \int_{\min\left(1, \frac{\epsilon}{\mu} \frac{\beta}{1+\beta}\right)}^1 d\eta (1-\eta^4) J_1^2\left(s\sqrt{1-\eta^2}\right) \frac{1}{\frac{\alpha_F^2(1-\eta^2)^2 s^2}{R_L^2(1-\mu^2)} + (v\mu\eta)^2} \right], \quad (35)$$

where $\epsilon = V_A/v$.

4.1. High values of $\mu > \epsilon$

For large pitch-angles $\mu > \epsilon$ we obtain

$$D_{\mu\mu}^S(\mu > \epsilon) \simeq \frac{(q-1)}{\alpha_F} (k_{\min}R_L)^{q-1} \left(\frac{\delta B}{B_0}\right)^2 (1-\mu^2)^{\frac{q+3}{2}} \times \int_{k_{\min}}^{\infty} R_L \sqrt{1-\mu^2} ds s^{-q} \times \left[\int_0^{\frac{\epsilon\beta}{\mu(1+\beta)}} d\eta (1-\eta^4) J_1^2\left(s\sqrt{1-\eta^2}\right) \times \frac{1}{(1-\eta^2)^2 s^2 + \frac{R_L^2(1-\mu^2)V_A^2 \eta^2 \frac{\beta}{1+\beta}}{\alpha_F^2}} + \int_{\frac{\epsilon\beta}{\mu(1+\beta)}}^1 d\eta (1-\eta^4) J_1^2\left(s\sqrt{1-\eta^2}\right) \times \frac{1}{(1-\eta^2)^2 s^2 + \frac{R_L^2(1-\mu^2)(v\mu\eta)^2}{\alpha_F^2}} \right]. \quad (36)$$

4.2. Low values of $\mu < \epsilon$

This case is important for treating damped waves for the same reason as discussed for fast mode waves (Sect. 3). For the small pitch-angles $\mu < \epsilon$, we obtain

$$D_{\mu\mu}^S(\mu < \epsilon) \simeq \alpha_F(q-1)(k_{\min}R_L)^{q-1} \left(\frac{\delta B}{B_0}\right)^2 (1-\mu^2)^{\frac{q+1}{2}} \times \int_{k_{\min}} R_L \sqrt{1-\mu^2} ds s^{-q} \times \left[\int_0^1 d\eta (1-\eta^4) J_1^2 \left(s \sqrt{1-\eta^2} \right) \frac{1}{\frac{\alpha_F^2(1-\eta^2)^2 s^2}{R_L^2(1-\mu^2)} + V_A^2 \eta^2 \frac{\beta}{1+\beta}} \right], \quad (37)$$

or for $\mu = 0$, we read

$$D_{\mu\mu}^S(\mu = 0) \simeq \frac{\Omega^2(q-1)R_L^2}{4\alpha_F} (k_{\min}R_L)^{q-1} \left(\frac{\delta B}{B_0}\right)^2 \int_{k_{\min}} R_L^\infty ds s^{-q} \left[\int_0^1 d\eta (1-\eta^4) J_1^2 \left(s \sqrt{1-\eta^2} \right) \frac{1}{(1-\eta^2)^2 s^2 + \frac{V_A^2 \eta^2 \frac{\beta}{1+\beta} R_L^2}{\alpha_F^2}} \right]. \quad (38)$$

In the last equation, $s = kR_L$.

5. Cosmic ray mean free path

5.1. Fast mode waves

In this section, we calculate the mean free path, which is connected with the spatial diffusion coefficient through

$$\lambda = \frac{3\kappa}{v} = \frac{3v}{4} \int_0^1 d\mu \frac{(1-\mu^2)^2}{D_{\mu\mu}}. \quad (39)$$

For the case in which we are interested, we can write

$$\lambda^{0F} = \frac{3\kappa}{v} = \frac{3v}{4} \frac{1}{D_{\mu\mu}(\mu=0)} \int_0^\epsilon d\mu = \frac{3}{4} \frac{V_A}{D_{\mu\mu}^F(\mu=0)} = 3 \frac{\alpha_F}{(q-1)V_A} (k_{\min}R_L)^{1-q} \left(\frac{B_0}{\delta B}\right)^2 \frac{1}{G}, \quad (40)$$

where

$$G = \int_{k_{\min}R_L}^\infty ds s^{-q} \int_0^1 d\eta (1-\eta^4) J_1^2 \left(s \sqrt{1-\eta^2} \right) \times \frac{1}{(1-\eta^2)^2 s^2 + \frac{V_A^2 R_L^2}{\alpha_F^2}}. \quad (41)$$

Now, we consider two limits: $k_{\min}R_L \ll 1$, and $k_{\min}R_L \gg 1$, where $k_{\min}R_L = T = E$ and is normalized with respect to $E_c = T_c = \frac{k_c}{k_{\min}} m_e c^2$. Expressing $k_{\min} = L_{\max}/2\pi$ in the terms of the longest wavelength of isotropic fast mode waves, $k_c = \Omega_{0,e}/v_A = \omega_{p,e}/c$ and for following plasma conditions ($v_A = 33.5 \frac{\text{km}}{\text{s}}$, $\frac{B_0}{\delta B} = 1$, Beck 2007), $T_c = 10.7 n_e^{1/2} (\frac{L_{\max}}{10 \text{ pc}}) \times 10^9 \text{ MV}$). For these values, the particle mean free path is measured by $\lambda_1 = \frac{9\alpha_F}{V_A} (\frac{B_0}{\delta B})^2$. We have used interplanetary plasma conditions that have been used in both models (Schlickeiser et al. 2010; Teufel & Schlickeiser 2002) for comparison. We note that for interstellar medium plasma conditions, λ_1 is one or two orders of magnitude larger than for interplanetary conditions, which is also a reasonable value.

For $k_{\min}R_L \gg 1$:

This case is treated in detail in Appendix A, where we derive

$$G(T \gg 1) = \frac{2}{5} \frac{10^{-14}}{q} T^{-(q+2)}, \quad (42)$$

$$\lambda^{0F}(T \gg 1) = \frac{15\alpha_F}{V_A} \frac{q}{q-1} \left(\frac{B_0}{\delta B}\right)^2 10^{14} T^3. \quad (43)$$

At relativistic rigidities, we find that $\lambda^0 \sim T^3$. As we consider certain positron energies 1–100 GeV, this case is not relevant. For $k_{\min}R_L \ll 1$:

This case is treated in detail in Appendix A, where we derive

$$G(T \ll 1) = \frac{1}{3} \frac{1}{q-1} T^{1-q}, \quad (44)$$

$$\lambda^{F0}(T \ll 1) = \frac{9\alpha_F}{V_A} \left(\frac{B_0}{\delta B}\right)^2. \quad (45)$$

In this energy limit, the mean free path is constant with respect to T , which is relevant for considered positron energies.

5.2. Slow mode waves

In this subsection, we calculate the mean free path which is connected with the spatial diffusion coefficient through

$$\lambda^S = \frac{3\kappa^S}{v} = \frac{3v}{4} \int_0^1 d\mu \frac{(1-\mu^2)^2}{D_{\mu\mu}^S}. \quad (46)$$

For the case for which we are interested, we can write

$$\lambda^{S0} = \frac{3\kappa^S}{v} = \frac{3v}{4} \frac{1}{D_{\mu\mu}^S(\mu=0)} \int_0^\epsilon d\mu = \frac{3}{4} \frac{V_A}{D_{\mu\mu}^S(\mu=0)} = 3 \frac{\alpha_F}{(q-1)V_A} (k_{\min}R_L)^{1-q} \left(\frac{B_0}{\delta B}\right)^2 \frac{1}{G}, \quad (47)$$

where

$$G = \int_{k_{\min}R_L}^\infty ds s^{-q} \int_0^1 d\eta (1-\eta^4) J_1^2 \left(s \sqrt{1-\eta^2} \right) \times \frac{1}{(1-\eta^2)^2 s^2 + \frac{V_A^2 \eta^2 \frac{\beta}{1+\beta} R_L^2}{\alpha_F^2}}. \quad (48)$$

We consider two limits: $k_{\min}R_L \ll 1$, and $k_{\min}R_L \gg 1$, where $k_{\min}R_L = T = E$ and is normalized with respect to E_c .

For $k_{\min}R_L \gg 1$:

This case is treated in detail in Appendix B, where we derive

$$G(T \gg 1) = \frac{\sqrt{2}}{\pi} \frac{|b/(b-1)| + |\log(1-b)|}{qp^2} T^{-(q+2)}, \quad (49)$$

$$\lambda^{0S}(T \gg 1) = \frac{3\alpha_F}{\sqrt{2}V_A} \frac{q}{(q-1)} \left(\frac{B_0}{\delta B}\right)^2 \times \frac{\pi p^2}{|b/(b-1)| + |\log(1-b)|} T^3, \quad (50)$$

where $T = k_{\min}R_L$ and $b \ll 1$.

At relativistic rigidities, we find that $\lambda^{0S} \sim T^3$.

For $k_{\min}R_L \ll 1$:

This case is treated in detail in Appendix B, where we derive

$$G(T \ll 1) = \frac{1}{3} \frac{1}{q-1} T^{1-q}, \quad (51)$$

$$\lambda^{0S}(T \ll 1) = \frac{9\alpha_F}{V_A} \left(\frac{B_0}{\delta B}\right)^2. \quad (52)$$

In this energy domain, the mean free path is constant with respect to T , which is important for cosmic ray positrons with Lorentz factor $\gamma < m_p/m_e = 1836$. Although the mean free path for slow magnetosonic waves has the same expression as in the case for fast waves for energies less than T_c , the low energy limit here is caused by plasma- β (Appendix B). However, it is always less than T_c and does not violate previous conditions.

The turbulence model considered in this paper ensures that all energy particles below the T_c value are scattered by the proposed resonant interaction.

Considering dynamical magnetic slab turbulence and random sweeping slab turbulence (Teufel & Schlickeiser 2002), there is a sharp cutoff of the turbulence power spectrum at k_{\min} . The consequence is that the mean free path for all particles with energies higher than 10^{10} eV with typical parameters rapidly grows and becomes larger than the size of ambient interstellar medium. For the slab plasma waves model (Schlickeiser et al. 2010) at rigidities less than 2×10^8 eV, the positron mean free path becomes infinitely large. It is because these positrons find no LH polarized slab waves with which to resonantly interact. In the turbulence model proposed in this paper, the positron mean free path does not depend on energy, in domain from 10^5 eV to 10^{12} eV.

The comparison of our result with previously reported turbulence models are given in Fig. 1, where the mean free path is in units of $\lambda_1 = 0.2\beta$ AU (AU = 1.5×10^{13} cm). To interpret the MeV positrons propagation and explain their diffusion, the model of the dynamical turbulence can be applied. However, this model fails to explain transport mechanisms for energetic positrons with energies of 100 GeV. In contrast, the slab gyroresonant plasma wave turbulence model is able to hold on energetic GeV positrons but fails in explaining the transport properties of MeV positrons. The isotropic damped magnetosonic plasma wave turbulence model, which is proposed in this paper, seems to be more plausible, since it covers energies in both domains. This model could be used in modeling turbulence that scatters positrons, resolving the problems stated by the results of either the INTEGRAL or PAMELA experiments.

The inclusion of viscous damping implies either steep turbulence spectra ($q > 2.4$) for isotropic turbulence with fixed values of k_{\max} and k_{\min} , or the existence of high wavenumber cutoff for isotropic turbulence with a spectral index $q = 5/3$ (Spanier & Schlickeiser 2005). To justify the use of k_{\max} and k_{\min} in our model, it is necessary to assume turbulence with a spectral index that is not less than 2.4. This value is higher than the Kolmogorov value of $5/3$ (Kolmogorov 1941) or Kraichan-Iroshnikov value of $3/2$ (Kraichnan 1965), but both theories consider an inertial range, where damping effects have been neglected. Interstellar medium has strong damping features, which does not mean that there is no inertial range. It could be that there is an intermediate regime between the inertial and dissipation range. Thus, the request for steep turbulence spectra is not in contradiction to neither Kolmogorov theory, or our calculation, in which there is only a restriction on q to be greater than 1.

The broadening of the resonance function could also be insured by nonlinear treatment of the specific turbulence model. Nonlinear theory (second order theory of Shalchi 2005) applied to the magnetostatic slab model (Shalchi et al. 2009) would lead to a broadened resonance function that is similar to the one obtained for the random sweeping model, which is linear (Teufel & Schlickeiser 2002). We have already mentioned that this linear model could be used to explain MeV positrons but fails for GeV positrons. Thus, we expect, at least mathematically, that

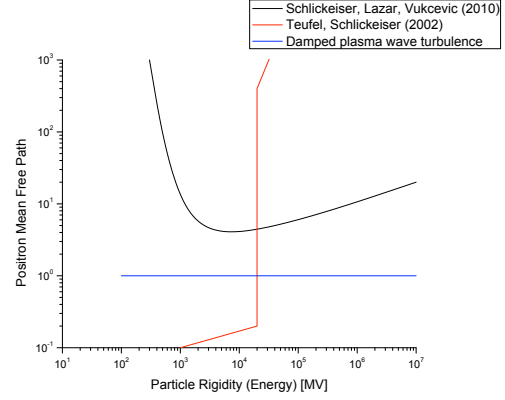


Fig. 1. The positron mean free path. The black line represents the mean free path obtained using the slab turbulence model and gyroresonant interactions, which exhibit a cutoff at particle energies less than 2×10^8 eV. The red line is the mean free path obtained using the dynamical magnetic slab turbulence, or the random sweeping slab turbulence model, which exhibit a sharp cutoff at particle energies of 10^{10} eV. The blue line is the mean free path obtained using isotropic magnetosonic damped plasma wave turbulence, which remains constant for particle energies from 10^5 eV to 10^{12} eV. All mean free paths are normalized with respect to the λ_1 value.

inclusion of nonlinear effects to the slab model would have the cutoff at the same wavenumbers as in the random sweeping linear model. However, it would be useful to compare timescales of nonlinear effects and damping effects within the same turbulence model, in order to make a general conclusion on the importance of each of them.

6. Summary and conclusion

We have investigated the implications of isotropically distributed interstellar damped plasma waves on the scattering mean free path on the cosmic ray positrons with a Lorentz factor $\gamma < m_p/m_e = 1836$. We show that inclusion of resonance broadening due to wave damping in the resonance function guarantees that dominance of transit-time damping also holds for cosmic ray particles at small pitch angle cosines $\mu \leq |V_a/v|$, unlike the case of negligible wave damping.

For small rigidities, or consequently low energies $T < T_c$, the mean free path is constant with respect to energy. The mean free path at high energies $T > T_c$ approaches a much steeper dependence, namely $\lambda \sim T^3$ for both fast and slow waves.

It is difficult to draw any general conclusion on the ratio of fast and slow modes mean free path, since there is an integral dependence on the pitch angle and the plasma-beta parameter are mixed in the latter case. For cold plasma, the mean free path of slow mode merges to the mean free path of the fast one, as expected. However, this turbulence model is able to ensure scattering of the cosmic ray positrons with Lorentz factor $\gamma < m_p/m_e = 1836$ via resonant interaction.

Appendix A: Evaluation of the function G for fast mode waves

The task is to calculate the function G (41):

$$G = \int_{k_{\min} R_L}^{\infty} ds s^{-q} \int_0^1 d\eta (1 - \eta^4) J_1^2 \left(s \sqrt{1 - \eta^2} \right) \times \frac{1}{(1 - \eta^2)^2 s^2 + \frac{V_A^2 R_L^2}{\alpha_F^2}}. \quad (\text{A.1})$$

First, it is possible to evaluate the term $\frac{V_A^2 R_L^2}{a_F^2} \sim 10^{14}$ for used plasma parameters (Sect. 5). We then evaluate G in two energy limits.

Case $G(k_{\min} R_L \gg 1)$

For energies $T \gg 1$ we substitute $s = xT$. Then, (A.1) reads as

$$\begin{aligned} G &= \int_1^\infty dx x^{-q} T^{-(1+q)} \int_0^1 d\eta (1-\eta^4) J_1^2 \left(xT \sqrt{1-\eta^2} \right) \\ &\times \frac{1}{(1-\eta^2)^2 x^2 + 10^{14}} = T^{-(1+q)} \int_1^\infty dx x^{-q} \\ &\times \left(\int_0^{1-\frac{1}{2xT}} d\eta (1-\eta^4) \right) \frac{1}{\pi xT \sqrt{1-\eta^2}} \frac{1}{(1-\eta^2)^2 x^2 + 10^{14}} \\ &+ \int_{1-\frac{1}{2xT}}^1 d\eta (1-\eta^4) \frac{1}{4} x^2 T^2 (1-\eta^2) \\ &\times \frac{1}{(1-\eta^2)^2 x^2 + 10^{14}} \Big), \end{aligned} \quad (\text{A.2})$$

where we use the approximations of Bessel functions for large and small arguments (Abramowitz & Stegun 1972):

$$J_\nu(z \gg 1) \approx \sqrt{\frac{2}{\pi \nu z}} \cos \left(\nu z - \frac{(2\nu+1)\pi}{4} \right), \quad (\text{A.3})$$

implying

$$\begin{aligned} J_1^2(z \gg 1) &= \frac{1}{\pi xT \sqrt{1-\eta^2}} \left(1 - \sin \left(2xT \sqrt{1-\eta^2} \right) \right) \\ &\approx \frac{1}{\pi xT \sqrt{1-\eta^2}} \end{aligned} \quad (\text{A.4})$$

($1/\xi \gg \sin \xi/\xi$) for the argument, $z = xT \ll 1$, and

$$J_\nu(z \ll 1) \approx \frac{(z/2)^\nu}{\Gamma(\nu+1)}, \quad (\text{A.5})$$

implying

$$J_1^2(z \ll 1) = \frac{1}{4} x^2 T^2 (1-\eta^2) \quad (\text{A.6})$$

for the argument $z = xT \gg 1$. We then obtain

$$\begin{aligned} T^{(1+q)} G(T \gg 1) &= \frac{T^2}{4} \int_1^\infty dx x^{-q+2} \int_{1-\frac{1}{2xT}}^1 d\eta (1-\eta^4) \\ &\frac{(1-\eta^2)}{(1-\eta^2)^2 x^2 + 10^{14}} \\ &+ \frac{1}{\pi T} \int_1^\infty dx x^{-(q+1)} \int_0^1 d\eta \frac{(1-\eta^4)}{\sqrt{1-\eta^2}} \frac{1}{(1-\eta^2)^2 x^2 + 10^{14}} \\ &- \frac{1}{\pi T} \int_1^\infty dx x^{-(q+1)} \int_{1-\frac{1}{2xT}}^1 d\eta \frac{(1-\eta^4)}{\sqrt{1-\eta^2}} \frac{1}{(1-\eta^2)^2 x^2 + 10^{14}} = \\ &I_3 + I_1 - I_2. \end{aligned} \quad (\text{A.7})$$

Next, we simplify further, namely keeping only terms with respect to $1-\eta$ of the lowest order, and we evaluate each integral:

$$\begin{aligned} I_2 &= \frac{1}{\pi T} \int_1^\infty dx x^{-(q+1)} \int_0^{\frac{1}{2xT}} dm \frac{4m}{\sqrt{2m}} \frac{1}{4m^2 x^2 + 10^{14}} \\ &= \frac{2}{3} \frac{10^{-14}}{\pi(q+3/2)} T^{-\frac{5}{2}}, \end{aligned} \quad (\text{A.8})$$

where we substitute $m = 1-\eta$.

$$I_3 = \frac{T^2}{4} \int_1^\infty dx x^{-q+2} \int_0^{\frac{1}{2xT}} dm 4m \frac{2m}{10^{14}} = \frac{1}{12} \frac{10^{-14}}{q} T^{-1}, \quad (\text{A.9})$$

where we have used the same substitution as in the previous case and where $10^{14} \gg 4m^2 x^2$. We note that $I_2 \ll I_3$.

$$I_1 = \frac{1}{\pi T} \int_1^\infty dx x^{-(q+1)} \int_0^1 d\eta \frac{(1-\eta^4)}{\sqrt{1-\eta^2}} \frac{1}{10^{14}} = \frac{5}{16} \frac{10^{-14}}{q} \frac{1}{T}. \quad (\text{A.10})$$

Combining all these three integrals, we obtain

$$G(T \gg 1) = \frac{2}{5} \frac{10^{-14}}{q} T^{-(q+2)}. \quad (\text{A.11})$$

Case $G(k_{\min} R_L \ll 1)$

For energies $T \ll 1$, we use the approximation for Bessel function (A.5). Then, (A.1) reads as

$$\begin{aligned} G(T \ll 1) &= \frac{1}{4} \int_{k_{\min} R_L}^1 ds s^{-q} \int_0^1 d\eta (1-\eta^4) \frac{(1-\eta^2) s^2}{(1-\eta^2)^2 s^2 + \frac{V_A^2 R_L^2}{a_F^2}} \\ &= \frac{1}{4} \int_T^1 ds s^{-q} \int_0^1 d\eta (1+\eta^2) - \frac{M^2}{4} \\ &\times \int_T^1 ds s^{-q} \int_0^1 d\eta (1+\eta^2) \\ &\times \frac{1}{(1-\eta^2)^2 s^2 + M^2} = I_5 - I_4, \end{aligned} \quad (\text{A.12})$$

where $M^2 = \frac{V_A^2 R_L^2}{a_F^2}$. We then evaluate each integral:

$$\begin{aligned} I_5 &= \frac{1}{4} \int_T^1 ds s^{-q} \int_0^1 d\eta (1+\eta^2) = \frac{1}{3(q-1)} (T^{1-q} - 1) \\ &\approx \frac{1}{3(q-1)} T^{1-q}, \end{aligned} \quad (\text{A.13})$$

since $T \ll 1$, and $q > 1$.

$$\begin{aligned} I_4 &= \frac{M^2}{4} \int_T^1 ds s^{-q} \int_0^1 d\eta (1+\eta^2) \frac{1}{(1-\eta^2)^2 s^2 + M^2} \\ &= \frac{1}{4} \int_T^1 ds s^{-q} I_6, \end{aligned} \quad (\text{A.14})$$

where

$$I_6 = \int_0^1 d\eta (1+\eta^2) \frac{1}{((1-\eta^2)^2 s^2/M^2) + 1}. \quad (\text{A.15})$$

The exact solution of integral I_6 reads as

$$\frac{(-1)^{1/4} \left(\frac{(-2i+n) \arctan \left(\frac{(-1)^{1/4}}{\sqrt{-i+n}} \right)}{\sqrt{-i+n}} + \frac{i(2i+n) \arctan \left(\frac{(-1)^{3/4}}{\sqrt{-i+n}} \right)}{\sqrt{-i+n}} \right)}{2n \sqrt{1+n^2}}, \quad (\text{A.16})$$

where $n^2 = M^2/s^2$. We can evaluate I_6 by

$$I_6 \approx \frac{1}{2n^3}, \quad (\text{A.17})$$

which for I_4 gives

$$I_4 \approx \frac{1}{8M^3} \frac{1}{4-q} (1 - T^{(4-q)}). \quad (\text{A.18})$$

To compare I_4 and I_5 and calculate $G(T \ll 1)$, we have to consider two cases, which are $(1 < q < 4)$ and steep $(4 < q < 6)$ turbulence spectrum.

For $(1 < q < 4)$ the integral $I_4 \sim \frac{1}{4-q}$, while $I_4 \sim \frac{1}{q-4} T^{q-4}$ for $(4 < q < 6)$. However, M^3 exists in both cases in the denominator of I_4 , which implies that $I_4 \ll I_5$. According to Eq. (A.12) then:

$$G(T \ll 1) = \frac{1}{3} \frac{1}{q-1} T^{1-q}. \quad (\text{A.19})$$

Appendix B: Evaluation of the function G for slow mode waves

The task is to calculate the function G (48),

$$G = \frac{\int_{k_{\min} R_L}^{\infty} ds s^{-q} \int_0^1 d\eta (1 - \eta^4) J_1^2 \left(s \sqrt{1 - \eta^2} \right)}{(1 - \eta^2)^2 s^2 + \frac{V_A^2 \eta^2 \frac{\beta}{1+\beta} R_L^2}{\alpha_F^2}}. \quad (\text{B.1})$$

and evaluate it in two energy limits.

Case $G(k_{\min} R_L \gg 1)$

For energies $T \gg 1$ we substitute $s = xT$. Then, (B.1) reads as

$$\begin{aligned} G &= \int_1^{\infty} dx x^{-q} T^{-(1+q)} \int_0^1 d\eta (1 - \eta^4) J_1^2 \left(xT \sqrt{1 - \eta^2} \right) \\ &\times \frac{1}{(1 - \eta^2)^2 x^2 + p^2 \eta^2} \\ &= T^{-(1+q)} \int_1^{\infty} dx x^{-q} \left(\int_0^{1-\frac{1}{2xT}} d\eta (1 - \eta^4) \frac{1}{\pi xT \sqrt{1 - \eta^2}} \right. \\ &\times \frac{1}{(1 - \eta^2)^2 x^2 + p^2 \eta^2} \\ &\left. + \int_{1-\frac{1}{2xT}}^1 d\eta (1 - \eta^4) \frac{1}{4} x^2 T^2 (1 - \eta^2) \frac{1}{(1 - \eta^2)^2 x^2 + p^2 \eta^2} \right), \end{aligned} \quad (\text{B.2})$$

where $p^2 = (V_A^2 R_L^2 \beta) / (\alpha_F^2 (1 + \beta))$. We have used

$$J_\nu(z \gg 1) \approx \sqrt{\frac{2}{\pi \nu z}} \cos \left(\nu z - \frac{(2\nu + 1)\pi}{4} \right), \quad (\text{B.3})$$

implying

$$\begin{aligned} J_1^2(z \gg 1) &= \frac{1}{\pi xT \sqrt{1 - \eta^2}} \left(1 - \sin \left(2xT \sqrt{1 - \eta^2} \right) \right) \\ &\approx \frac{1}{\pi xT \sqrt{1 - \eta^2}} \end{aligned} \quad (\text{B.4})$$

$(1/\xi \gg \sin \xi/\xi)$ for the argument, $z = xT \ll 1$, and

$$J_\nu(z \ll 1) \approx \frac{(z/2)^\nu}{\Gamma(\nu + 1)}, \quad (\text{B.5})$$

implying

$$J_1^2(z \ll 1) = \frac{1}{4} x^2 T^2 (1 - \eta^2) \quad (\text{B.6})$$

for the argument $z = xT \gg 1$. We then obtain

$$\begin{aligned} T^{(1+q)} G(T \gg 1) &= \frac{T^2}{4} \int_1^{\infty} dx x^{-q+2} \int_{1-\frac{1}{2xT}}^1 d\eta (1 - \eta^4) \\ &\times \frac{(1 - \eta^2)}{(1 - \eta^2)^2 x^2 + p^2 \eta^2} + \frac{1}{\pi T} \int_1^{\infty} dx x^{-(q+1)} \\ &\int_0^1 d\eta \frac{(1 - \eta^4)}{\sqrt{1 - \eta^2}} \frac{1}{(1 - \eta^2)^2 x^2 + p^2 \eta^2} - \frac{1}{\pi T} \int_1^{\infty} dx x^{-(q+1)} \\ &\int_{1-\frac{1}{2xT}}^1 d\eta \frac{(1 - \eta^4)}{\sqrt{1 - \eta^2}} \frac{1}{(1 - \eta^2)^2 x^2 + p^2 \eta^2} \\ &= I_3 + I_1 - I_2. \end{aligned} \quad (\text{B.7})$$

Next, we evaluate each integral in turn as in the case of fast mode waves.

$$\begin{aligned} I_2 &= \frac{1}{\pi T} \int_1^{\infty} dx x^{-(q+1)} \int_0^{\frac{1}{2xT}} dm \frac{4m}{\sqrt{2m}} \frac{1}{4m^2 x^2 + p^2 (1 - m)^2} \\ &= \frac{1}{\pi T} \int_1^{\infty} dx x^{-(q+1)} I'_2(m, x), \end{aligned} \quad (\text{B.8})$$

where we substitute $m = 1 - \eta$.

$$\begin{aligned} I_3 &= \frac{T^2}{4} \int_1^{\infty} dx x^{-q+2} \int_0^{\frac{1}{2xT}} dm \frac{8m^2}{p^2 (1 - m)^2 + 4m^2 x^2} \\ &= \frac{T^2}{4} \int_1^{\infty} dx x^{-q+2} I'_3(m, x), \end{aligned} \quad (\text{B.9})$$

where we have used the same substitution as in the previous case.

$$\begin{aligned} I_1 &= \frac{1}{\pi T} \int_1^{\infty} dx x^{-(q+1)} \int_0^1 dm \frac{4m}{\sqrt{2m}} \frac{1}{p^2 (1 - m)^2 + 4m^2 x^2} \\ &= \frac{1}{\pi T} \int_1^{\infty} dx x^{-(q+1)} I'_1(m, x). \end{aligned} \quad (\text{B.10})$$

To compare functions under integration with respect to m , we write out the following integrals

$$I'_2(m, x) = \int_0^{\frac{1}{2xT}} dm \frac{4m}{\sqrt{2m}} \frac{1}{4m^2 x^2 + p^2 (1 - m)^2} \quad (\text{B.11})$$

$$= \frac{2\sqrt{2}}{p^2} \int_0^{\frac{1}{2xT}} dm f_1, \quad (\text{B.12})$$

$$I'_3(m, x) = \int_0^{\frac{1}{2xT}} dm \frac{8m^2}{p^2 (1 - m)^2 + 4m^2 x^2} = \frac{8}{p^2} \int_0^{\frac{1}{2xT}} dm f_2, \quad (\text{B.13})$$

$$I'_{1(m,x)} = \int_0^1 dm \frac{4m}{\sqrt{2m}} \frac{1}{p^2 (1 - m)^2 + 4m^2 x^2} = \frac{2\sqrt{2}}{p^2} \int_0^1 dm f_1, \quad (\text{B.14})$$

where $f_1 = \frac{m}{(1-m)^2}$ and $f_2 = \frac{m^2}{(1-m)^2}$. We have approximated the denominator as $(1-m)^2$, as long as $\frac{4v^2}{p^2} \ll 1$ holds (which is ensured by consideration of $T \gg 1$). Analyzing f_1 and f_2 in given intervals of integration we deduce that $I_2 < I_3 < I_1$. However, this case is not of particular interest, so we make a rough estimation on G .

Integral I'_1 diverges for $m = 1$, so we integrate to $m = b < 1$. Combining all, we obtain

$$G(T \gg 1) = \frac{\sqrt{2}}{\pi} \frac{|b/(b-1)| + |\log(1-b)|}{qp^2} T^{-(q+2)}. \quad (\text{B.15})$$

Case $G(k_{\min} R_L \ll 1)$

For energies $T \ll 1$, we use the approximation for Bessel function (B.5). Then, (B.1) reads as

$$\begin{aligned} G(T \ll 1) &= \frac{1}{4} \int_{k_{\min} R_L}^1 ds s^{-q} \int_0^1 d\eta (1 - \eta^4) \\ &\times \frac{(1 - \eta^2)s^2}{(1 - \eta^2)^2 s^2 + \frac{V_A^2 R_L^2 \eta^2 \beta}{\alpha_F^2 (1 + \beta)}} \\ &= \frac{1}{4} \int_T^1 ds s^{-q} \int_0^1 d\eta (1 + \eta^2) - \frac{p^2}{4} \\ &\int_T^1 ds s^{-q} \int_0^1 d\eta (1 + \eta^2) \\ &\times \frac{\eta}{(1 - \eta^2)^2 s^2 + p^2 \eta^2} \\ &= I_5 - I_4, \end{aligned} \quad (\text{B.16})$$

where $p^2 = \frac{V_A^2 R_L^2 \beta}{\alpha_F^2 (1 + \beta)}$. We then evaluate each integral.

$$\begin{aligned} I_5 &= \frac{1}{4} \int_T^1 ds s^{-q} \int_0^1 d\eta (1 + \eta^2) = \frac{1}{3(q-1)} (T^{1-q} - 1) \\ &\simeq \frac{1}{3(q-1)} T^{1-q}, \end{aligned} \quad (\text{B.17})$$

since $T \ll 1$.

To estimate I_4 , we write

$$\begin{aligned} I_4 &= \frac{p^2}{4} \int_T^1 ds s^{-q} \int_0^1 d\eta (1 + \eta^2) \frac{\eta^2}{(1 - \eta^2)^2 s^2 + p^2 \eta^2} \\ &= \frac{1}{4} \int_T^1 ds s^{-q} I_6, \end{aligned} \quad (\text{B.18})$$

where

$$I_6 = \int_0^1 d\eta (1 + \eta^2) \frac{\eta^2}{((1 - \eta^2)^2 w^2) + \eta^2} \quad (\text{B.19})$$

and $w^2 = s^2/p^2$. Here, we compare functions in integrals I_5 with respect to η , namely $f_1 = (1 + \eta^2)$, and in I_6 namely $f_2 = (1 + \eta^2) \frac{\eta^2}{((1 - \eta^2)^2 w^2) + \eta^2}$.

We find that $I_5 \gg I_6$ for $w^2 \gg 1$ over the interval $[0, 1]$. For $10^{-14} < w^2 < 1$, we still have $I_5 > I_4$. Only at $w^2 \leq 10^{-14}$, $I_5 < I_6$ (low energy value is caused by this limitation; namely, we consider $T \ll 1$). However, this treatment is valid as long as $T > \frac{\beta}{1+\beta}$, which is always less than 1.

As long as I_5 dominates, we obtain

$$G(T \ll 1) = \frac{1}{3} \frac{1}{q-1} T^{1-q}. \quad (\text{B.20})$$

References

- Abdo, A. A., Ackermann, M., Ajello, M., et al. 2009, *Phys. Rev. Lett.* 102, 1101
 Abramowitz, M., & Stegun, I. A. 1972, *Handbook of Mathematical functions* 1966
 Achterberg, A. 1979, *A&A*, 76, 276
 Adriani, O., Barbarino, G. C., Bazilevskaya, G. A., et al. 2009, *Nature*, 458, 607
 Aguilar, M., et al. 2013, *Phys. Rev. Lett.*, 110, 141102
 Arvanitaki, A., Dimopoulos, S., Dubovsky, S., et al. 2009, *Phys. Rev. D*, 80, 55011
 Beck, R. 2007, *EAS Pub. Ser.*, 23, 19
 Bieber, J. W., Wanner, W., & Matthaeus, W. M. 1996, *J. Geophys. Res.*, 101, 2511
 Boehm, C., Hooper, D., Silk, J., et al. 2004, *Phys. Rev. Lett.*, 92, 1301
 Clayton, D. D. 1973, *Nature Phys. Sci.*, 244, 137
 Dogan, A., Spanier, F., Vainio, R., & Schlickeiser, R. 2006, *J. Plasma Phys.*, 72, 419
 Fedorenko, V. N. 1992, *Sov. Sci. Rev. E*, 8, 4
 Guessoum, N., Jean, P., & Prantzos, N. 2006, *A&A*, 457, 753
 Higdon, J. C., Lingenfelter, R. E., & Rothschild, R. E. 2009, *ApJ*, 698, 350
 Hooper, D., Stebbins, A., & Zurek, K. N. 2009, *PRD*, 79, 103513
 Jokipii, J. R. 1966, *ApJ* 146, 480
 Knödseder, J., Jean, P., Lonjou, V., et al. 2005, *A&A*, 441, 513
 Kolmogorov, A. N. 1941, *Dokl. Akad. Nauk. SSSR*, 30, 301
 Kraichnan, R. 1965, *Phys. Fluids*, 8, 1835
 Kubo, R. 1957, *J. Phys. Soc. Jpn.* 12, 570
 Matthaeus, W. H., & Smith, C. W. 1981, *Phys. Rev. A* 24, 2135
 Milne, P. A., Kurfess, J. D., Kinzer, R. L., & Leising, M. D. 2002, *New Astron. Rev.*, 46, 553
 Palmer, I. D. 1982, *Rew. Geophys. Space Phys.*, 20, 335
 Pohl, M., & Eichler, D. 2010, *ApJ*, 712, L53
 Ramaty, R., & Lingenfelter, R. E. 1979, *Nature*, 278, 127
 Ramaty, R., Stecker, F. W., & Misra, D. 1970, *J. Geophys. Res.*, 75, 1141
 Schlickeiser, R. 2002, *Cosmic Ray Astrophysics* (Berlin: Springer)
 Schlickeiser, R. 2003, *Lect. Not. Phys.*, 612, 230
 Schlickeiser, R., & Miller, J. A. 1998, *ApJ* 492, 352
 Schlickeiser, R., & Vainio, R. 1999, *Astrophys. Space Sci.*, 264, 457
 Schlickeiser, R., Lazar, M., & Vukcevic, M. 2010, *ApJ*, 719, 1497
 Shalchi, A. 2005, *Phys. Plasmas*, 12, 052905
 Shalchi, A., & Schlickeiser, R. 2004, *A&A*, 420, 821
 Shalchi, A., Škoda, T., Tautz, R. C., & Schlickeiser, R. 2009, *Phys. Rev. D*, 80, 023012
 Spanier, F., & Schlickeiser, R. 2005, *A&A*, 436, 1
 Sturrock, P. A. 1971, *ApJ*, 164, 529
 Teufel, A., & Schlickeiser, R. 2002, *A&A*, 393, 703
 Teufel, A., Lerche, I., & Schlickeiser, R. 2003, *A&A* 397, 776
 Vukcevic, M., & Schlickeiser, R. 2007, *A&A*, 467, 15

THE INFLUENCE OF DISSIPATION RANGE POWER SPECTRA AND PLASMA-WAVE POLARIZATION ON COSMIC-RAY SCATTERING MEAN FREE PATH

R. SCHLICHEISER^{1,2}, M. LAZAR^{1,2}, AND M. VUKCEVIC^{1,3}

¹ Institut für Theoretische Physik, Lehrstuhl IV: Weltraum- und Astrophysik, Ruhr-Universität Bochum, D-44780 Bochum, Germany; rsch@tp4.rub.de

² Research Department Plasmas with Complex Interactions, Ruhr-Universität Bochum, D-44780 Bochum, Germany; mlazar@tp4.ruhr-uni-bochum.de

³ Military Academy, Pavla Jurisica Sturma 33, 11000 Belgrade, Serbia; vuk.mira@gmail.com

Received 2010 May 5; accepted 2010 June 23; published 2010 July 30

ABSTRACT

The influence of the polarization state and the dissipation range spectral steepening of slab plasma waves on the scattering mean free path of single-charged cosmic-ray particles is investigated in a turbulence model, where the crucial scattering of cosmic-ray particles with small pitch-angle cosines is caused by resonant cyclotron interactions with slab plasma waves. Analytical expressions for the mean free path of protons, antiprotons, negatrons, and positrons are derived for the case of constant frequency-independent magnetic helicity values σ and different values of the dissipation range spectral index k for characteristic interplanetary and interstellar plasma conditions. The positron mean free path is not affected by the dissipation range spectral index k as these particles can only cyclotron-resonate for rigidity values larger than $R_0 = m_p c = 938$ MV. Proton and antiproton mean free paths are only slightly affected by the dissipation range spectral index k at small rigidities $R < R_0$. The negatron mean free path is severely affected by the dissipation range spectral index k at rigidities smaller than R_0 . At high rigidities $R \gg R_0$, all particle species approach the same power-law dependence $\propto R^{2-s}$ determined by the inertial range spectral index $s = 5/3$. The magnetic helicity value σ affects the value of the mean free path. At all rigidities, the ratio of the antiproton to proton mean free paths equals the constant $(1 + \sigma)/(1 - \sigma)$, which also agrees with the ratio of the negatron to the proton and positron mean free paths at relativistic rigidities. At relativistic rigidities the positron and proton mean free paths agree, as do the negatron and antiproton mean free paths.

Key words: cosmic rays – diffusion – magnetic fields – plasmas – Sun: particle emission

Online-only material: color figures

1. INTRODUCTION

The scattering mean free path of cosmic-ray particles in interplanetary and interstellar turbulent magnetic fields is a key quantity for particle astrophysics, as it determines the diffusive escape time from cosmic systems, the anisotropy of galactic cosmic rays, the acceleration time scale of diffusive shock acceleration, the modulation of galactic and anomalous cosmic rays in the expanding solar wind, and, via its rigidity dependence, the chemical composition of ultra-high-energy cosmic rays. The scattering mean free path results from resonant particle-wave interactions of cosmic-ray particles with the turbulent component of cosmic magnetic fields and thus depends on the nature and geometry of cosmic turbulent magnetic fields (Schlickeiser 2002). In situ measurements of plasma turbulence in the solar wind indicate that the turbulent magnetic field is a mixture of slab (i.e., parallel to the ordered background magnetic field) waves, a dominating two-dimensional component (Bieber et al. 1996), with a negligible contribution to particle scattering (Shalchi & Schlickeiser 2004), and obliquely propagating magnetosonic waves that, due to their compressive nature, reveal themselves through electron density fluctuations. In the magnetostatic limit, the scattering rate from the two-dimensional component vanishes (Shalchi & Schlickeiser 2004), so that particle scattering is solely due to resonant interactions with the slab Alfvén waves and obliquely propagating fast magnetosonic waves.

Schlickeiser & Miller (1998) and Schlickeiser & Vainio (1999) have investigated the quasilinear interactions of charged particles with these two plasma modes. A cosmic-ray particle of given velocity v , Lorentz factor $\gamma = (1 - (v^2/c^2))^{-1/2}$, pitch-angle cosine μ , mass m , charge $q_i = e|Z_i|Q$ with $Q = \text{sgn}(Z_i)$,

and gyrofrequency $\Omega_c = Q\Omega$ with $\Omega = q_i B_0/(mc\gamma)$ interacts with waves whose wavenumber k , cosine of propagation angle $\eta = k_{\parallel}/k$, and real frequency f obey the resonance condition:

$$f(k) = v\mu k\eta + n\Omega_c \quad (1)$$

for the entire $n \in [-\infty, \infty]$. For slab ($\eta = 1$) Alfvén waves, only gyroresonant interactions with $n = \pm 1$ are possible. In contrast, for obliquely propagating fast magnetosonic waves, besides gyroresonance interactions ($n \neq 1$), also the $n = 0$ resonance is possible due to their compressive magnetic field component. The $n = 0$ interactions are referred to as transit-time damping (TTD). Using $n = 0$, the resonance condition (1) requires the parallel cosmic-ray velocity $v\mu = f/(k\eta) \geq f/k \simeq V_A$ to be greater than the finite phase velocity of magnetosonic waves, given by the Alfvén speed. TTD interactions therefore only occur for cosmic-ray particles with pitch-angle cosines $|\mu| \geq V_A/v = \epsilon$. At these pitch-angle cosines, TTD interactions provide most of the particle scattering.

For energetic particles, the crucial scattering in the interval of small $|\mu| \leq V_A/v = \epsilon \ll 1$ is then provided only by gyroresonances with slab plasma waves that below the non-relativistic electron gyrofrequency consist of the right-handed (RH) polarized Alfvén–Whistler-electron cyclotron branch and the left-handed (LH) polarized Alfvén-proton cyclotron branch, and gyroresonances with fast magnetosonic waves. If slab-mode waves and obliquely distributed magnetosonic waves have comparable intensities, the TTD scattering rates of energetic particles at pitch-angle cosines $|\mu| > \epsilon$ become so large that the mean free path is well approximated with an integral of the slab-mode ($D_{\mu\mu}^{\text{slab}}$) contribution and the contribution from

gyroresonant interactions with magnetosonic waves ($D_{\mu\mu}^{\text{g-ms}}$) that extends from $\mu = -\epsilon \ll 1$ to ϵ (Schlickeiser & Miller 1998; Schlickeiser 1999; Vainio 2000):

$$\lambda \simeq \frac{3v}{8} \int_{-\epsilon}^{\epsilon} d\mu \frac{(1 - \mu^2)}{D_{\mu\mu}^{\text{slab}}(\mu) + D_{\mu\mu}^{\text{g-ms}}(\mu)} \simeq \frac{3V_A}{4[D_{\mu\mu}^{\text{slab}}(0) + D_{\mu\mu}^{\text{g-ms}}(0)]}. \quad (2)$$

According to Schlickeiser & Miller (1998) for similar turbulence power spectra of slab and magnetosonic waves, the magnetosonic contribution $D_{\mu\mu}^{\text{g-ms}}(0) \simeq \epsilon D_{\mu\mu}^{\text{slab}}(0)$ for energetic particles ($\epsilon \ll 1$) is much smaller than the slab contribution, so that

$$\lambda \simeq \frac{3V_A}{4D_{\mu\mu}^{\text{slab}}(0)}, \quad (3)$$

which will be used in the following. We note, however, that this latter reduction is not justified for cosmic-ray positrons with Lorentz factors $\gamma < m_p/m_e = 1836$. We will demonstrate below that these positrons find no LH polarized slab waves to resonantly interact with, so that here $D_{\mu\mu}^{\text{slab}}(0) \rightarrow 0$. In this case, the contribution from gyroresonant interactions with magnetosonic waves provides small but finite scattering. This subject will be studied in a separate, forthcoming investigation as the calculation of $D_{\mu\mu}^{\text{g-ms}}(0)$ is rather involved.

For gyroresonant interactions with slab Alfvén waves of cosmic-ray particles with $\mu = 0$, the resonance condition (1) reduces to the cyclotron condition $f = \pm\Omega Z$, implying with $f > 0$ that the scattering of positively ($Q = 1$) charged particles, such as protons (p^+) and positrons (e^+), at $\mu = 0$ is caused by resonant cyclotron interactions with the LH polarized slab waves, whereas negatively ($Q = -1$) charged particles, such as negatrons (e^-) and antiprotons (p^-), cyclotron-interact with the RH polarized slab waves. For a net polarization of slab waves, i.e., non-zero values of the magnetic helicity σ , different values of the scattering mean free path for positively and negatively charged cosmic-ray particles result. Such a difference is of high interest for the interpretation of the recently observed dramatic rise in the positron fraction of galactic cosmic-ray electrons (Adriani et al. 2009) between 10 GeV and 300 GeV.

Besides the net polarization of slab waves, the mean free path of energetic particles can also be influenced by the observed steepening of magnetic field fluctuation power spectra in the solar wind. In situ spacecraft measurements of plasma turbulence in the solar wind yield magnetic fluctuation spectra $J(f) \propto f^{-\alpha}$ which are power laws in the observed frequency f . At small frequencies $f \leq 0.2$ Hz $\simeq \Omega_p$ below the non-relativistic proton gyrofrequency, the spectral index is measured to be about the Kolmogorov value $-5/3$ (Smith et al. 2006; Podesta et al. 2007), which therefore is referred to as the “inertial range.” In the range $f \in [0.2, 0.5]$ Hz, the measurements indicate a distinct spectral break to steeper spectra (Leamon et al. 1998; Smith et al. 2006; Alexandrova et al. 2008). At higher observed frequencies up to 100 Hz, higher spectral indices with $2 < \alpha < 4.5$ are measured (Denskat et al. 1983; Bale et al. 2005; Sahraoui et al. 2009; Kiyani et al. 2009; Alexandrova et al. 2009). These higher frequency range spectra are referred to as “dissipation range” again by analogy with neutral fluid turbulence (Saito et al. 2008). Because high frequency turbulence above the spectral breakpoint is relatively weak ($|\delta\vec{B}|^2 \ll B_0^2$), this dissipation regime may be thought

of as an ensemble of weakly interacting fluctuations which are individually described by linear dispersion theory. Then a likely explanation for higher spectral indices is that these fluctuations are weakly damped dispersive waves (Stawicki et al. 2001; Alexandrova et al. 2008).

It is the purpose of this work to quantitatively investigate the influences of a net polarization of slab plasma waves and of the established spectral steepening of magnetic fluctuation spectra in the dissipation range on the quasilinear scattering mean free paths of cosmic-ray, and especially solar energetic, particles. Because of the measured small turbulence levels ($q_L = |\delta\vec{B}|^2/B_0^2 \ll 1$), the application of quasilinear particle transport theory, which is a perturbation theory to the lowest order in q_L , is well justified. Of particular interest are differences in the rigidity dependence of the mean free path of cosmic-ray protons, antiprotons, negatrons, and positrons caused by either (1) the dissipation range steepening of magnetic fluctuation power spectra or (2) different wave powers in RH and LH polarized slab waves, which via resonant cyclotron interactions determine the relevant scattering rate of energetic particles.

2. QUASILINEAR SCATTERING MEAN FREE PATH

The pitch-angle scattering Fokker Planck coefficient for cosmic-ray particles with $\mu = 0$ is caused by resonant cyclotron interactions with the LH and RH polarized slab waves so that

$$D_{\mu\mu}^{\text{slab}}(0) = \pi^2 \frac{\Omega^2}{B_0^2} \left[\int_0^{\Omega_e} df P_{s,\text{RH}}(f) \delta(f + \Omega Q) + \int_0^{\Omega_p} df P_{s,\text{LH}}(f) \delta(f - \Omega Q) \right], \quad (4)$$

where $\Omega = \Omega_0/\gamma$ denotes the absolute value of the particle’s gyrofrequency. Equation (4) accounts for the non-existence of LH polarized slab waves at wave frequencies above the non-relativistic proton cyclotron frequency.

The power spectra of LH, $P_{s,\text{LH}}(f) = (1+\sigma)J_s(f)/2$, and RH, $P_{s,\text{RH}}(f) = (1-\sigma)J_s(f)/2$, polarized slab waves are related to the total power $J_s(f) = P_{s,\text{LH}}(f) + P_{s,\text{RH}}(f)$ of the slab mode as a function of wave frequency,

$$(\delta B_s)^2 = 2\pi \int_{f_0}^{\infty} df J_s(f), \quad (5)$$

where $f_0 = 10^{-4}\Omega_p$ denotes the lowest observed frequency of plasma waves. For constant, frequency-independent magnetic helicity values σ , we obtain

$$\begin{aligned} D_{\mu\mu}^{\text{slab}}(0) &= \pi^2 \frac{\Omega^2}{2B_0^2} [(1-\sigma)J_s(-\Omega Q)H[-Q]H[\Omega_e + \Omega Q] \\ &\quad + (1+\sigma)J_s(\Omega Q)H[Q]H[\Omega_p - \Omega Q]] \\ &= \frac{\pi^2 \Omega^2}{B_0^2} J_s(\Omega) G(\sigma, \Omega, Q), \end{aligned} \quad (6)$$

where $H[x]$ denotes the Heaviside step function and with the charge-sign-dependent function:

$$\begin{aligned} G(\sigma, \Omega, Q) &= (1-\sigma)H[\Omega_e + \Omega Q]H[-Q] \\ &\quad + (1+\sigma)H[\Omega_p - \Omega Q]H[Q]. \end{aligned} \quad (7)$$

Accounting for the slab contribution to the observed turbulence that additionally contains oblique magnetosonic turbulence and two-dimensional turbulence, by the slab factor

$\eta = (\delta B_s)^2 / (\delta B_{\text{total}})^2 \simeq 0.15$ (Bieber et al. 1996) in the solar wind, we relate $J_s(f) = \eta J(f)$ to the observed magnetic fluctuation spectra which we represent as

$$J(f) = \frac{J_0 f^{-s}}{\left[1 + \frac{f}{\Omega_p}\right]^k} H[f - f_0]. \quad (8)$$

Here, $s = 5/3$ represents the inertial range spectral index, whereas k accounts for the measured steepening in the dissipation range. We then obtain for Equation (6)

$$D_{\mu\mu}^{\text{slab}}(0) = \frac{\pi^2 \eta J_0 \Omega^2 \Omega_0^{-s}}{2B_0^2} \frac{H[\Omega - f_0]}{\left[1 + \frac{\Omega}{\Omega_p}\right]^k} G(\sigma, \Omega, Q). \quad (9)$$

Consequently, the mean free path (Equation (3)) becomes

$$\lambda(\gamma) = \frac{3V_A B_0^2}{2\pi^2 \eta J_0 G(\sigma, \Omega, Q)} \left(\frac{\gamma}{\Omega_0}\right)^{2-s} \times \left[1 + \frac{\Omega_0}{\Omega_p \gamma}\right]^k H\left[\frac{\Omega_0}{f_0} - \gamma\right]. \quad (10)$$

J_0 is related to the total fluctuating magnetic field component $(\delta B_{\text{total}})^2$ as

$$(\delta B_{\text{total}})^2 = 2\pi \int_{f_0}^{\infty} df J(f) = 2\pi J_0 \int_{f_0}^{\infty} df \frac{f^{-s}}{\left[1 + \frac{f}{\Omega_p}\right]^k}, \quad (11)$$

where we inserted Equation (7). For $s + k > 1$, the integral can be solved in terms of hypergeometric functions so that

$$(\delta B_{\text{total}})^2 = \frac{2\pi J_0}{s + k - 1} \frac{f_0^{1-s}}{\left(1 + \frac{f_0}{\Omega_p}\right)^k} \times F\left(k, 1; s + k; \frac{1}{1 + \frac{f_0}{\Omega_p}}\right) \simeq \frac{2\pi J_0}{s - 1} f_0^{1-s}, \quad (12)$$

where the latter approximation holds because of the small observed value $f_0 = 10^{-4} \Omega_p$. Replacing J_0 in Equation (10), we obtain

$$\lambda(\gamma) = \frac{3}{\pi(s-1)\eta G(\sigma, \Omega, Q)} \frac{B_0^2}{(\delta B_{\text{total}})^2} \frac{V_A}{\Omega_0} \left(\frac{\Omega_0}{f_0}\right)^{s-1} \times \gamma^{2-s} \left[1 + \frac{\Omega_0}{\Omega_p \gamma}\right]^k H\left[\frac{\Omega_0}{f_0} - \gamma\right]. \quad (13)$$

Expressing the Alfvén speed $V_A = \Omega_p c / \omega_{p,p}$ in terms of the proton plasma frequency $\omega_{p,p}$, we find

$$\lambda(\gamma) = \lambda_0 \frac{\Omega_p}{\Omega_0} \left(\frac{\Omega_0}{f_0}\right)^{s-1} \frac{\gamma^{2-s}}{G(\sigma, \Omega, Q)} \times \left[1 + \frac{\Omega_0}{\Omega_p \gamma}\right]^k H\left[\frac{\Omega_0}{f_0} - \gamma\right] \quad (14)$$

with the constant

$$\lambda_0 = \frac{3c}{\pi \eta (s-1) \omega_{p,p}} \frac{B_0^2}{(\delta B_{\text{total}})^2}. \quad (15)$$

Table 1
Function G for Different Cosmic-ray Particles

| Particle | Q | G |
|-------------|-----|---|
| Protons | 1 | $(1 + \sigma)H[\gamma - 1]$ |
| Antiprotons | 1 | $(1 - \sigma)H[\gamma - 1]$ |
| Negatrons | -1 | $(1 - \sigma)H[\gamma - 1]$ |
| Positrons | 1 | $(1 + \sigma)H[\gamma - \alpha], \alpha = m_p/m_e = 1836$ |

The charge-sign-dependent function G is calculated in Table 1 for cosmic-ray protons, antiprotons, positrons (e^+), and negatrons (e^-). Antiprotons and negatrons interact with RH polarized slab waves for all values of the particle Lorentz factor, whereas protons interact with LH polarized slab waves for all values of the particle Lorentz factor. However, positrons interact with LH polarized slab waves only if their Lorentz factor is higher than the mass ratio $\alpha = 1836$. Because there are no LH polarized slab waves above the proton cyclotron frequency, only the mean free path of negatrons at Lorentz factors $\gamma < \alpha$ will be heavily influenced by the spectral steepening of the magnetic fluctuation power spectrum in the dissipation range. The absence of LH polarized slab waves above the proton cyclotron frequency can be best seen from the plot of the dispersion relation $f = \omega = \omega(k_{\parallel})$ shown as a dashed line in Figure 1 of Steinacker & Miller (1992).

In the next section, we will calculate the rigidity dependence of the mean free path for the four particle species adopting the following standard interplanetary plasma parameters: the gas density $n_e = 10n_1 \text{ cm}^{-3}$, the turbulence level $b = \delta B_{\text{total}}/B_0 = 0.1b_{0.1}$, the slab ratio $\eta = 0.15\eta_{0.15}$, the inertial spectral index $s = 5/3$ and $f_0 = 10^{-4}f_{0,-4}\Omega_p$. For these values, the mean free path (Equation (14)) is given by

$$\lambda(\gamma) = \lambda_1 \left(\frac{\Omega_p}{\Omega_0}\right)^{2-s} \frac{\gamma^{2-s}}{G(\sigma, \Omega, Q)} \times \left[1 + \frac{\Omega_0}{\Omega_p \gamma}\right]^k H\left[\frac{\Omega_0}{f_0} - \gamma\right] \quad (16)$$

with the constant

$$\lambda_1 = \lambda_0 \left(\frac{\Omega_p}{f_0}\right)^{s-1} = \frac{0.22}{f_{0,-4}^{2/3} \eta_{0.15} b_{0.1}^2 n_1^{1/2}} \text{ AU}, \quad (17)$$

whose value compares favorably well with the observed particle mean free paths in the interplanetary medium (Dröge 2000).

We note that in the interstellar medium the observed electron density fluctuation spectrum (Armstrong et al. 1995) extends to much smaller frequencies $f_{0,-4} = 10^{-4}$ yielding $n_1 = 0.1$ for the constant $\lambda_1 = 2.3 \times 10^{15} \text{ cm}$, which again is a reasonable value.

3. MEAN FREE PATH FOR PROTONS, ANTIPROTONS, NEGATONS, AND POSITONS

For cosmic-ray protons, antiprotons, negatons, and positons, we derive the mean free paths from Equation (16) and Table 1 as

$$\lambda_{p^+}(\gamma_p) = \frac{\lambda_1}{1 + \sigma} \gamma_p^{2-s} \left[1 + \frac{1}{\gamma_p}\right]^k H\left[\frac{\Omega_p}{f_0} - \gamma_p\right], \quad (18)$$

$$\lambda_{p^-}(\gamma_p) = \frac{1 + \sigma}{1 - \sigma} \lambda_{p^+}(\gamma_p), \quad (19)$$

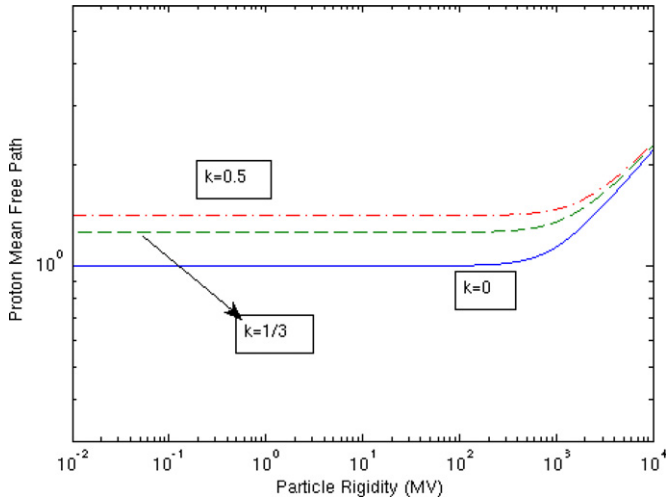


Figure 1. Scattering mean free path of cosmic-ray protons and antiprotons in units of $\lambda_1/(1+\sigma)$ and $\lambda_1/(1-\sigma)$, respectively, as a function of particle rigidity for three values of the dissipation range spectral index $k = 0$ (full curve), $k = 1/3$ (dashed curve), and $k = 0.5$ (dot-dashed curve).

(A color version of this figure is available in the online journal.)

$$\lambda_{e^+}(\gamma_e) = \frac{\lambda_1}{1+\sigma} \left(\frac{\gamma_e}{\alpha}\right)^{2-s} \left[1 + \frac{\alpha}{\gamma_e}\right]^k \times H[\gamma_e - \alpha] H\left[\frac{\alpha\Omega_p}{f_0} - \gamma_e\right], \quad (20)$$

and

$$\lambda_{e^-}(\gamma_e) = \frac{\lambda_1}{1-\sigma} \left(\frac{\gamma_e}{\alpha}\right)^{2-s} \left[1 + \frac{\alpha}{\gamma_e}\right]^k H\left[\frac{\alpha\Omega_p}{f_0} - \gamma_e\right], \quad (21)$$

respectively. For these four singly charged particle species, the rigidity $R = p$ equals the particle momentum so that the Lorentz factors are

$$\gamma_{p,e} = \sqrt{1 + \left(\frac{R}{m_{p,e}c}\right)^2}. \quad (22)$$

For solar wind turbulence parameters, these mean free paths are shown in Figures 1–3 as a function of particle rigidity for different values of the dissipation range spectral index k .

Figure 1 indicates that the proton and antiproton mean free paths are only slightly affected by the dissipation range spectral index k at small rigidities. In agreement with Equations (18) and (19), the proton and antiproton mean free paths approach the constant values

$$\lambda_{p^+,p^-}(R_p \rightarrow 0) = \frac{2^k \lambda_1}{1 \pm \sigma}. \quad (23)$$

At relativistic rigidities $R \gg R_0 = m_p c = 938$ MV, both mean free paths increase $\propto R^{2-s} = R^{1/3}$. At all rigidities, the ratio of the antiproton to proton mean free paths equals the constant $(1+\sigma)/(1-\sigma)$.

The positron mean free path shown in Figure 2 is not affected by the dissipation range spectral index k . In order to resonate with LH polarized slab waves, the positron rigidity has to be larger than $R \geq \alpha m_e c = R_0$. At lower rigidities, the positron mean free path is infinitely large for this type of turbulence model. At high rigidities $R \gg R_0$, the positron mean free path

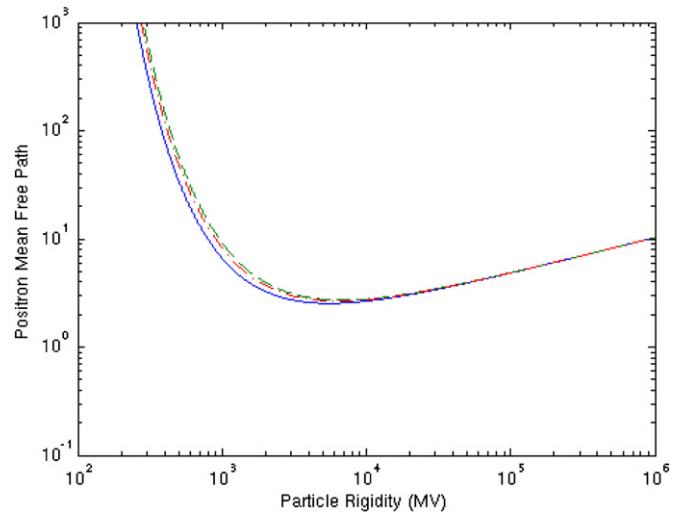


Figure 2. Scattering mean free path of cosmic-ray positrons in units of $\lambda_1/(1+\sigma)$ as a function of particle rigidity for solar wind scattering conditions and three values of the dissipation range spectral index $k = 0$ (full curve), $k = 1/3$ (dashed curve), and $k = 0.5$ (dot-dashed curve).

(A color version of this figure is available in the online journal.)

equals the same power-law dependence of the proton mean free path

$$\lambda_{e^+}(R \gg R_0) = \frac{\lambda_1}{1+\sigma} \left(\frac{R}{m_p c}\right)^{2-s} = \lambda_p(R \gg R_0). \quad (24)$$

The negatron mean free path shown in Figure 3 is heavily influenced by the dissipation range spectral index at negatron rigidities below R_0 . In agreement with Equation (20), the negatron mean free path approaches the constant value:

$$\lambda_{e^-}(R_e \rightarrow 0) = \frac{\lambda_1}{1-\sigma} \frac{(1+\alpha)^k}{\alpha^{2-s}} \simeq \frac{\lambda_1}{1-\sigma} \alpha^{k+2-s}. \quad (25)$$

At high rigidities $r \gg R_0$, the negatron mean free path approaches the power-law dependence:

$$\begin{aligned} \lambda_{e^-}(R \gg R_0) &= \frac{\lambda_1}{1-\sigma} \left(\frac{R}{m_p c}\right)^{2-s} = \frac{1+\sigma}{1-\sigma} \lambda_p(R \gg R_0) \\ &= \frac{1+\sigma}{1-\sigma} \lambda_{e^+}(R \gg R_0), \end{aligned} \quad (26)$$

which differs from the positron and the proton mean free path by the constant factor $(1+\sigma)/(1-\sigma)$, reflecting that negatrons interact with RH polarized waves, whereas the positively charged protons and positrons interact with LH polarized waves. Only for the case of linearly ($\sigma = 0$) polarized slab waves, all four particle species have the same value of the mean free path at the same relativistic rigidity.

Dröge (2000, 2003) has compared the rigidity dependence of proton and electron mean free paths for several solar flare events with numerically calculated mean free paths including also the dissipation range steepening for linearly ($\sigma = 0$) polarized slab waves. In Figure 4, we therefore show the electron and proton mean free paths for the dissipation range spectral index $k = 1/2$ and two different values of the magnetic helicity $\sigma = -0.7, 0.5$. One notices that non-zero values of the magnetic helicity have a drastic influence on the absolute values of the proton and electron mean free paths. In agreement with Equation (26), a negative value of σ , indicating more RH than LH polarized slab

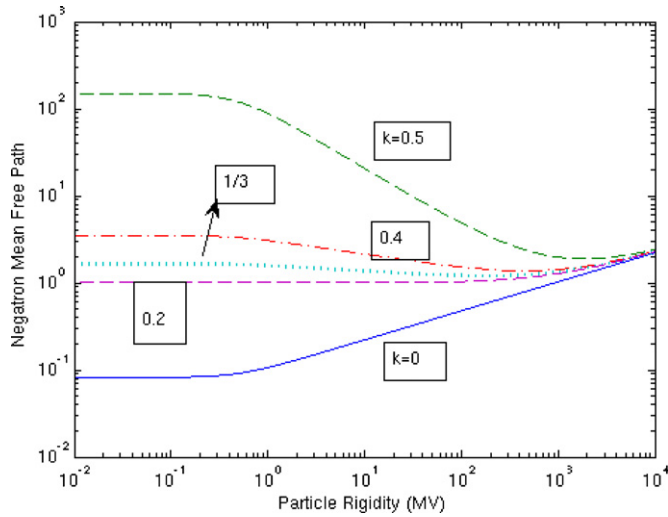


Figure 3. Scattering mean free path of cosmic-ray negatrons in units of $\lambda_1/(1-\sigma)$ as a function of particle rigidity for solar wind scattering conditions and five values of the dissipation range spectral index.

(A color version of this figure is available in the online journal.)

waves, implies a smaller electron compared to the proton mean free path. Electrons are scattered more often by the excess of RH polarized waves than protons, implying a smaller mean free path that is inversely proportional to the scattering rate. Alternatively, the excess of LH polarized waves implied by positive values of σ lead to smaller proton mean free path compared to the electron mean free path. By fitting the two parameters k and σ to the measured proton and negatron mean free paths of individual solar flare events, it is therefore possible to infer the dissipation range spectral index and the magnetic helicity state for each event. The same difference results for the mean free paths of relativistic negatrons and positrons: for positive $\sigma > 0$ the positron mean free path is a factor $(1-\sigma)/(1+\sigma)$ smaller than the negatron mean free path, whereas for negative $\sigma < 0$ the positron mean free path is larger than the negatron mean free path by the same factor.

4. SUMMARY AND CONCLUSIONS

We have investigated the influence of the polarization state and the dissipation range spectral steepening of slab plasma waves on the scattering mean free path of single-charged cosmic-ray particles in a turbulence model, where the crucial scattering of cosmic-ray particles with small pitch-angle cosines is caused by resonant cyclotron interactions with slab plasma waves. Because positively (negatively) charged cosmic rays resonate with the LH (RH) polarized slab waves, different values of the scattering mean free path for positively and negatively charged cosmic-ray particles result for non-zero magnetic helicity values σ . The mean free paths are also affected by the observationally established steepening of the power spectrum of magnetic fluctuations at frequencies above the non-relativistic proton gyrofrequency. Analytical expressions for the mean free path of protons, antiprotons, negatrons, and positrons are derived for the case of constant frequency-independent magnetic helicity values and different values of the dissipation range spectral index k for characteristic interplanetary and interstellar plasma conditions.

The positron mean free path is not affected by the dissipation range spectral index k as these particles can only cyclotron-resonate for rigidity values larger than $R_0 = m_p c = 938$ MV. Proton and antiproton mean free paths are only slightly affected

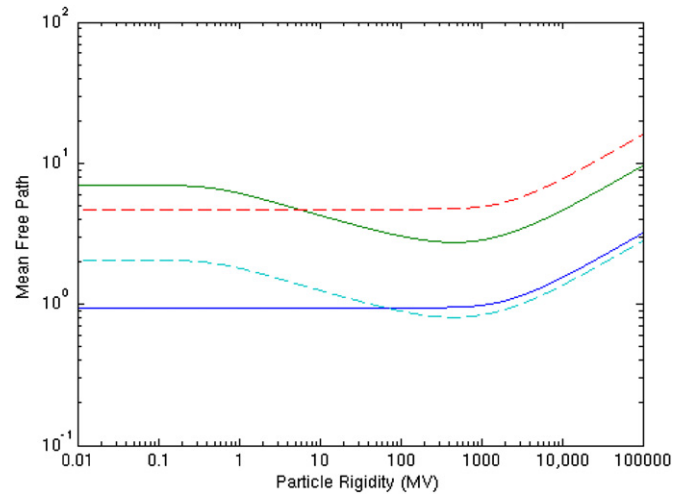


Figure 4. Scattering mean free path of cosmic-ray negatrons and protons in units of λ_1 as a function of particle rigidity for the dissipation range spectral index $k = 1/2$ and the two magnetic helicity values $\sigma = 0.5$ (full curves) and $\sigma = -0.7$ (dashed curves). The proton curves are constants at rigidities less than 500 MV, whereas the electron curves exhibit a dip near 500 MV.

(A color version of this figure is available in the online journal.)

by the dissipation range spectral index k at small rigidities $R < R_0$. The negatron mean free path is severely affected by the dissipation range spectral index k at rigidities smaller than R_0 . At high rigidities $R \gg R_0$, all particle species approach the same power-law dependence $\propto R^{2-s}$ determined by the inertial range spectral index $s = 5/3$.

The magnetic helicity value σ affects the value of the mean free path. At all rigidities, the ratio of the antiproton to proton mean free paths equals the constant $(1+\sigma)/(1-\sigma)$, which also agrees with the ratio of the negatron to the proton and positron mean free paths at relativistic rigidities. At relativistic rigidities, the positron and proton mean free paths agree, as do the negatron and antiproton mean free paths. Using the measured rigidity variations of proton and negatron mean free paths of individual solar flare events, it is therefore possible to infer the dissipation range spectral index and the magnetic helicity state for each event.

The reported charge-sign-dependent differences in the mean free paths distinguish this plasma-wave interaction model of cosmic-ray particles from other magnetostatic transport models such as the dynamical turbulence and random sweeping model (Bieber et al. 1994), which omit finite frequency effects and thus the influence of wave polarization on the particle scattering at small pitch-angle cosines. Establishing experimentally therefore differences in the scattering rates of positively and negatively charged particles, as e.g., by positron/electron-ratio and antiproton/proton-ratio observations, would therefore favor this plasma-wave interaction model.

We thank the referee for his/her constructive comments. R.S. acknowledges support from the Deutsche Forschungsgemeinschaft through grant Schl 201/19-1. This work was started when M.V. was a visiting guest scientist of the Research Department Plasmas with Complex Interactions at Ruhr-University Bochum.

REFERENCES

- Adriani, O., et al. 2009, *Nature*, **458**, 607
 Alexandrova, O., Carbone, V., Veltri, P., & Sorriso-Valvo, L. 2008, *ApJ*, **674**, 1153

- Alexandrova, O., Saur, J., Lacombe, C., Mangeney, A., Mitchell, J., Schwartz, S. J., & Robert, P. 2009, *Phys. Rev. Lett.*, **103**, 165003
- Armstrong, J. W., Rickett, B. J., & Spangler, S. R. 1995, *ApJ*, **443**, 209
- Bale, S. D., Kellog, P. J., Mozer, F. S., Horbury, T. S., & Reme, H. 2005, *Phys. Rev. Lett.*, **94**, 215002
- Bieber, J. W., Matthaeus, W. H., Smith, C.W., Wanner, W., Kallenrode, M.-B., & Wibberenz, G. 1994, *ApJ*, **420**, 294
- Bieber, J. W., Wanner, W., & Matthaeus, W. M. 1996, *J. Geophys. Res.*, **101**, 2511
- Denskat, K. U., Beinroth, H. J., & Neubauer, F. M. 1983, *Z. Geophys.*, **54**, 60
- Dröge, W. 2000, *ApJ*, **537**, 1073
- Dröge, W. 2003, *ApJ*, **589**, 1027
- Kiyani, K. H., Chapman, S. C., Khotyaintsev, Yu. V., Dunlop, M. W., & Sahraoui, F. 2009, *Phys. Rev. Lett.*, **103**, 075006
- Leamon, R. J., Smith, C. W., Ness, N. F., Matthaeus, W. M., & Wong, H. K. 1998, *J. Geophys. Res.*, **103**, 4775
- Podesta, J. J., Roberts, D. A., & Goldstein, M. L. 2007, *ApJ*, **664**, 543
- Sahraoui, F., Goldstein, M. L., Robert, P., & Khotyaintsev, Yu. V. 2009, *Phys. Rev. Lett.*, **102**, 231102
- Saito, S., Gary, S. P., Li, H., & Narita, Y. 2008, *Phys. Plasmas*, **15**, 102305
- Schlickeiser, R. 1999, *A&A*, **351**, 382
- Schlickeiser, R. 2002, *Cosmic Ray Astrophysics* (Berlin: Springer)
- Schlickeiser, R., & Miller, J. A. 1998, *ApJ*, **492**, 352
- Schlickeiser, R., & Vainio, R. 1999, *Astrophys. Space Sci.*, **264**, 457
- Shalchi, A., & Schlickeiser, R. 2004, *ApJ*, **604**, 861
- Smith, C. W., Hamilton, K., Vasquez, B. J., & Leamon, R. J. 2006, *ApJ*, **645**, L85
- Stawicki, O., Gary, S. P., & Li, H. 2001, *J. Geophys. Res.*, **106**, 8273
- Steinacker, J., & Miller, J. A. 1992, *ApJ*, **393**, 764
- Vainio, R. 2000, *ApJS*, **131**, 519

Confinement and anisotropy of ultrahigh-energy cosmic rays in isotropic plasma wave turbulence

I. Modification of the Hillas limit due to turbulence geometry^{*}

M. Vukcevic^{1,2} and R. Schlickeiser¹

¹ Institut für Theoretische Physik, Lehrstuhl IV: Weltraum- und Astrophysik, Ruhr-Universität Bochum, 44780 Bochum, Germany
 e-mail: rsch@tp4.ruhr-uni-bochum.de

² Department of Physics, University of Montenegro, Podgorica, Montenegro

Received 14 December 2006 / Accepted 22 February 2007

ABSTRACT

Context. The mean free path and anisotropy of galactic cosmic rays is calculated in weak plasma wave turbulence that is isotropically distributed with respect to the ordered uniform magnetic field.

Aims. The modifications on the value of the Hillas energy, above which cosmic rays are not confined to the Galaxy, are calculated. The original determination of the Hillas limit has been based on the case of slab turbulence where only parallel propagating plasma waves are allowed.

Methods. We use quasilinear cosmic ray Fokker-Planck coefficients to calculate the mean free path and the anisotropy in isotropic plasma wave turbulence.

Results. In isotropic plasma wave turbulence the Hillas limit is enhanced by about four orders of magnitude to $E_c = 2.03 \times 10^5 A n_e^{1/2} (L_{\max}/10 \text{ pc})$ PeV resulting from the dominating influence of transit-time damping interactions of cosmic rays with obliquely propagating magnetosonic waves.

Conclusions. Below the energy E_c the cosmic ray mean free path and the anisotropy exhibit the well known $E^{1/3}$ energy dependence. At energies higher than E_c both transport parameters steepen to a E^3 -dependence. This implies that cosmic rays even with ultrahigh energies of several hundreds of EeV can be rapidly pitch-angle scattered by interstellar plasma turbulence, and are thus confined to the Galaxy.

Key words. ISM: cosmic rays – ISM: magnetic fields – plasmas – scattering

1. Introduction

To unravel the nature of cosmic sources that accelerate cosmic rays to ultrahigh energies has been identified as one of the eleven fundamental science questions for the new century (Turner et al. 2002). Cosmic rays with energies up to at least 10^{14} eV are likely accelerated at the shock fronts associated with supernova remnants (for review see Blandford & Eichler 1987). Radio emissions and X-rays give conclusive evidence that electrons are accelerated there to near-light speed (Koyama et al. 1995, 1997; Tanimori et al. 2001; Allen et al. 1997; Slane et al. 1999; Borkowski et al. 2001). The HESS observations of supernova remnants up to ~ 100 TeV provide direct evidence of very high energy particle acceleration in the shocks (Aharonian et al. 2004, 2005), while the leptonic or hadronic nature of these gamma-rays is currently being disputed (e.g. Enomoto et al. 2002; Reimer & Pohl 2002). The supernova remnant origin would be consistent with the observed GeV excess of diffuse galactic gamma radiation from the inner Galaxy (Büsching et al. 2001), although the GeV excess has been found to be present in all directions including galactic latitudes where no supernova remnants are present and the outer Galaxy (Strong et al. 2004). This indicates that the origin of the GeV excess is more complex

and is not straightforwardly connected with supernova remnants in the inner Galaxy.

More puzzling are the much higher energy cosmic rays with energies as large as $10^{20.5}$ eV. It has been argued (Lucek & Bell 2000; Bell & Lucek 2001; Hillas 2006) that, due to the amplification of the magnetic field in the shock, the acceleration of cosmic rays in young supernova remnants is possible up to $\sim 10^{18}$ eV. This implies that such particles may have a Galactic origin. For ultrahigh-energy (10^{18} – $10^{20.5}$ eV) cosmic rays an extragalactic origin is favored by many researchers. Extragalactic ultrahigh-energy cosmic rays (UHECRs) coming from cosmological distances ≥ 50 Mpc should interact with the universal cosmic microwave background radiation (CMBR) and produce pions. For an extragalactic origin of UHECRs the detection or non-detection of the Greisen-Kuzmin-Zatsepin cutoff resulting from the photopion attenuation in the CMBR will have far-reaching consequences not only for astrophysics but also for fundamental particle physics as e.g. the breakup of Lorentz symmetry (Coleman & Glashow 1997) or the non-commutative quantum picture of spacetime (Amelio-Camelia et al. 1998).

Radio synchrotron radiation intensity and polarisation surveys of our own and external galaxies (for review see Sofue et al. 1986) have revealed that the interstellar medium is transversely by large-scale ordered magnetic fields with superposed plasma wave turbulence. The Galactic magnetic field has a regular and a random component of about equal strength. The

^{*} Appendices are only available in electronic form at <http://www.aanda.org>

turbulent field has a broad spectrum of scales with the largest one being 10–100 pc (e.g. Beck 2007, and references therein). This could be compared with the gyroradius of ~ 1 pc for 10^{15} eV particles, or ~ 1 kpc for 10^{18} eV particles. The conventional size of the Galactic halo derived from abundances of radioactive isotopes in cosmic rays is about 4–6 kpc (Ptuskin & Soutoul 1998; Strong & Moskalenko 1998; Webber & Soutoul 1998). The turbulent magnetic field may thus present a mechanism for isotropization of Galactic cosmic rays up to 10^{17} – 10^{18} eV (see, e.g., Candia et al. 2003).

According to the current understanding (reviewed in Schlickeiser 2002) the relativistic charged particles (hereafter referred to as cosmic ray particles) in these space plasmas are confined and accelerated by resonant interactions in these weakly random electromagnetic fields. In the presence of low-frequency magnetohydrodynamic plasma waves, whose magnetic field component is much larger than their electric field component, the particle's phase space distribution function adjusts rapidly to a quasi-equilibrium through pitch-angle diffusion, which is close to the isotropic distribution. The isotropic part of the phase space distribution function $F(z, p, t)$ obeys the *diffusion-convection-equation*

$$\begin{aligned} \frac{\partial F}{\partial t} - S_0 = \frac{\partial}{\partial z} \left[\kappa \frac{\partial F}{\partial z} \right] - V \frac{\partial F}{\partial z} \\ + \frac{p}{3} \frac{\partial V}{\partial z} \frac{\partial F}{\partial p} + \frac{1}{p^2} \frac{\partial}{\partial p} \left[p^2 A_M \frac{\partial F}{\partial p} - p^2 \dot{p}_{\text{Loss}} F \right] - \frac{F}{T_c} \end{aligned} \quad (1)$$

where the parallel spatial diffusion coefficient κ , the cosmic ray bulk speed V and the momentum diffusion coefficient A are determined by pitch-angle averages of three Fokker-Planck coefficients

$$\kappa = \frac{v}{3} \lambda = \frac{v^2}{8} \int_{-1}^1 d\mu \frac{(1 - \mu^2)^2}{D_{\mu\mu}(\mu)}, \quad (2)$$

$$V = u + \frac{1}{3p^2} \frac{\partial}{\partial p} (p^3 D), \quad D = \frac{3v}{4p} \int_{-1}^1 d\mu (1 - \mu^2) \frac{D_{\mu p}(\mu)}{D_{\mu\mu}(\mu)}, \quad (3)$$

$$A_M = \frac{1}{2} \int_{-1}^1 d\mu \left[D_{pp}(\mu) - \frac{D_{\mu p}^2(\mu)}{D_{\mu\mu}(\mu)} \right]. \quad (4)$$

In Eq. (1) the space coordinate z is parallel to the uniform background magnetic field \mathbf{B}_0 , S_0 is the source term, \dot{p}_{Loss} and T_c describe continuous and catastrophic momentum loss processes. See also Appendix A for a glossary and definitions of important symbols.

For many years the theoretical development of the resonant wave-particle interactions has mainly concentrated on the special case that the plasma waves propagate only parallel or antiparallel to the ordered magnetic field – the so-called slab turbulence. In this case only cosmic ray particles with gyroradii R_L smaller than the longest parallel wavelength $L_{\parallel, \text{max}}$ of the plasma waves can resonantly interact. Obviously this condition is equivalent to a limit on the maximum particle rigidity R :

$$R = \frac{p}{Z} \leq e B_0 L_{\parallel, \text{max}}. \quad (5)$$

An alternative way to express the condition (5) is

$$E_{15}/Z \leq 40 \cdot \left(\frac{B_0}{4 \mu \text{ G}} \right) \left(\frac{L_{\parallel, \text{max}}}{10 \text{ pc}} \right), \quad (6)$$

where E_{15} denotes the cosmic ray particle energy in units of 10^{15} eV. The limit set by the right hand side of Eq. (6) is referred to as Hillas limit (Hillas 1984). According to this limit, cosmic ray protons of energies larger than $40 \text{ PeV} = 4 \times 10^{16} \text{ eV}$ cannot be confined or accelerated in the Milky Way, and an extragalactic origin for this cosmic ray component has to be invoked. Moreover, as the cosmic ray mean free path in case of spatial gradients is closely related to the cosmic ray anisotropy (Schlickeiser 1989, Eq. (94)), the Hillas limit (6) implies strong anisotropies at energies above 40 PeV which have not been observed by the KASCADE experiment (Antoni et al. 2004; Hörandel et al. 2006).

It is the purpose of this work to investigate how the Hillas limit (6) is affected if we discard the assumption of purely slab plasma waves, i.e. if we allow for oblique propagation angles θ of the plasma waves with respect to the ordered magnetic field component. There is ample observational evidence that obliquely propagating magnetohydrodynamic plasma waves exist in the interstellar medium (Armstrong et al. 1995; Lithwick & Goldreich 2001; Cho et al. 2002). In particular, we will consider the alternative extreme limit that the plasma waves propagation angles are isotropically distributed around the magnetic field direction. It has been emphasised before by Schlickeiser & Miller (1998) referred to as SM) that oblique propagation angles of fast magnetosonic waves leads to an order of magnitude quicker stochastic acceleration rate as compared to the slab case, since the compressional component of the obliquely propagating fast mode waves allows the effect of transit-time damping acceleration of cosmic ray particles. Here we will demonstrate that the obliqueness of fast mode and shear Alfvén wave propagation also modifies the resulting parallel spatial diffusion coefficient and the Hillas limit.

2. Relevant magnetohydrodynamic plasma modes

Most cosmic plasmas have a small value of the plasma beta $\beta_p = c_s^2/V_A^2$, which is defined by the ratio of the ion sound c_s to Alfvén speed V_A , and thus indicates the ratio of thermal to magnetic pressure. For low-beta plasmas the two relevant magnetohydrodynamic wave modes are the

- (1) incompressional *shear Alfvén waves* with dispersion relation

$$\omega_R^2 = V_A^2 k_{\parallel}^2 \quad (7)$$

at parallel wavenumbers $|k_{\parallel}| \ll \Omega_{p,0}/V_A$, which have no magnetic field component along the ordered background magnetic field δB_z ($\parallel \mathbf{B}_0$) = 0,

- (2) the *fast magnetosonic waves* with dispersion relation

$$\omega_R^2 = V_A^2 k^2, \quad k^2 = k_{\parallel}^2 + k_{\perp}^2 \quad (8)$$

for wavenumbers $|k| \ll \Omega_{p,0}/V_A$, which have a compressive magnetic field component $\delta B_z \neq 0$ for oblique propagation angles $\theta = \arccos(k_{\parallel}/k) \neq 0$.

In the limiting case (commonly referred to as slab model) of parallel (to \mathbf{B}_0) propagation ($\theta = k_{\perp} = 0$) the shear Alfvén waves become the left-handed circularly polarised Alfvén-ion-cyclotron waves, whereas the fast magnetosonic waves become the right-handed circularly polarised Alfvén-Whistler-electron-cyclotron waves.

Schlickeiser & Miller (1998) investigated the quasilinear interactions of charged particles with these two plasma waves. In case of negligible wave damping the interactions are of resonant nature: a cosmic ray particle of given velocity v , pitch angle

cosine μ and gyrofrequency $\Omega_c = \Omega_{c,0}/\gamma$ interacts with waves whose wavenumber and real frequencies obey the condition

$$\omega_R(k) = v\mu k_{\parallel} + n\Omega_c, \quad (9)$$

for entire $n = 0, \pm 1, \pm 2, \dots$

2.1. Resonant interactions of shear Alfvén waves

For shear Alfvén waves only interactions with $n \neq 0$ are possible. These are referred to as *gyroresonances* because inserting the dispersion relation (7) in the resonance condition (9) yields for the resonance parallel wavenumber

$$k_{\parallel,A} = \frac{n\Omega_c}{\pm V_A - v\mu}, \quad (10)$$

which apart from very small values of $|\mu| \leq V_A/v$ typically equals the inverse of the cosmic ray particle's gyroradius, $k_{\parallel,A} \simeq n/R_L$ and higher harmonics.

2.2. Resonant interactions of fast magnetosonic waves

In contrast, for fast magnetosonic waves the $n = 0$ resonance is possible for oblique propagation due its compressive magnetic field component. The $n = 0$ interactions are referred to as *transit-time damping*, hereafter TTD. Inserting the dispersion relation (8) into the resonance condition (9) in the case $n = 0$ yields

$$v\mu = \pm V_A / \cos \theta \quad (11)$$

as necessary condition which is independent from the wavenumber value k . Apparently all super-Alfvénic ($v \geq V_A$) cosmic ray particles are subject to TTD provided their parallel velocity $v\mu$ equals at least the wave speeds $\pm V_A$. Hence Eq. (11) is equivalent to the two conditions

$$|\mu| \geq V_A/v, \quad v \geq V_A. \quad (12)$$

Additionally, fast mode waves also allow gyroresonances ($n \neq 0$) at wavenumbers

$$k_F = \frac{n\Omega_c}{\pm V_A - v\mu \cos \theta}, \quad (13)$$

which is very similar to Eq. (10).

2.3. Implications for cosmic ray transport

The simple considerations of the last two subsections allow us the following immediate conclusions:

(1) With TTD-interactions alone, it would not be possible to scatter particles with $|\mu| \leq V_A/v$, i.e., particles with pitch angles near 90° . Obviously, these particles have basically no parallel velocity and cannot catch up with fast mode waves that propagate with the small but finite speeds $\pm V_A$. In particular this implies that with TTD alone it is not possible to establish an isotropic cosmic ray distribution function. Gyroresonances are needed to provide the crucial finite scattering at small values of μ .

(2) Conditions (11) and (12) reveal that TTD is no gyroradius effect. It involves fast mode waves at all wavenumbers provided the cosmic ray particles are super-Alfvénic and have large enough values of μ as required by Eq. (12). Because gyroresonances occur at single resonant wavenumbers only, see Eqs. (10) and (13), their contribution to the value of the Fokker-Planck

coefficients in the interval $|\mu| \geq V_A/v$ is much smaller than the contribution from TTD. Therefore for comparable intensities of fast mode and shear Alfvén waves, TTD will provide the overwhelming contribution to all Fokker-Planck coefficients $D_{\mu\mu}$, $D_{\mu p}$ and D_{pp} in the interval $|\mu| \geq V_A/v$. At small values of $|\mu| < V_A/v$ only gyroresonances contribute to the values of the Fokker-Planck coefficients involving according to Eqs. (10) and (13) wavenumbers at $k_{\parallel,A} = k_R \simeq \pm n\Omega_c/V_A$.

(3) The momentum diffusion coefficient (4)

$$A_M = \frac{1}{2} \int_{-1}^1 d\mu [D_{pp}(\mu) - \frac{D_{\mu p}^2(\mu)}{D_{\mu\mu}(\mu)}] = A_T + A_2 \quad (14)$$

has contributions both from transit-time damping of fast mode waves,

$$A_T \simeq \int_{V_A/v}^1 d\mu D_{pp}^{\text{TTD}}(\mu), \quad (15)$$

and from second-order Fermi gyroresonant acceleration by shear Alfvén waves (Schlickeiser 1989)

$$A_2 = \frac{1}{2} \int_{-1}^1 d\mu \left[D_{pp}^A(\mu) - \frac{[D_{\mu p}^A(\mu)]^2}{D_{\mu\mu}^A(\mu)} \right]. \quad (16)$$

(4) On the other hand, the spatial diffusion coefficient (2)

$$\kappa = \frac{v^2}{8} \int_{-1}^1 d\mu (1 - \mu^2)^2 D_{\mu\mu}^{-1}(\mu) \quad (17)$$

is given by the integral over the *inverse* of the Fokker-Planck coefficient $D_{\mu\mu}$, so here the small values of $D_{\mu\mu}$ due to gyroresonant interactions in the interval $|\mu| < V_A/v$ determine the spatial diffusion coefficient and the corresponding parallel mean free path

$$\kappa = v\lambda/3 \simeq \frac{v^2}{8} \int_{-V_A/v}^{V_A/v} \frac{d\mu}{D_{\mu\mu}^G(\mu)}. \quad (18)$$

The gyroresonances can be due to shear Alfvén waves or fast magnetosonic waves. For relativistic cosmic rays the relevant range of pitch angle cosines $|\mu| \leq v_A/v$ is very small allowing us the approximation $D_{\mu\mu}^G(\mu) \simeq D_{\mu\mu}^G(0)$ so that

$$\kappa = v\lambda/3 \simeq \frac{v^2}{4} \frac{\epsilon}{D_{\mu\mu}^G(0)} = \frac{vV_A}{4D_{\mu\mu}^G(0)}. \quad (19)$$

(5) According to Eq. (90) of Schlickeiser (1989) the streaming cosmic ray anisotropy due to spatial gradients in the cosmic ray density is given by

$$\delta = \frac{F_{\max} - F_{\min}}{F_{\max} + F_{\min}} = \frac{1}{2F} \frac{v}{4} \frac{\partial F}{\partial z} \int_{-1}^1 d\mu (1 - \mu^2) D_{\mu\mu}^{-1}(\mu) \quad (20)$$

which also is determined by the smallest value of $D_{\mu\mu}$ around $\mu = 0$. Approximating again $D_{\mu\mu}(\mu) \simeq D_{\mu\mu}^G(0)$ for $|\mu| \leq \epsilon = V_A/v$ we derive with Eq. (19) the direct proportionality of the cosmic ray anisotropy with the parallel mean free path, i.e.

$$\delta \simeq \frac{v}{8} \frac{\partial F}{\partial \ln z} \frac{2V_A}{vD_{\mu\mu}^G(0)} = \frac{V_A}{4} \frac{1}{D_{\mu\mu}^G(0)} \frac{\partial F}{\partial \ln z} = \frac{1}{3} \lambda \frac{\partial F}{\partial \ln z}. \quad (21)$$

Introducing the characteristic spatial gradient of the cosmic ray density $\langle z \rangle^{-1} \equiv (1/F) |\partial F / \partial z|$ Eq. (21) reads

$$\delta = \frac{\lambda}{3\langle z \rangle}. \quad (22)$$

Cosmic ray gradients derived from diffuse galactic GeV gamma-ray emissivities (Strong & Mattox 1996) suggest a value of $\langle z \rangle \simeq 2$ kpc.

3. Quasilinear cosmic ray mean free path and anisotropy isotropic plasma wave turbulence

Throughout this work we consider isotropic linearly polarised magnetohydrodynamic turbulence so that the components of the magnetic turbulence tensor for plasma mode j is

$$P_{lm}^j(\mathbf{k}) = \frac{g^j(k)}{8\pi k^2} \left(\delta_{lm} - \frac{k_l k_m}{k^2} \right). \quad (23)$$

The magnetic energy density in wave component j then is

$$(\delta B)_j^2 = \int d^3k \sum_{i=1}^3 P_{ii}(\mathbf{k}) = \int_0^\infty dk g^j(k). \quad (24)$$

We adopt a Kolmogorov-like power law dependence (index $q > 1$) of $g^j(k)$ above the minimum wavenumber k_{\min}

$$g^j(k) = g_0^j k^{-q} \quad \text{for } k > k_{\min}. \quad (25)$$

The normalisation (24) then implies

$$g_0^j = (q-1)(\delta B)_j^2 k_{\min}^{q-1}. \quad (26)$$

Moreover we adopt a vanishing cross helicity of each plasma mode, i.e. equal intensity of forward and backward moving waves, so that g_0^j refers to the total energy density of each mode.

According to Eq. (30) of SM the Fokker-Planck coefficients $D_{\mu\mu}^F$ and $D_{pp}^F = \epsilon^2 p^2 D_{\mu\mu}$ with $\epsilon = V_A/v$ for fast mode waves are the sum of contributions from transit-time damping (T) and gyroresonant interactions (G):

$$D_{\mu\mu}^F(\mu) = \frac{\pi\Omega^2(1-\mu^2)}{4B_0^2} [D_T(\mu) + D_G(\mu)] \quad (27)$$

with

$$\begin{aligned} D_T(\mu) &= (q-1)(\delta B)_F^2 |\Omega|^{-1} (R_L k_{\min})^{q-1} H[|\mu| - \epsilon] \\ &\times \frac{1 + (\epsilon/\mu)^2}{|\mu|} [(1-\mu^2)(1 - (\epsilon/\mu)^2)]^{q/2} \\ &\times \int_U^\infty ds s^{-(1+q)} J_1^2(s), \end{aligned} \quad (28)$$

where the lower integration boundary is

$$U = k_{\min} R_L \sqrt{(1-\mu^2)(1 - (\epsilon/\mu)^2)}, \quad (29)$$

and $\eta = \cos \theta$. $R_L = v/|\Omega|$ denotes the gyrofrequency of the cosmic ray particle, H is the Heaviside' step function and $J_1(s)$ is the Bessel function of the first kind.

The gyroresonant contribution from fast mode waves is

$$\begin{aligned} D_G(\mu) &= \frac{q-1}{2} (\delta B)_F^2 k_{\min}^{q-1} \sum_{n=1}^\infty \sum_{j=\pm 1} \int_{-1}^1 d\eta (1+\eta^2) \\ &\times \int_{k_{\min}}^\infty dk k^{-q} [J_n'(k R_L \sqrt{(1-\eta^2)(1-\mu^2)})^2 \\ &\times [\delta(k[v\mu\eta - jV_A] + n\Omega) + \delta(k[v\mu\eta - jV_A] - n\Omega)]. \end{aligned} \quad (30)$$

On the other hand shear Alfvén waves provide only gyroresonant ($n \neq 1$) interactions yielding

$$\begin{aligned} (D_{\mu\mu}^A, D_{\mu p}^A, D_{pp}^A) &= \pi(q-1)\Omega^2(1-\mu^2) k_{\min}^{q-1} \frac{(\delta B)_A^2}{32B_0^2} \sum_{n=1}^\infty \\ &\times \sum_{j=\pm 1} ([1-j\mu\epsilon]^2, j\epsilon p[1-j\mu\epsilon], (\epsilon p)^2) \int_{-1}^1 d\eta (1+\eta^2) \\ &\times \int_{k_{\min}}^\infty dk k^{-q} [\delta([v\mu - jV_A]\eta k + n\Omega) \\ &+ \delta([v\mu - jV_A]\eta k - n\Omega)] \left[(J_{n-1}(k R_L \sqrt{(1-\mu^2)(1-\eta^2)}) \right. \\ &\left. + J_{n+1}(k R_L \sqrt{(1-\mu^2)(1-\eta^2)}) \right]^2. \end{aligned} \quad (31)$$

According to SM at particle pitch-angles outside the interval $|\mu| \geq \epsilon$ transit-time damping provides the dominant and overwhelming contribution to these Fokker-Planck coefficients. This justifies the approximations to derive Eqs. (19) and (21) for the cosmic ray mean free path and anisotropy, respectively. Both transport parameters are primarily fixed by the small but finite scattering due to gyroresonant interactions in the interval $|\mu| < \epsilon$. We then derive

$$\begin{aligned} \lambda &\simeq \frac{3v}{8} \int_{-\epsilon}^\epsilon d\mu (1-\mu^2)^2 [D_{\mu\mu}^F(\mu) + D_{\mu\mu}^A(\mu)]^{-1} \\ &\simeq \frac{3v\epsilon}{4[D_{\mu\mu}^F(\mu=0) + D_{\mu\mu}^A(\mu=0)]}, \end{aligned} \quad (32)$$

and

$$\delta = \frac{1}{3} \lambda \frac{\partial F}{\partial \ln z} \simeq \frac{v\epsilon}{4[D_{\mu\mu}^F(\mu=0) + D_{\mu\mu}^A(\mu=0)]} \frac{\partial F}{\partial \ln z}. \quad (33)$$

In the following, we consider both transport coefficients for positively charged cosmic ray particles with $\Omega > 0$ especially in the limit $k_{\min} R_L \gg 1$.

3.1. Gyroresonant Fokker-Planck coefficients at $\mu = 0$

At $\mu = 0$ the contribution from shear Alfvén waves to the pitch-angle Fokker-Planck coefficient is according to Eq. (23)

$$\begin{aligned} D_{\mu\mu}^A(\mu=0) &\simeq \frac{\pi(q-1)\Omega^2 k_{\min}^{q-1} (\delta B)_A^2}{16B_0^2} \sum_{n=1}^\infty \int_{k_{\min}}^\infty dk k^{-q-1} \\ &\times \left(1 + \frac{n^2 \Omega^2}{V_A^2 k^2} \right) H \left[k - \frac{n\Omega}{V_A} \right] \left[J_{n-1} \left(R_L \sqrt{k^2 - \frac{n^2 \Omega^2}{V_A^2}} \right) \right. \\ &\left. + J_{n+1} \left(R_L \sqrt{k^2 - \frac{n^2 \Omega^2}{V_A^2}} \right) \right]^2, \end{aligned} \quad (34)$$

where we readily performed the η -integration. Substituting $t = R_L [k^2 - (n^2 \Omega^2 / V_A^2)]^{1/2}$, and using $V_A/\Omega = \epsilon R_L$, Eq. (34) reduces to

$$\begin{aligned} D_{\mu\mu}^A(\mu=0) &\simeq \frac{\pi(q-1)\Omega(\delta B)_A^2}{16\epsilon B_0^2} [k_{\min} R_L]^{q-1} \sum_{n=1}^\infty \int_{U_A}^\infty dt t \\ &\times \left(t^2 + \frac{2n^2}{\epsilon^2} \right) \left[t^2 + \frac{n^2}{\epsilon^2} \right]^{-(q+4)/2} (J_{n-1}(t) + J_{n+1}(t))^2 \end{aligned} \quad (35)$$

where

$$U_A = \max\left(0, \left[R_L^2 k_{\min}^2 - \frac{n^2}{\epsilon^2}\right]^{1/2}\right). \quad (36)$$

Likewise the contribution from gyroresonant interactions with fast mode waves is according to Eqs. (27) and (30)

$$D_{\mu\mu}^F(\mu = 0) \simeq \frac{\pi(q-1)\Omega^2 k_{\min}^{q-1} (\delta B)_F^2}{4V_A B_0^2} \left[\frac{V_A}{\Omega}\right]^q \sum_{n=1}^{\infty} \times n^{-q} H\left[n - \frac{k_{\min} V_A}{\Omega}\right] \int_{-1}^1 d\eta (1 + \eta^2) \left(J'_n\left(\frac{n}{\epsilon} \sqrt{1 - \eta^2}\right)\right)^2 \quad (37)$$

where we performed the k -integration. With $V_A/\Omega = \epsilon R_L$, Eq. (37) becomes

$$D_{\mu\mu}^F(\mu = 0) \simeq \frac{\pi(q-1)\Omega(\delta B)_F^2}{4B_0^2} [k_{\min} R_L \epsilon]^{q-1} \sum_{n=1}^{\infty} n^{-q} \times H[n - \epsilon R_L k_{\min}] \int_{-1}^1 d\eta (1 + \eta^2) \left(J'_n\left(\frac{n}{\epsilon} \sqrt{1 - \eta^2}\right)\right)^2. \quad (38)$$

The Bessel function integral in Eq. (38)

$$I_1 = \int_{-1}^1 d\eta (1 + \eta^2) \left(J'_n\left(\frac{n}{\epsilon} \sqrt{1 - \eta^2}\right)\right)^2 \quad (39)$$

has been calculated asymptotically by SM to lowest order in the small quantity $\epsilon = V_A/v \ll 1$ as

$$I_1 \simeq \frac{3}{2} \frac{\epsilon}{n} \quad (40)$$

yielding

$$D_{\mu\mu}^F(\mu = 0) \simeq \frac{3\pi(q-1)\Omega\epsilon(\delta B)_F^2}{4B_0^2} [k_{\min} R_L \epsilon]^{q-1} \times \sum_{n=1}^{\infty} n^{-(q+1)} H[n - \epsilon R_L k_{\min}]. \quad (41)$$

In Appendix B we evaluate the Bessel function integral in Eq. (35)

$$I_2 = \int_{U_A}^{\infty} dt t \left(t^2 + \frac{2n^2}{\epsilon^2}\right) \left[t^2 + \frac{n^2}{\epsilon^2}\right]^{-(q+4)/2} \times (J_{n-1}(t) + J_{n+1}(t))^2 \quad (42)$$

for small and large values of $k_{\min} R_L \epsilon$.

For values $k_{\min} R_L \epsilon \leq 1$ we obtain approximately

$$I_2(k_{\min} R_L \epsilon \leq 1) \simeq \frac{8}{\pi} \epsilon^{q+2} n^{-q} [1 + (-1)^n 1.00813] \quad (43)$$

yielding

$$D_{\mu\mu}^A(\mu = 0, k_{\min} R_L \epsilon \leq 1) \simeq \frac{(q-1)\Omega\epsilon^2(\delta B)_A^2}{2^{1+q} B_0^2} \times [k_{\min} R_L \epsilon]^{q-1} [2.00813\zeta(q) + 0.00813\zeta(q, 0.5)], \quad (44)$$

in terms of the zeta and the generalised zeta functions of Riemann (Whittaker & Watson 1978).

For values of $k_{\min} R_L \epsilon > 1$ we obtain Eq. (43) for values of $n \geq N+1$, where $N = \inf[k_{\min} R_L \epsilon]$ is the largest integer smaller than $\epsilon R_L k_{\min}$, while for smaller n

$$I_2(k_{\min} R_L \epsilon > 1, n = N) \simeq 4\epsilon^{q+2} N^{-(q+1)} \quad (45)$$

and

$$I_2(k_{\min} R_L \epsilon > 1, n \leq N-1) \simeq \frac{4n^2}{\pi(q+3)} U_A^{-(q+3)}. \quad (46)$$

According to Eq. (35) this yields

$$D_{\mu\mu}^A(\mu = 0, k_{\min} R_L \epsilon > 1) \simeq \frac{(q-1)\Omega\epsilon^2(\delta B)_A^2}{2B_0^2} [k_{\min} R_L \epsilon]^{q-1} \left[\frac{\pi}{2N^{q+1}} + \frac{\epsilon}{2(q+3)} \sum_{n=1}^{N-1} n^{-(q+1)} \left[\left(\frac{R_L k_{\min} \epsilon}{n} \right)^2 - 1 \right]^{-(q+3)/2} + \sum_{n=N+1}^{\infty} n^{-q} [1 + (-1)^n 1.00813] \right]. \quad (47)$$

Comparing the Fokker-Planck coefficients from fast mode waves (41) and Alfvén waves (Eqs. (44) and (47)) we note that the latter one is always smaller by the small ratio $\epsilon = V_A/v$ than the first one:

$$D_{\mu\mu}^A(\mu = 0) \simeq \epsilon D_{\mu\mu}^F(\mu = 0) \quad (48)$$

so that the gyroresonant contribution from Alfvén waves can be neglected in comparison to the gyroresonant contribution from fast mode waves.

3.2. Cosmic ray mean free path

Neglecting $D_{\mu\mu}^A(\mu = 0)$ we obtain for the cosmic ray mean free path (32)

$$\lambda(\gamma) \simeq \frac{3v\epsilon}{4D_{\mu\mu}^F(\mu = 0)} = \frac{1}{\pi(q-1)} \frac{B_0^2}{(\delta B)_F^2} \frac{R_L (k_{\min} R_L \epsilon)^{1-q}}{\sum_{n=1}^{\infty} n^{-(q+1)} H[n - \epsilon R_L k_{\min}]}, \quad (49)$$

which exhibits the familiar Lorentzfator dependence $\propto \beta\gamma^{2-q} \simeq \gamma^{2-q}$ at Lorentzfactors $\gamma \leq \gamma_c$ below a critical Lorentz factor defined by

$$\gamma_c = k_c/k_{\min} \quad (50)$$

with $k_c = \Omega_{0,p}/V_A = \omega_{p,i}/c$ being the inverse ion skin length. The Lorentzfator dependence $\lambda \propto \gamma^{2-q}$ especially holds at rigidities $1 \leq k_{\min} R_L \leq \epsilon = c/V_A$, in a rigidity range where the slab turbulence model would predict an infinitely large mean free path.

Expressing $k_{\min} = 2\pi/L_{\max}$ in terms of the longest wavelength of isotropic fast mode waves $L_{\max} = 10$ pc yields

$$\gamma_c = \frac{\omega_{p,i} L_{\max}}{2\pi c} = 2.16 \times 10^{11} n_e^{1/2} \left(\frac{L_{\max}}{10 \text{ pc}} \right). \quad (51)$$

The corresponding cosmic ray hadron energy is

$$E_c = A\gamma_c m_p c^2 = 2.03 \times 10^5 A n_e^{1/2} \left(\frac{L_{\max}}{10 \text{ pc}} \right) \text{ PeV} \quad (52)$$

which is four orders of magnitude larger than the Hillas limit (6) for equal values of the maximum wavelength. This difference demonstrates the dramatic influence of the plasma turbulence geometry (slab versus isotropically distributed waves) on the confinement of cosmic rays in the Galaxy. With isotropically distributed fast mode waves, even ultrahigh energy cosmic rays obey the scaling $\lambda\gamma^{q-2} = \text{const.}$

Only, at ultrahigh Lorentz factors $\gamma > \gamma_c$ or energies $E > E_c$ the mean free path (49) approaches the much steeper dependence

$$\lambda(\gamma > \gamma_c) \simeq \frac{1}{\pi(q-1)} \frac{B_0^2}{(\delta B)_F^2} R_L (k_{\min} R_L \epsilon)^2 \propto \beta \gamma^3 \simeq \gamma^3, \quad (53)$$

independent from the turbulence spectral index q . Here the mean free path quickly attains very large values greater than the typical scales of the Galaxy.

3.3. Anisotropy

Because of the direct proportionality between mean free path and anisotropy, the cosmic ray anisotropy (33) shows the same behaviour as a function of energy:

$$\delta(E) \simeq \frac{1}{3\pi(q-1)} \frac{B_0^2}{(\delta B)_F^2} \frac{\partial F}{\partial \ln z} \times \frac{R_L (k_{\min} R_L \epsilon)^{1-q}}{\sum_{n=1}^{\infty} n^{-(q+1)} H[n - \epsilon R_L k_{\min}]} \quad (54)$$

which is proportional $\delta(E \leq E_c) \propto E^{2-q}$ at energies below E_c and $\delta(E > E_c) \propto E^3$ at energies above E_c . In particular we obtain no drastic change in the energy dependence of the anisotropy at PeV energies. Quantitatively, with Eq. (22), $q = 5/3$ and $V_A = 20 \text{ km s}^{-1}$ we find

$$\delta(E) = 0.152 \left(\frac{L_{\max}}{10 \text{ pc}} \right) \left(\frac{\langle z \rangle}{2 \text{ kpc}} \right)^{-1} \left(\frac{(B_0/\delta B)_F}{10} \right)^2 \times \frac{(E/E_c)^{1/3}}{\sum_{n=1}^{\infty} n^{-(8/3)} H[n - (E/E_c)]}. \quad (55)$$

At $E_c = 20 \text{ EeV}$ energies we calculate an anisotropy of less than 15 percent, whereas at smaller energies the anisotropy values decrease proportional to $(E/E_c)^{1/3}$.

4. Summary and conclusions

We have investigated the implications of isotropically distributed interstellar magnetohydrodynamic plasma waves on the scattering mean free path and the spatial anisotropy of high-energy cosmic rays. We demonstrate a drastic modification of the energy dependence of both cosmic ray transport parameters compared to previous calculations that have assumed that the plasma waves propagate only parallel or antiparallel to the ordered magnetic field (slab turbulence). In case of slab turbulence cosmic rays with Larmor radius R_L resonantly interact with plasma waves with wave vectors at $k_{\text{res}} = R_L^{-1}$. If the slab wave turbulence power spectrum vanishes for wavenumbers less than k_{\min} , as a consequence then cosmic rays with Larmor radii larger than k_{\min}^{-1} cannot be scattered in pitch-angle, causing the so-called Hillas limit for the maximum energy $E_{15}^H = 40Z \cdot (B_0/4 \mu\text{G})(L_{\parallel, \max}/10 \text{ pc})$ of cosmic rays being confined in the Galaxy. At about these energies this would imply a drastic increase in the spatial anisotropy of cosmic rays that has not been detected by KASCADE and other air shower experiments.

In case of isotropically distributed interstellar magnetohydrodynamic waves we demonstrated that the Hillas energy E^H is modified to a limiting total energy that is about 4 orders of magnitude larger $E_c = 2.03 \times 10^5 A n_e^{1/2} (L_{\max}/10 \text{ pc}) \text{ PeV}$, where A denotes the mass number and L_{\max} the maximum wavenumber of isotropic plasma waves. Below this energy the cosmic ray mean free path and the anisotropy exhibit the well known E^{2-q} energy

dependence, where $q = 5/3$ denotes the spectral index of the Kolmogorov spectrum. At energies higher than E_c both transport parameters steepen to a E^3 -dependence. This implies that cosmic rays even with ultrahigh energies of several tens of EeV can be rapidly pitch-angle scattered by interstellar plasma turbulence, and are thus confined to the Galaxy.

The physical reason for the four orders of magnitude higher value of the limiting energy is the occurrence of dominating transit-time damping interactions of cosmic rays with magnetosonic plasma waves due to their compressive magnetic field component along the ordered magnetic field. This $n = 0$ resonance is not a gyroresonance implying that cosmic rays interact with plasma waves at all wavenumbers provided that the cosmic ray parallel speed (transit speed) equals the parallel phase speed of magnetosonic waves. Only at small values of the cosmic ray pitch-angle cosine $|\mu| \leq \epsilon = V_A/v$, where the cosmic ray particles spiral at nearly ninety degrees with very small parallel speeds less than the minimum magnetosonic phase speed V_A , gyroresonant interactions are necessary to scatter cosmic rays. However, the gyroresonance condition of cosmic rays at $\mu = 0$ reads $k_{\text{res}} = (R_L \epsilon)^{-1}$ instead of the slab condition $k_{\text{res}} = (R_L)^{-1}$ causing the limiting energy enhancement from E^H to E_c by the large factor $\epsilon^{-1} = c/V_A \simeq \mathcal{O}(10^4)$.

Acknowledgements. Partial support by the Deutsche Forschungsgemeinschaft through Sonderforschungsbereich 591 is acknowledged.

References

- Abramowitz, M., & Stegun, I. A. 1972, *Handbook of Mathematical Functions* (Washington: National Bureau of Standards)
- Aharonian, F., Akhperjanian, A. G., Aye, K.-M., et al. 2004, *Nature*, 432, 75
- Aharonian, F., Akhperjanian, A. G., Aye, K.-M., et al. 2005, *A&A*, 437, L7
- Allen, G. E., Keohane, J. W., Gotthelf, E. V., et al. 1997, *ApJ*, 487, L97
- Amelio-Camelia, G., Ellis, J., Mavromatos, N. E., Nanopoulos, D. V., & Srakar, S. 1998, *Nature*, 393, 763
- Antoni, T., Apel, W. D., Badea, A. F., et al. 2004, *ApJ*, 604, 687
- Armstrong, J. W., Rickett, B. J., & Spangler, S. R. 1995, *ApJ*, 443, 209
- Beck, R. 2007, *EAS Publ. Ser.*, 23, 19 [arXiv:astro-ph/0603531]
- Bell, A. R., & Lucek, S. G. 2001, *MNRAS*, 321, 433
- Blandford, R. D., & Eichler, D. 1987, *Phys. Rep.*, 154, 1
- Borkowski, K. J., Rho, J., Reynolds, S. P., & Dyer, K. K. 2001, *ApJ*, 550, 334
- Büsching, I., Pohl, M., & Schlickeiser, R. 2001, *A&A*, 377, 1056
- Candia, J., Mollerach, S., & Roulet, E. 2003, *JCAP*, 5, 3
- Coleman, S., & Glashow, S. L. 1997, *Phys. Lett. B*, 405, 249
- Cho, Y., Lazarian, A., & Vishniac, E. 2002, *ApJ*, 566, 49
- Enomoto, R., Tanimori, T., Naito, T., et al. 2002, *Nature*, 416, 823
- Hillas, A. M. 1984, *ARA&A*, 22, 425
- Hillas, A. M. 2006, *J. Phys.: Conf. Ser.*, 47, 168
- Hörandel, J. R., Kalmykov, N. N., Timokhin, A. V. 2006, *J. Phys. Conf. Ser.*, 47, 132
- Koyama, K., Petre, R., Gotthelf, E. V., et al. 1995, *Nature*, 378, 255
- Koyama, K., Kinugasa, K., Matsuzaki, K., et al. 1997, *PASJ*, 49, L7
- Lithwick, Y., & Goldreich, P. 2001, *ApJ*, 567, 479
- Lucek, S. G., & Bell, A. R. 2000, *MNRAS*, 314, 65
- Ptuskín, V. S., & Soutoul, A. 1998, *A&A*, 337, 859
- Reimer, O., & Pohl, M. 2002, *A&A*, 390, L43
- Schlickeiser, R. 1989, *ApJ*, 336, 243
- Schlickeiser, R. 2002, *Cosmic Ray Astrophysics* (Berlin: Springer)
- Schlickeiser, R., & Miller, J. A. 1998, *ApJ*, 492, 352 (SM)
- Slane, P., Gaensler, B. M., Dame, T. M., et al. 1999, *ApJ*, 525, 357
- Sofue, Y., Fujimoto, M., & Wielebinski, R. 1986, *ARA&A*, 24, 459
- Strong, A. W., & Mattox, J. R. 1996, *A&A*, 308, L21
- Strong, A. W., & Moskalenko, I. V. 1998, *ApJ*, 509, 212
- Strong, A. W., Moskalenko, I. V., & Reimer, O. 2004, *ApJ*, 613, 962
- Tanimori, T., Hayami, Y., Kamei, S., et al. 1998, *ApJ*, 497, L25
- Turner, M. S., et al. 2002, *Report to the National Academy of Science*
- Webber, W. R., & Soutoul, A. 1998, *ApJ*, 506, 335
- Whittaker, E. T., & Watson, G. N. 1978, *A Course of Modern Analysis* (Cambridge: Cambridge University Press)

Online Material

Appendix A: Glossary and definitions of important symbols

$A = m/m_p$: cosmic ray particle mass or nucleon number

A_M : momentum diffusion coefficient of cosmic rays

β : cosmic ray velocity in units of c

$\beta_p = c_S^2/V_A^2$: plasma beta

B_0 : uniform magnetic field strength

δB : strength of total fluctuating magnetic fields

δB_F : strength of fast magnetosonic plasma wave magnetic fields

δB_A : strength of shear Alfvén plasma wave magnetic fields

c : vacuum speed of light

$c_S = \sqrt{2k_B T/m_p}$: ion sound speed

$\gamma = E/mc^2 = (1 - \beta^2)^{-1/2}$: cosmic ray Lorentz factor

$\gamma_c = E_c/mc^2$: critical cosmic ray Lorentz factor where the energy dependence of the mean free path changes

D_{ij} : Fokker-Planck coefficient

$\delta(p)$: cosmic ray anisotropy

$E = \gamma mc^2$: total kinetic energy of cosmic ray particle

$E_c = \gamma_c mc^2$: critical cosmic ray total kinetic energy where the energy dependence of the mean free path changes

$\epsilon = V_A/c$: ratio of Alfvén speed to speed of light

$F(z, p, t)$: isotropic part of cosmic ray phase space density

$g^j(k) \propto k^{-q}$: magnetic field turbulence spectrum of plasma wave mode j

$J_n(x)$: Bessel function of first kind and order n

$\mathbf{k} = (k_x, k_y, k_z)$: plasma wave vector and its cartesian components

$k_{\parallel} = k_z = k \cos \theta$: component of plasma wave vector parallel to uniform magnetic field

$k_{\perp} = \sqrt{k_x^2 + k_y^2} = k \sin \theta$: component of plasma wave vector perpendicular to uniform magnetic field

$k_{\min} = 2\pi/\lambda_{\max}$: minimum wavenumber of plasma waves

$k_c = \omega_{p,i}/c$: inverse ion skin length

$\kappa = v\lambda/3$: spatial diffusion coefficient of cosmic rays parallel to uniform magnetic field

$\lambda = 3\kappa/v$: parallel mean free path of cosmic rays

$\lambda_{\max} = 2\pi/k_{\min}$: maximum wavenumber of plasma waves

L_{\max} : maximum wavenumber of isotropic fast magnetosonic waves

$L_{\parallel, \max}$: maximum wavenumber of parallel propagating (slab) plasma waves

$m = Am_p$: mass of cosmic ray particle

m_p : proton mass

$\mu = p_{\parallel}/p$: pitch angle cosine of cosmic ray particle

n_e : number density of electrons in interstellar medium

ω_R : real part of plasma wave frequency

$\omega_{p,i} = \sqrt{4\pi n_e e^2/m_p}$: proton plasma frequency in interstellar ionized gas

$\Omega_{c,0} = |ZeB_0/mc|$: nonrelativistic gyrofrequency of cosmic ray particle in uniform magnetic field B_0

$\Omega_c = \Omega_{c,0}/\gamma$: relativistic gyrofrequency of cosmic ray particle in uniform magnetic field B_0

$\Omega_{p,0} = eB_0/m_p c$: nonrelativistic gyrofrequency of proton in uniform magnetic field B_0

p : total momentum of cosmic ray particle

\dot{p}_{Loss} : continuous momentum loss rate of cosmic ray particle

$P_{lm}^j(\mathbf{k})$: magnetic turbulence tensor for plasma mode j

q : spectral index of turbulence power law spectrum

$R = p/Z$: rigidity of cosmic ray particle

$R_L = v/\Omega_c$: gyroradius of cosmic ray particle in uniform magnetic field B_0

T : temperature of interstellar gas

T_c : catastrophic loss time of cosmic ray particle

$\theta = \arccos(k_{\parallel}/k)$: propagation angle of plasma wave with respect to uniform magnetic field direction

u : velocity of plasma wave-carrying interstellar gas

$v = \beta c$: velocity of cosmic ray particle

V : cosmic ray bulk speed

$V_A = B_0/\sqrt{4\pi m_p n_e}$: Alfvén velocity

Z : cosmic ray particle charge or atomic number

Appendix B: Asymptotic calculation of the integral (42)

The task is to calculate the integral (42)

$$I_2 = \int_{U_A}^{\infty} dt t \left(t^2 + \frac{2n^2}{\epsilon^2} \right) \left[t^2 + \frac{n^2}{\epsilon^2} \right]^{-(q+4)/2} \left[(J_{n-1}(t) + J_{n+1}(t))^2 \right], \quad (56)$$

for small and large values of $k_{\min} R_L$ using the approximations of Bessel functions for small and large arguments (Abramowitz & Stegun 1972), yielding

$$J_n^2(t \ll 1) \simeq \frac{t^{2n}}{2^{2n} \Gamma^2[n+1]}, \quad (57)$$

and

$$J_n^2(t \gg 1) \simeq \frac{1}{\pi t} [1 + (-1)^n \sin(2t)]. \quad (58)$$

According to Eq. (36)

$$U_A = \max \left(0, \left[R_L^2 k_{\min}^2 - \frac{n^2}{\epsilon^2} \right]^{1/2} \right),$$

the lower integration boundary $U_A = 0$ in the case $k_{\min} R_L \epsilon \leq 1$ which includes in particular the limit $k_{\min} R_L \ll 1$ because $\epsilon \ll 1$.

4.1. Case $k_{\min} R_L \epsilon \leq 1$

With the identity

$$J_{n-1}(t) + J_{n+1}(t) = \frac{2n J_n(t)}{t} \quad (59)$$

we obtain

$$I_2(k_{\min} R_L \epsilon \leq 1) = 4n^2 \left[W \left[\frac{q+2}{2} \right] + \frac{n^2}{\epsilon^2} W \left[\frac{q+4}{2} \right] \right] \quad (60)$$

where

$$W[\alpha] \equiv \int_0^{\infty} dt t^{-1} \frac{J_n^2(t)}{\left[t^2 + \frac{n^2}{\epsilon^2} \right]^\alpha}. \quad (61)$$

With the asymptotics (57) and (58) we obtain

$$\begin{aligned} W[\alpha] &\simeq \left(\frac{\epsilon}{n} \right)^{2\alpha} \left[\frac{1}{2^{2n} \Gamma^2[n+1]} \int_0^1 dt t^{2n-1} \right. \\ &\quad \left. + \frac{1}{\pi} \int_1^{n/\epsilon} dt t^{-2} [1 + (-1)^n \sin(2t)] \right. \\ &\quad \left. + \frac{1}{\pi} \int_{n/\epsilon}^{\infty} dt t^{-2(1+\alpha)} [1 + (-1)^n \sin(2t)] \right] \\ &\simeq \left(\frac{\epsilon}{n} \right)^{2\alpha} \left[\frac{1}{\pi} \left[1 + (-1)^n 1.00813 - \frac{\epsilon}{n} \right. \right. \\ &\quad \left. \left. - \frac{(-1)^n}{2} \left(\frac{\epsilon}{n} \right)^2 \cos \left(\frac{2n}{\epsilon} \right) \right] + \frac{1}{n 2^{2n+1} \Gamma^2[n+1]} \right] \\ &\quad + \frac{1}{\pi(1+2\alpha)} \left(\frac{\epsilon}{n} \right)^{1+2\alpha} + \frac{(-1)^n}{\pi} j_1, \end{aligned} \quad (62)$$

where we use

$$2 \int_1^{\infty} dx x^{-2} \sin x = 2(\sin(1) - Ci(1)) = 1.00813$$

and where

$$\begin{aligned} j_1 &= \int_{n/\epsilon}^{\infty} dt t^{-2-2\alpha} \sin 2t = 2^{2\alpha} \left[i^{-2-2\alpha} \Gamma \left[-(1+2\alpha), -2i \frac{n}{\epsilon} \right] \right. \\ &\quad \left. + (-i)^{-2-2\alpha} \Gamma \left[-(1+2\alpha), 2i \frac{n}{\epsilon} \right] \right] \end{aligned} \quad (63)$$

in terms of the incomplete gamma function. For large arguments $(n/\epsilon) \gg 1$ we obtain asymptotically

$$j_1 \simeq \frac{1}{2} \left(\frac{\epsilon}{n} \right)^{2+2\alpha} \cos \left(\frac{2n}{\epsilon} \right). \quad (64)$$

Collecting terms we find to lowest order in $\frac{\epsilon}{n} \ll 1$

$$W[\alpha] \simeq \frac{1}{\pi} \left(\frac{\epsilon}{n} \right)^{2\alpha} \left[1 + (-1)^n 1.00813 + \frac{\pi}{n 2^{2n+1} \Gamma^2[n+1]} \right] \quad (65)$$

so that

$$\begin{aligned} I_2(k_{\min} R_L \epsilon \leq 1) &\simeq \frac{8}{\pi} \epsilon^{q+2} n^{-q} \\ &\times \left[1 + (-1)^n 1.00813 + \frac{\pi}{n 2^{2n+1} \Gamma^2[n+1]} \right]. \end{aligned} \quad (66)$$

4.2. Case $k_{\min} R_L \epsilon > 1$

In this case $U_A = 0$ for $n \geq N+1$, and $U_A = \sqrt{(R_L k_{\min})^2 - (n/\epsilon)^2}$ for $n \leq N$, where

$$N = \inf[\epsilon R_L k_{\min}] \quad (67)$$

denotes the largest integer smaller than $\epsilon R_L k_{\min}$. Hence we obtain again Eq. (66) for $n \geq N+1$

$$\begin{aligned} I_2(k_{\min} R_L \epsilon > 1, n \geq N+1) &\simeq \frac{8}{\pi} \epsilon^{q+2} n^{-q} \\ &\times \left[1 + (-1)^n 1.00813 + \frac{\pi}{n 2^{2n+1} \Gamma^2[n+1]} \right]. \end{aligned} \quad (68)$$

For values of $n \leq N$ we find that

$$I_2(k_{\min} R_L \epsilon > 1, n \leq N) = 4n^2 \left[V \left[\frac{q+2}{2} \right] + \frac{n^2}{\epsilon^2} V \left[\frac{q+4}{2} \right] \right] \quad (69)$$

where

$$V[\alpha] \equiv \int_{U_A}^{\infty} dt t^{-1} \frac{J_n^2(t)}{\left[t^2 + \frac{n^2}{\epsilon^2} \right]^\alpha} = \left(\frac{\epsilon}{n} \right)^{2\alpha} \int_{\epsilon U_A/n}^{\infty} dt t^{-1} \frac{J_n^2(nt/\epsilon)}{[1+t^2]^\alpha}. \quad (70)$$

We may express

$$k_{\min} R_L \epsilon = N(1 + \phi) \quad (71)$$

with $\phi < 1/N$, so that the lower integration boundary in (70) is

$$\begin{aligned} \frac{\epsilon}{n} U_A &= \left[\left(\frac{k_{\min} R_L \epsilon}{n} - 1 \right) \left(\frac{k_{\min} R_L \epsilon}{n} + 1 \right) \right]^{1/2} \\ &= \frac{N}{n} \left[\left(1 + \phi - \frac{n}{N} \right) \left(1 + \phi + \frac{n}{N} \right) \right]^{1/2}. \end{aligned} \quad (72)$$

In cases where $N \geq 2$, Eq. (72) yields that for all values of n such that $1 \leq n \leq N - 1$ the lower integration boundary $\frac{\epsilon}{N} U_A$ is greater unity. Using the expansion (58) in this case we find that

$$\begin{aligned} V[\alpha, n \leq N - 1] &\simeq \frac{1}{\pi} \left(\frac{\epsilon}{N} \right)^{2\alpha+1} \int_{\epsilon U_A/N}^{\infty} dt t^{-2-2\alpha} \\ &\times \left[1 + (-1)^n \sin \left(\frac{2nt}{\epsilon} \right) \right] \simeq \frac{1}{\pi(1+2\alpha)} U_A^{-(2\alpha+1)} \\ &\times \left[1 + (-1)^n \frac{1+2\alpha}{2U_A} \cos(2U_A) \right] \simeq \frac{U_A^{-(2\alpha+1)}}{\pi(1+2\alpha)} \end{aligned} \quad (73)$$

In the remaining case $n = N$ the lower integration boundary (72)

$$\frac{\epsilon}{N} U_A = \sqrt{\phi(2+\phi)} \leq \sqrt{2.5\phi} < 1 \quad (74)$$

is smaller unity, so that we approximate Eq. (70) in this case by

$$\begin{aligned} V[\alpha, n = N] &\simeq \left(\frac{\epsilon}{N} \right)^{2\alpha} \left[\int_{\epsilon U_A/N}^1 dt t^{-1} J_N^2 \left(\frac{Nt}{\epsilon} \right) \right. \\ &+ \left. \int_1^{\infty} dt t^{-1-2\alpha} J_N^2 \left(\frac{Nt}{\epsilon} \right) \right] \simeq \left(\frac{\epsilon}{N} \right)^{2\alpha} \\ &\times \left[j_2 + \frac{\epsilon}{\pi N(1+2\alpha)} \left(1 + (-1)^n (1+2\alpha) \frac{\epsilon}{2N} \cos \left(\frac{2N}{\epsilon} \right) \right) \right] \end{aligned} \quad (75)$$

where we approximate

$$\begin{aligned} j_2 &= \int_{\epsilon U_A/N}^1 dt t^{-1} J_N^2 \left(\frac{Nt}{\epsilon} \right) < \\ &\int_0^{\infty} dt t^{-1} J_N^2 \left(\frac{Nt}{\epsilon} \right) = \frac{1}{2N} \end{aligned} \quad (76)$$

by its upper limit to obtain

$$V[\alpha, n = N] \simeq \frac{\left(\frac{\epsilon}{N} \right)^{2\alpha}}{2N}. \quad (77)$$

Collecting terms in Eq. (69) we derive

$$I_2(k_{\min} R_L \epsilon > 1, n = N) \simeq 4\epsilon^{q+2} N^{-(q+1)} \quad (78)$$

and

$$I_2(k_{\min} R_L \epsilon > 1, n \leq N - 1) \simeq \frac{4n^2}{\pi(q+3)} U_A^{-(q+3)} \quad (79)$$

SPIRAL SOLITON SOLUTION FOR DISK GALAXIES

M. Savković¹ and Z. Yoshida²¹ *Studentska 43, 11070 Belgrade, Serbia and Montenegro*² *Graduate School of Frontier Sciences, The University of Tokyo, Tokyo 113-656, Japan*

(Received: September 10, 2003; Accepted: November 5, 2003)

SUMMARY: In this paper, weakly nonlinear dynamics of spiral galaxies is studied, using reductive perturbation method. One primarily aims at the derivation of possible soliton solution for two dimensional geometry, in the state of marginal stability. In order to use proper coordinate transformation, it was necessary to analyze stability of the linearized system of equations, and to define proper parameter regime. Such parameter regime is in agreement with the observational data, too. The influence of finite-thickness of the galaxy disk on dispersive properties of the system is studied, extending approximate solution of Poisson's equation. For both cases, infinitesimally thin disk and disk of finite thickness, the same type of NLS equation is derived, but with different coefficients for nonlinear and dispersive terms. This means that corresponding soliton solutions have different properties. By comparing soliton properties with observational data it is possible to control validity of approximation for different geometry of the model.

Key words. Galaxies: spiral – Galaxies: kinematics and dynamics – Methods: analytical

1. INTRODUCTION

Spirals are rather common structures produced in many different systems such as atmospheric flows, some self-catalyzed chemical reactions, a variety of networks (neurons, circuits or ecosystems), and some life forms. The seminal work of Lin and Shu (Bertin 2000) succeeded in producing a spiral solution of a linearized density wave equation. In the present work, we consider a nonlinear dispersive wave model to study nearly collisionless dynamics of the spiral galaxies, using reductive perturbation method (Jaffrey and Taniuti 1964), with the emphasis on possible soliton solutions. Two different geometries of the disk are discussed, and the corresponding solutions of the nonlinear equation are given.

2. GOVERNING EQUATIONS

The density wave model consists of transport equations for the mass density ρ and the momentum ρv , together with the Poisson's equation that relates the density to the gravitational potential ϕ . The equilibrium state of the system is described as a rotation with an angular velocity $\Omega(r)$ about z-axis under the balance of centrifugal and gravitational forces in a frame rotating with constant angular velocity Ω_0 . Then, the equilibrium velocity is $v_{0\phi} = (\Omega - \Omega_0)r$, where $\Omega^2 r = -\partial\phi_0/\partial r$. The quantities ϕ_0 and ρ_0 are the equilibrium potential and the density, respectively. The dispersive property originates from the coupled Poisson's equation, which is a second-order elliptic partial differential equation.

Case (a): The model of Lin and Shu assumes delta function for the density in z -direction and approximates Poisson's equation by

$$\frac{\partial \phi(r, z=0)}{\partial r} = \pm 2\pi i G \sigma, \quad (1)$$

in the vicinity of spiral arms, where σ represents surface mass density (Lin and Shu 1964). Here, the geometry of the model is infinitely thin disk.

Case (b): In this paper we propose more realistic solution, introducing in the z -direction Gaussians instead of delta function, $f(z)$ for potential and $g(z)$ for density. Then, we can approximately express Poisson's equation in dimensionless form as follows:

$$A \nabla_{\perp}^2 \hat{\phi} + B \hat{\phi} = \hat{\phi}, \quad (2)$$

where $\hat{\phi}, \hat{\rho}$ are two-dimensional (r and φ dependent) potential and density, respectively, $A = -a/(4\pi Gc)$, $B = -b/(4\pi Gc)$ are constants dependent on thickness of the disk L by way of a, b and c given by:

$$a = (1/2L) \int_{-L}^L f(z) dz, \quad b = (1/2L) \int_{-L}^L f''(z) dz, \\ c = (1/2L) \int_{-L}^L g(z) dz, \quad (3)$$

and ∇_{\perp}^2 denotes two-dimensional Laplacian in the plane perpendicular to z .

3. NONLINEAR EQUATION WITH SPIRAL SOLITON SOLUTION

Case (a): Let us first examine two-dimensional fluid model of the infinitesimally thindisk galaxy (Lin-Shu approximation). We normalize r and φ by means of the wave length of the carrier wave in the radial direction, $2\pi R/\lambda$, where R is the radial size of

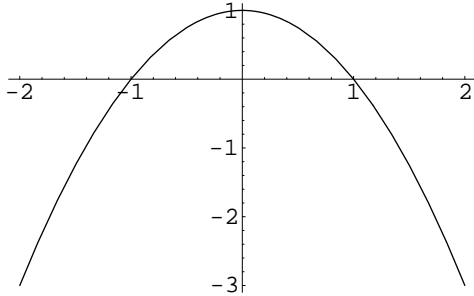


Fig. 1. Marginal stability curve for the zero thickness fluid model. x axis represents wave number k normalized by critical wave number k_2 , and y axis represents Doppler shifted frequency ω^2 normalized by epicyclic frequency κ^2 .

the galaxy and $\lambda \gg 1$ is a dimensionless constant resulting from the Lin-Shu derivation; t is normalized by the period of the carrier wave $2\pi/\omega$, ρ by ρ_0 , both components of velocity by the phase velocity $\omega R/\lambda$, ϕ by $\omega^2 R^2/\lambda^2$ and G by $\omega^2 R/(2\rho_0\lambda)$. Introducing $\tau = t + \varphi/\Omega$, the set of governing equations will be somewhat reduced. Before making the choice of transformation of coordinates and expansion of variables, it is necessary to discuss parameter regime. Dispersion relation in this case will be (Fig. 1):

$$\omega^2 = \kappa^2 - 2\pi G \rho_0 |k|. \quad (4)$$

Stability parameter is defined by $k_2 = \kappa^2/(2\pi G \rho_0)$, so that all waves with $k < k_2$ are purely stable. For this regime, dark soliton solution has already been obtained (Kondoh et al. 2000). The problem is that this solution has dark soliton solution with diminishing density, and has no spiral pattern.

Taking into account initial limitation on k , namely $k > k_1$ (where $k_1 = \max\{1/r, f'/f\}$, $f = \rho_0(r)$ and prime denotes the derivative with respect to r), we find that observational data suggest $k \approx k_2$. Marginal stability, as introduced above in terms of local dispersion relation, defines a very important condition for the basic state. In fact, if the system is far on the side of instability, then it can be expected from it to be subject to rapidly growing perturbations, which are bound to change the properties of the basic state on a short dynamical time scale. In astrophysical applications, it is often said that violently unstable models are just the wrong choice of basic state (Bertin 2000). The relevant regimes for the galaxy disk must be close to the instability threshold. In this case, a new transformation of variables has to be introduced according to Watanabe (Watanabe 1969), different from the stable case (the reason being that, in marginal stability, frequency goes to zero, so that the group velocity becomes infinite). Stretched coordinates and expansion of variables in our case are given as:

$$\xi = \varepsilon(\tau - cr), \quad \eta = \varepsilon^2 r, \\ \rho = \rho_0 + \sum_{n=1}^{\infty} \sum_{m=-\infty}^{\infty} \varepsilon^n \rho^{n,m}(\xi, \eta) e^{i(kr - \omega t)}, \quad (5) \\ \nu_{fi} = r\Omega + \sum_{n=1}^{\infty} \sum_{m=-\infty}^{\infty} \varepsilon^n \nu_{\varphi}^{n,m}(\xi, \eta) e^{i(kr - \omega t)}.$$

Substituting (5) into governing equations (the transport equations of mass density and momentum), and using Lin-Shu solution (1) instead of Poisson's equation, we derive the nonlinear equation:

$$i \frac{\partial \rho^{1,1}}{\partial \eta} + P \frac{\partial^2 \rho^{1,1}}{\partial \xi^2} + Q |\rho^{1,1}|^2 \rho^{1,1}, \quad (6)$$

in which $P = -k_2/\kappa^2 = -1/2(\partial k/\partial \omega^2) < 0$, and $Q = -(3/2)\kappa^2/(k_2 \rho_0^2) < 0$, so that $PQ > 0$. This

type of equation has bright soliton solution moving in the ξ direction:

$$\begin{aligned}\rho^{1,1}(\xi, \eta) &= \rho_0 \frac{e^{i\nu}}{ch(\sqrt{(B/2A)}\rho_0(\xi - 2A\eta))}, \\ \psi &= A \left(\frac{B}{2A}\rho_a^2 - 1 \right) \eta + \xi.\end{aligned}\quad (7)$$

Going back to the original coordinates, one obtains the solitary structure solution with enhanced density along the spiral, which explains the observed pattern (see Fig. 2).

Case (b): We extend nonlinear analysis to the more realistic case, taking the finite thickness effect into account by way of the Poisson's equation (2). It will yield for k (marginal stability case), a NLS equation with the coefficients A and B dependent of n ($B/A = n$ that includes information about the thickness). Since these coefficients determine the amplitude, width and velocity of the soliton, a comparison with the structure observed, makes it possible to decide when the finite thickness approximation is necessary for a given galaxy.

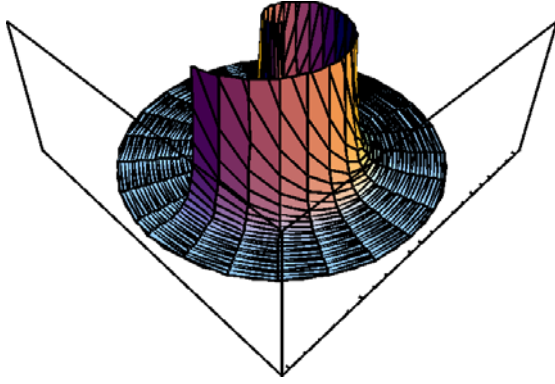


Fig. 2. Enhanced density along the spiral in 3d; solution of Eq.(4).

4. CONCLUSION

In this paper we studied weakly nonlinear dynamics of different galaxy models, using reductive perturbation method, with the emphasis on possible soliton solutions. For 2-dimensional model, using Lin-Shu approximation, the NLS equation was derived. Solution is the bright soliton, propagating along the spiral. Having established the solitary solution, we eliminate the main difficulty from the linear theory, that is the problem of searching generators of spiral wave and mechanism that maintains waves on a long time scale (quasi-stationarity assumption). We extended the 2-dimensional analysis for galaxies by solving the Poisson's equation in a different manner and obtaining NLS equation. The latter is with coefficients different for nonlinear and dispersive terms, which means different properties of soliton. Comparing the evaluated soliton properties with the observational data, one can control the validity of approximations used in either of the models.

Acknowledgements – Ms. M. Savković, is grateful to Dr. Vazha Berezhiani for his encouragement and very useful discussion on solution of NLS.

REFERENCES

- Bertin, G.: 2000, *Dynamics of Galaxies*, Cam. Univ. Press.
- Jaffrey, A., Taniuti, T.: 1964, *Non-linear Wave Propagation: with Applications to Physics and Magnetohydrodynamics*, Academic Press.
- Kondoh, S., Teramoto, R., Yoshida, Z.: 2000, *Phys. Review E*, **61**(5), 5710.
- Lin, C. C., Shu, F.H.: 1964, *Astrophys. J.*, **140**, 646.
- Watanabe, T.J.: 1969, *Phys. Soc. Jpn.*, **27**, 1341.

СПИРАЛНО СОЛИТОНСКО РЕШЕЊЕ ЗА ДИСКОЛИКЕ ГАЛАКСИЈЕ

М. Савковић¹ и Z. Yoshida²¹ Студентска 43, 11070 Нови Београд, Србија и Црна Гора² Graduate School of Frontier Sciences, The University of Tokyo, Tokyo 113-656, Japan

UDK 524.726

Оригинални научни рад

У овом раду је проучавана слабо нелинеарна динамика спиралних галаксија, употребом редуктивне пертурбационе методе. Основни циљ је одређивање могућег солитонског решења за дводимензиону геометрију, за систем који је у стању граничне стабилности. У циљу употребе одговарајуће трансформације координата неопходно је претходно извршити анализу линеаризованог система једначина и дефинисати одговарајући режим параметара. Режим параметара дефинисан на овај начин у сагласности је са посматрачким подацима. Проучен је утицај коначне дебљине галактичког диска на дисперзивне особине система,

решавајући Поасонову једначину у проширеном облику у односу на претходно апроксимативно решење Поасонове једначине које су предложили Лин и Шу. У оба случаја, за бесконачно танак диск, као и за диск коначне дебљине, изведен је исти облик нелинеарне Шредингерове једначине, али са различитим коефицијентима уз нелинеарни и дисперзивни члан. Ово значи да одговарајућа солитонска решења имају различите особине. Поређењем особина солитона са посматрачким подацима могуће је контролисати да ли је коришћена апроксимација за геометрију модела оправдана.